

75526

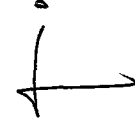
AN ANALYTICAL AND NUMERICAL STUDY OF THE PRIMARY AND
SECONDARY SUBSTRATE EFFECTS IN DROPWISE CONDENSATION

A MASTER'S THESIS
in
Mechanical Engineering
Middle East Technical University

T. C.
Yükseköğretim Kurulu
Dokümantasyon Merkez

By
AYDIN, Mahmut
September, 1991

Approval of the Graduate School of Natural and Applied Sciences



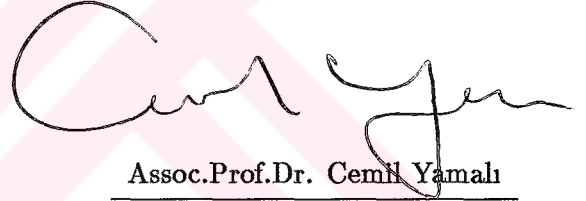
for Prof.Dr. Alpay ANKARA
Director

I certify that this thesis satisfies all the requirements as a thesis for the degree of Master of Science in Mechanical Engineering.



Prof.Dr. Rüknettin Oskay
Chairman of the Department

We certify that we have read this thesis and that in our opinion it is fully adequate, in scope and quality, as a thesis for the degree of Master of Science in Mechanical Engineering.



Assoc.Prof.Dr. Cemil Yamalı
Supervisor

Examining Committee in Charge:

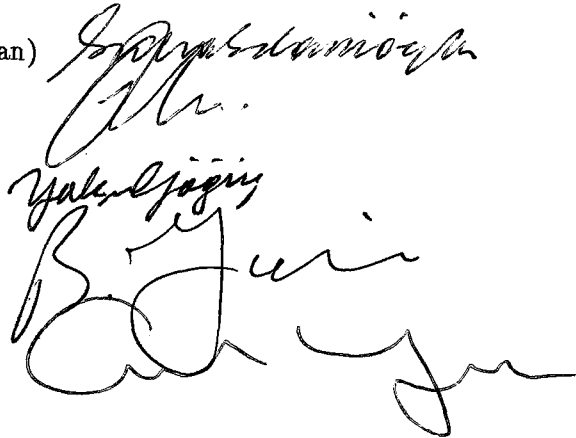
Prof.Dr. Suha Selamoğlu (Chairman)

Prof.Dr. Orhan Yeşin

Prof.Dr. Yalçın Göğüş

Assoc.Prof.Dr. Birol Yücel

Assoc.Prof.Dr. Cemil Yamalı



ABSTRACT

AN ANALYTICAL AND NUMERICAL STUDY OF THE PRIMARY AND SECONDARY SUBSTRATE EFFECTS IN DROPWISE CONDENSATION

AYDIN, Mahmut

M.S. Thesis, Department of Mechanical Engineering

Supervisor: Assoc.Prof.Dr. Cemil YAMALI

September 1991, 95 pages

In this work, the effect of the substrate material on dropwise condensation heat transfer is studied by solving the temperature distribution in the substrate material analytically. A solution to the temperature distribution under a single and isolated droplet is found by using Hankel transformation method. A simple resistance model that replaces the droplet on the condensation surface is assumed. Model also considers, an interfacial heat transfer coefficient at the interface of the vapor and condensate.

By superimposing the solutions found for single droplets the interaction effects between the neighboring droplets are found. Total dropwise condensation heat

transfer is calculated by integrating heat transfer rate through individual droplets over the entire droplet population. Computations showed that the primary substrate effect reduces the dropwise condensation heat transfer rate considerably (around 30 %). However, secondary substrate effect does not reduce the dropwise condensation heat transfer rate significantly.

Key words: Dropwise condensation, Interfacial heat transfer coefficient, Substrate effect, Dropsize distribution, Primary substrate effect, Secondary substrate effect.

SCIENCE CODE: 625.05.04



ÖZET

DAMLACIK YOĞUNLAŞMASINDA YÜZEY MALZEMESİNİN ÖZELLİKLERİNİN BİRİNCİL VE İKİNCİL ETKİLERİNİN ANALİTİK VE NÜMERİK OLARAK İNCELENMESİ

Mahmut AYDIN

Yüksek Lisans Tezi, Makina Müh. Bölümü

Tez Yöneticisi: Doç.Dr. Cemil YAMALI

Eylül 1991, 95 sayfa

Bu çalışmada yoğuşma yüzeyinin termal özelliklerinin damlacık yoğuşması, ısı iletimi üzerindeki etkisi, malzeme içinde oluşan sıcaklık dağılımı analitik ve nümerik olarak çözümlenmiştir. Tek ve izole bir damlacık halinde malzemedeki sıcaklık dağılımı Hankel Transformasyonu yardımıyla çözülmüştür. Damlacık yerine direnç modeli kullanılarak oluşturulan model aynı zamanda buhar damla ara yüzey ısı transfer katsayısını da ele almıştır. Damlaların birbiri üzerinde oluşturdukları etkiler

süperpozisyon tekniđi kullanılarak hesaplanmıřtır. Toplam ısı transferi, yüzeydeki belirli damlalar için hesaplanıp tüm yüzey üzerinden belirli bir dağılıma göre entegre edilmiştir. Hesaplamalar sonunda, birincil malzeme yüzey etkisinin (% 30 civarında) ikincil malzeme yüzey etkisine göre çok daha fazla olduđu bulunmuřtur.

Anahtar Kelimeler: Damlacık yođuřması, Ara yüzey ısı transferi katsayısı, Malzeme yüzey etkisi, Damlacık büyüklük dağılımı, Birincil malzeme yüzey etkisi, İkincil malzeme yüzey etkisi.

BİLİM DALI KODU : 625.05.04

ACKNOWLEDGMENTS

I'm indebted to my supervisor, Assoc.Prof.Dr. Cemil Yamalı for his help and friendly guidance in this endeavour. Special thanks go to Dr. Necdet Kural for his helpful suggestions. Finally, thanks are extended to my family for their patience and support.

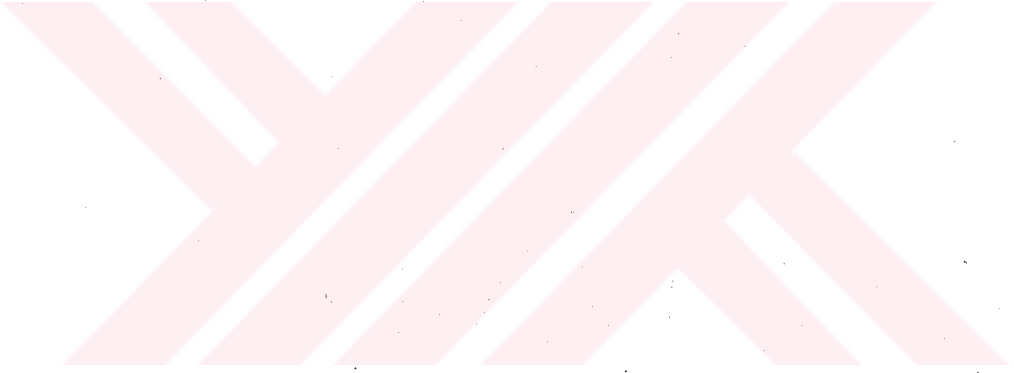


TABLE OF CONTENTS

	Page
ABSTRACT	iii
ÖZET	v
ACKNOWLEDGMENTS	vii
LIST OF FIGURES	x
NOMENCLATURE	xiii
 CHAPTER I : INTRODUCTION	 1
1.1 The Aim of the Present Work	4
 CHAPTER II : MECHANISM OF DROPWISE CONDENSATION	 5
2.1 Formation of Droplets	6
2.2 Heat Transfer Through the Droplet	8
2.2.1 Dropsize Distribution	9
2.3 Effects of Non-Condensable Gases	10
2.4 Substrate Effect	11
2.5 The Effect of Sweeping	12
 CHAPTER III : ANALYTIC MODEL	 13
3.1 Interfacial Heat Transfer Coefficient	15
3.2 Mathematical Model for the Substrate Effect in Dropwise Condensation	17
3.3 Temperature Distribution in and Heat Flux Through an Isolated Droplet Resting on a Semi-Infinite Substrate with Known Thermal Properties .	20
3.4 Temperature Distribution in the Substrate Under Two Neighboring Droplets	27
3.5 Total Substrate Effect in Dropwise Condensation	32

3.6	Total Primary Substrate Effect	34
3.7	Total Secondary Substrate Effect	35
CHAPTER IV : RESULTS OF COMPUTATION AND DISCUSSION		38
4.1	Computation Results for the Temperature Distribution Under an Iso- lated Droplet	38
4.2	Computation Results for the Temperature Distribution Under Two Neighboring Droplets	55
4.3	Computation Results of the Total Substrate Effect	63
4.3.1	Total Primary Substrate Effect	63
4.3.2	Total Secondary Substrate Effect	67
4.4	Total Dropwise Condensator Heat Transfer Including the Substrate Effect	68
4.5	Comparison with Experimental Results	68
CHAPTER V : CONCLUSIONS AND RECOMMENDATION		70
	REFERENCES	72
	APPENDICES	75
	A. FLOW CHART OF THE SOLUTION PROCEDURE	75
	B. LIST OF THE MAIN PROGRAM	76
	C. LIST OF THE PROGRAM TO CALCULATE THE NEIGHBOR EFFECT	85
	D. LIST OF THE PROGRAM TO CALCULATE DOUBLE INTEGRATION OF THE HEAT FLUX	89
	E. LIST OF THE PROGRAM TO CALCULATE THE MESH POINTS OF THE TEMPERATURE DISTRIBUTION PROBLEM	92
	F. LIST OF THE PROGRAM TO DRAW THE ISOTHERM LINES	94

LIST OF FIGURES

		Page
Figure 3.1	Thermal resistance associated to the edge of the droplet.	18
Figure 3.2	Isolated droplet resting on a semi-infinite solid substrate	21
Figure 3.3	Two neighboring droplets resting on a semi-infinite solid surface	28
Figure 3.4	Differential area of influence at a distance of x from the droplet of concern	36
Figure 4.1	Isotherms under an isolated droplet of radius 2 mm.	39
Figure 4.2	Isotherms under an isolated droplet of radius 1 mm.	39
Figure 4.3	Isotherms under an isolated droplet of radius 1 mm.	40
Figure 4.4	Isotherms under an isolated droplet of radius 0.01 mm.	41
Figure 4.5	Variation of the stainless steel substrate surface temperature under an isolated droplet as a function of radial distance ($r = 2mm$).	44
Figure 4.6	Variation of the stainless steel substrate surface temperature under an isolated droplet as a function of radial distance ($r = 1mm$).	46
Figure 4.7	Variation of the stainless steel substrate surface temperature under an isolated droplet as a function of radial distance ($r = 0.1mm$).	47
Figure 4.8	Variation of the stainless steel substrate surface temperature under an isolated droplet as a function of radial distance ($r = 0.01mm$).	48
Figure 4.9	Variation of the nickel substrate surface temperature under an isolated droplet as a function of radial distance ($r = 2mm$).	49

Figure 4.10	Variation of the copper substrate surface temperature under an isolated droplet as a function of radial distance ($r = 2mm$).	50
Figure 4.11	Surface local heat flux under an isolated droplet versus nondimensional radial distance ($r = 2mm$).	51
Figure 4.12	Surface local heat flux under an isolated droplet versus nondimensional radial distance ($r = 1mm$).	52
Figure 4.13	Surface local heat flux under an isolated droplet versus nondimensional radial distance ($r = 0.1mm$).	53
Figure 4.14	Surface local heat flux under an isolated droplet versus nondimensional radial distance ($r = 0.01mm$).	54
Figure 4.15	Isotherms under two neighboring droplets of radius 2 mm and axial distance 4.0 mm.	55
Figure 4.16	Isotherms under two neighboring droplets of radius 2 mm and radial distance 4.02 mm.	56
Figure 4.17	Isotherms under two neighboring droplets of radius 2 mm and radial distance 4.04 mm.	56
Figure 4.18	Isotherms under two neighboring droplets of radius 2 mm and radial distance 4.06 mm.	57
Figure 4.19	Isotherms under two neighboring droplets of radius 2 mm and radial distance 4.08 mm.	57
Figure 4.20	Isotherms under two neighboring droplets of radius 2 mm and radial distance 4.10 mm.	58
Figure 4.21	Temperature of the substrate surface along the line joining the center of the droplets ($x = 4.0mm, d_1 = 2mm, d_2 = 2mm$).	59
Figure 4.22	Temperature of the substrate surface along the line joining the center of the droplets ($x = 4.06mm, d_1 = 2mm, d_2 = 2mm$).	60
Figure 4.23	Temperature of the substrate surface along the line joining the center of the droplets ($x = 4.08mm, d_1 = 2mm, d_2 = 2mm$).	61

Figure 4.24	Temperature of the substrate surface along the line joining the center of the droplets ($x = 4.10mm$, $d_1 = 2mm$, $d_2 = 2mm$).	62
Figure 4.25	Total heat flux through the droplet of concern ($d = 1mm$) under the influence of the neighboring droplet ($d = 1mm$) versus center to center distance between the droplets.	64
Figure 4.26	Total heat flux through the droplet of concern ($d = 0.1mm$) under the influence of the neighboring droplet ($d = 1mm$) versus center to center distance between the droplets.	65
Figure 4.27	Total heat flux through the droplet of concern ($d = .01mm$) under the influence of the neighboring droplet ($d = 1mm$) versus center to center distance between the droplets.	66



NOMENCLATURE

T_{sat}	vapor saturation temperature
f_{c0}	fractional area occupied by droplets in the coalescence region
P_v	pressure of vapor
T_v	vapor temperature
G	gas constant
T_i	temperature of liquid-vapor interface
v_1	drop specific volume of droplet
σ	surface tension
h_{fg}	latent heat of evaporation
h_i	equivalent interfacial heat transfer coefficient for the liquid-vapor interface
r^*	critical droplet radius
T_s	temperature of substrate surface
r	droplet base radius
T_d	temperature of droplet
k_s	thermal conductivity of substrate material
k_v	thermal conductivity of droplet
T_∞	Substrate temperature at infinite distance
w	net rate of condensation per unit area
γ	condensation coefficient
θ	contact angle

J_0	Bessel function of order zero
α	variable of Hankel transformation
P_i^{**}	equilibrium pressure corresponding to the interface temperature
P_r^{**}	equilibrium pressure corresponding to droplet radius of curvature
R	radius of curvature at the point of interest
R^*	critical droplet radius
ρ_1	liquid density
ΔT	difference between the vapor and the interface temperature
z	axial direction
f_{01}	primary substrate effect per unit droplet
f_{12}	secondary substrate effect per unit droplet
Q_{01}	total primary substrate effect
Q_{dc}	total dropwise heat transfer under the influence of primary and secondary substrate effects
Q_{12}	total secondary substrate effect
q_{II}	total secondary substrate effect per unit droplet

CHAPTER I

INTRODUCTION

Since it was first reported in 1930 by Schmidt, dropwise condensation has been of interest to many investigators. It has higher heat transfer coefficients than those achieved with filmwise condensation. This holds promise for commercial heat exchangers [1]. Recent concern for more effective energy utilization and development of alternative energy conversion processes has amplified interest in condensation phenomena in general and dropwise condensation in particular since improved condensation heat transfer coefficient could clearly improve power plant performance. Reduction of condenser surface area could result in substantially lower capital costs. The economic viability of power production schemes involving relatively small overall temperature differences (such as the use of ocean thermal gradients and other power generation concepts) is highly dependent on efficient condensation; since, minimization of heat exchanger surface is crucial for these designs.

The advantage of dropwise condensation for such uses, and the prospect of using high-surface-energy materials (such as plastics) in condensers, which will make dropwise condensation more easily attainable, points up, the need for a detailed understanding of dropwise condensation phenomena.

Condensation is a phenomena frequently encountered in nature, defined as the phase change from the vapor state to the liquid or the solid state. This can take place within a bulk vapor when its temperature is below the saturation temperature corresponding to its pressure or on a solid surface whose temperature is below the saturation temperature of the vapor. In the latter case, the vapor temperature itself

may be either at saturation or superheated. In any case, condensation requires a certain amount of subcooling.

During the phase, process energy in the form of the latent heat must be removed from the region of condensation, either by convection, diffusion or radiation. A pressure decrease occurs in the region where condensation is taking place, and as a result mass diffuses toward this region. The combined mass and heat transfer characterizes the condensation phenomena. The precise onset of condensation has not been clearly identified, but it is believed that the process is initiated with a nucleus formed by a group of vapor molecules within the vapor bulk or on a solid surface. In this sense it is a nucleation phenomenon.

The condensation phenomenon can be classified as:

- 1) Bulk condensation
- 2) Surface condensation

Bulk condensation takes place within the bulk of vapor away from any solid or liquid boundaries. In this type of condensation nucleation takes place either randomly within the bulk of the vapor (homogeneous nucleation), or on foreign particles entrained in the vapor (heterogeneous nucleation).

Surface condensation is the condensation taking place on a subcooled solid surface when exposed to vapor. Because of its wide application in industry, it is the most important one, from the engineering point of view.

Surface condensation can be classified further as either dropwise or filmwise condensation depending upon the characteristics of the condenser surface employed. Either one or both of these can take place on a surface. Filmwise condensation is the most widely observed mode, and occurs if the liquid wets the condenser surface, resulting in the coverage of the surface by liquid condensation film.

The first analytical formulation of filmwise condensation was made by Nusselt, considering a parabolic velocity profile and a linear temperature variation across the condensate film. This treatment neglected the momentum changes in the condensate flow and a so-called interfacial resistance. Latter becomes significant for liquid metal

condensation, especially at low vapor pressures. Nevertheless, simple analysis of the Nusselt predicts the heat transfer in filmwise condensation quite well. Subsequent modifications to the theory of Nusselt include incorporating the effects of interfacial resistance, interfacial shear stress, transition to turbulent flow within the film, and superheated vapor [3]. Dropwise condensation occurs if the condensate does not wet the condenser surface. Heat transfer coefficients can be predicted satisfactorily for dropwise condensation and ideal film condensation. The ratio of the dropwise-to-filmwise coefficient may be as high as 10 or 20 [4]. Until 1965 dropwise condensation was achieved by coating the condenser surface with an organic promoter. Unfortunately, these promoters (waxes, oils, greases, soaps) wash off rapidly and condensation becomes filmwise. Continuous injection of promoters in the steam gives long-lived dropwise condensation but these added materials are not wanted in commercial systems containing pumps and turbines. Polymer coatings such as Teflon can produce dropwise condensation, but if thickness is great enough to give durability, the heat transfer benefits are cancelled by the thermal resistance of the low-thermal conductivity coating. Thin coatings of noble metals can serve as promoters of dropwise condensation. These have good thermal conductivities and the possibility of permanence. For example, an electro plate of Gold $200\mu\text{m}$ thick on copper was found to produce dropwise condensation for over 2500 hours.

In dropwise condensation vapor in contact with a subcooled surface form microscopic droplets on the surface, which then grow by the direct condensation on the droplets and by coalescences between the droplets, until certain size is reached. The droplets then leave the surface by the action of body forces and/or vapor shear. Unlike filmwise condensation, the physical processes taking place in dropwise condensation are complex and random when viewed on a detailed scale. More over the parameters affecting dropwise condensation are more difficult to control (e.g., the number of nucleation sites, and noncondensable gases). The major portion of the heat transfer with dropwise condensation takes place on droplets of microscopic sizes. Elaborate optical techniques are necessary to understand the phenomena and to obtain data of such small dimensions.

Because of the above factors, dropwise condensation provides a challenging field

of study, experimentally and analytically. Only in recent years have significant improvements been made in analyzing the events taking place in dropwise condensation.

1.1 The Aim of the Present Work

The goals that are planned to achieve in this work can be summarized as follows:

- a) In order to see the effect of substrate material on the dropwise condensation heat transfer, the temperature distribution in the substrate material as a result of the heat flux through an individual droplet will be formulated and solved analytically.
- b) The effect of various droplets at different sizes on heat transfer rate of the neighboring droplets will be formulated and solved.
- c) Total substrate effect in the dropwise condensation will be evaluated.

CHAPTER II

MECHANISM OF DROPWISE CONDENSATION

If a surface on which dropwise condensation is taking place is studied in detail, it will be observed that surface is covered by droplets of varying sizes. These sizes vary from very small microscopic dimensions to couple of millimeters. During the dropwise condensations droplets on the surface are swept by falling droplets. In the swept area the average droplet size is naturally smaller therefore, the sweeping results in variations of the droplet sizes. If a region on the condensation surface is not allowed to be swept by falling droplets, in other words if the sweeping effect is eliminated then, in the unswept region, the average droplet size and the droplet size distribution is almost the same in such regions. If the size of the droplets are made nondimensional by a characteristic length such as the average droplet size or maximum droplet size in the distribution then it will be observed that the droplet size distribution is almost the same for different condensation conditions although the average droplet size might be different from situation to situation. This situation is usually observed in magnified picture of the condensation surfaces on which dropwise condensation is taking place. This observation is extensively used in the analytical study of the dropwise condensation.

If a condensation surface is studied locally, there will be variations in the average droplet size from one location to another location. On the other hand, if a reasonably large condensation surface is taken on which varies dropwise condensation processes (i.e., sweeping of the surface, formation of the new droplet, growth of the newly formed droplets etc.) are taken place randomly and the time average of all these processes taking place on the surface is considered then one can consider the dropwise condensation

on such surface somewhat independent of time, that is, local processes are function of time but general characteristics of average process can be considered as independent of the time.

Dropwise condensation processes occur in a cycle. It starts with the formation of a droplet in a nucleation site [5]. A droplet so formed grows with direct condensation on it then, it starts coalescences with neighbouring droplets. From that point on dropwise condensation continues with the growth of droplets by direct condensation and coalescences with other droplets. As a result of the coalescences number of droplets in the unit area decreases as the size of the droplets increase and large percents the surface covered by the droplets.

When a droplet reaches a certain size, due to its weight, it starts sliding on the surface and, during its journey on the surface it sweeps, dry areas are formed on which new droplets can nucleate. In order to be able to form a realistic analytical model for dropwise condensation, it is essential to understand various processes that make up dropwise condensation phenomena.

2.1 Formation of Droplets

Because of the difficulties encountered in examining the formation and growth of the microscopic droplets, different models are proposed by various investigators on the formation of the droplets and the transfer of latent heat to the condensation surface. The proposed models on the formation of droplets can be divided in two groups, according to the explanation of how the dry area between the droplets behave during the condensation.

One group claims the dry area between the droplets is inactive as far as the condensation is concerned and no phase change occurs and the only mode of heat transfer on this area is convection. According to the models proposed by the second group condensation takes place in the empty area among the droplets and the resulting latent heat is transferred to the surface.

Jacob [2] introduced the first model to explain the formation of droplets. Ac-

According to this model, condensation starts with the formation of a thin film on the condensation surface. When this film reaches to a critical thickness, it fractures and forms a droplet. Emmons assumed a re-evaporation mechanism between the droplets which results high heat transfer coefficient there. According to this model, molecules condense and re-evaporate which result in a superheated vapor blanket between the droplets. Erb and Thelen [6] also assumed a re-evaporation mechanism among the droplets. According to this model vapor between the droplets on the bare surface is supercooled due to the heat transfer with the condensation surface. Some of this vapor condenses while the remaining vapor which captures the resulting latent heat becomes saturated. Erb and Thelen claims that the high heat transfer rate in dropwise condensation is caused by violent eddy currents, that results from the above mentioned condensation and latent heat release process. According to the models mentioned above, majority of the heat transfer takes place in the area between the droplets and, heat transfer through the droplets is (due to the high thermal resistance of the droplets) only a small fraction of the total heat transfer in dropwise condensation.

Models considered above somehow missed the point that droplets, although they have a large thermal resistance, have a small thermal resistance at the edge and therefore it is possible that heat transfer at those regions are considerably large. Although the condensation models described above are explained in detail in the related documents, it will be fair to say that none of the models described above is based on careful experimental observations and measurements. All these models are based on the general understanding of the physical principles by individual investigators. The first experimental studies of the mechanism of the dropwise condensation are made by Welch and Westwater [7] by using high speed cameras. In their films they observed that coalescences occur between droplets even at microscopic sizes and there are empty spaces available between the droplets. Since the magnification they used in their studies is not large enough, they couldn't study the growth of a single droplet. Mc Cormic and Bear [8], in their experimental study, examined the growth and collapse of individual droplets and found that the formation of the droplets took place at specific sites. They used a magnification factor of 600 in their study which made it possible to study the individual droplets. In their studies they took 50 control droplets, 25-50 of which is found to form at specific sites. The small surface to vapor temperature difference

($0.95 - 7.6^\circ$) made it possible to reach relatively large critical (formation) sizes. This made the examination of droplets of critical sizes possible.

Umur and Griffith [9] also made experiments to prove that the formation of droplets occur as a result of nucleation and therefore, they tried to disrepute the film formation hypothesis. They claimed that if there is any film formation on the condensation surface, this occurs due to two reasons. Either condensation between droplets forms a film or a condensate film is left behind the moving droplets. Their analytical and experimental studies have shown that such a film formation is not possible. Another study related to the impossibility of a condensate film formation in dropwise condensation is made by Ivanovskii [10]. By studying the dropwise condensation of mercury and electrical resistance it has on the surface, he concluded that no condensate film formed on the condensation surface, otherwise such a film would reduce the electrical resistance below the values measured during the experiment.

Mc Cormick and Westwater [11] realized from the pictures that they obtained in their experiments that dropwise condensation is essentially a nucleation phenomenon. On the picture taken with the help of a microscope (magnification of 400) they observed the formation and coalescences of droplets and also the formation of new droplets in the area left by coalescing droplets.

In brief, the latest studies clearly show that formation of droplets occurs as a result of nucleation and no film formation between droplets takes place and majority of the condensation takes place along the edge of the droplets.

2.2 Heat Transfer Through the Droplet

Since condensation occurs on the droplets of varying sizes in the dropwise condensation, to find the total heat transfer rate, the amount of heat transfer through a single droplet as a function of its radius and the size distribution over the condensation surface should be known.

In order to find the heat transfer through a single droplet the following points should be considered:

- a) Heat conduction through a single droplet
- b) Heat conduction in the substrate material
- c) The existence and the variation of the interfacial heat transfer coefficient at the vapor-liquid interface
- d) Interference of heat conduction through a single droplet with the heat conduction in the neighboring droplets

One can argue that the large number of coalescences and the continuous growth of droplets make the dropwise condensation a highly unsteady process and therefore heat transfer in dropwise condensation should be considered in terms of the unsteady equations. One can meet these arguments by stating the fact that although the individual droplets go through unsteady processes, the overall process, if it is considered in terms of the average terms (for instance the dropsize distribution), is steady. Also, the fact that the time period needed to reach steady state for an individual droplet is much shorter than the period needed for the condensation vapor on the droplet, makes a quasi-steady type of an analysis for the heat conduction for an individual droplet reasonable.

First calculation model for heat transfer through an individual droplet is proposed by Fatica and Katz [12]. In that model, in order to avoid an anomaly of a mathematical singular point at the edge of the droplet, they omit the heat transfer at the region close to the droplet. Hurst and Olson [13], later, showed that in those neglected regions 83-98 % of the total drop heat transfer took place.

2.2.1 Dropsize Distribution

In the analytical modelling of the dropwise condensation, the dropwise distribution is studied with two different point of views.

- i) In the pioneering studies, an average dropsize distribution is considered. In that model an average dropsize distribution that results from the sweeping, coalescences, growth and departing of completely random processes is taken to calculate the total heat transfer in dropwise condensation.

ii) If a surface on which dropwise condensation is taking place is studied carefully, it will be seen that each point on the surface is at a different level of growth. In other words, each point on the surface has a different elapsed time period from the last sweeping that took place at the point to the present time. Regions close to the top of the condensation surface is swept less frequently therefore, the average droplet size there will be larger compared to the region close to the bottom. Also, droplet size distribution is affected by direct condensation at very small sizes, when they reach a critical size growth take place as a result of direct condensation and coalescences together. Therefore, droplet size distribution should have a different character from that point on. This fact is observed in the analytical and experimental work of Griffith [14].

Le Fevre and Rose [15] proposed the following expression to calculate the fraction of surface covered by the droplets in the size range r to r_{\max} .

$$f_{co} \left(\frac{r}{r_{\max}} \right) = 1 - \left(\frac{r}{r_{\max}} \right)^{1/n}.$$

This expression can be used for a surface swept by departing droplets as well as for unswept surfaces. The effect of sweeping can be introduced in to the expression above by choosing a suitable value for n . It is shown by Tanaka [16] that for an unswept surface the value of n is close to 3.

2.3 Effects of Non-Condensable Gases

Majority of industrial systems that involve condensation has small amount of non-condensable gases in it. The source of the non-condensable gases is either the dissolved gases or atmospheric air that diffuses into the system. The dissolved gases in water usually reduces the calculated film condensation coefficient up to 50 %. Hasson [17] has shown that non-condensable gases decrease the heat transfer rate appreciately. He concluded that non-condensable gases that are carried by vapor acts as a barrier and reduces the condensation rate. It is found that heat transfer coefficient in condensation is inversely proportional to the percentage of air in the vapor. In dropwise condensation the non-condensable gases not only reduces the heat transfer coefficient but also cause

oscillations in temperature measurements which makes the temperature measurements extremely difficult.

2.4 Substrate Effect

As far as the effect of substrate material properties are concerned the opinions differ. A group of scientist claim that thermal properties of substrate has an important effect on the rate of heat transfer, in dropwise condensation whereas others claim that substrate is not a factor in dropwise condensation.

Tanner et.al. [18] showed that a copper substrate has a condensation heat transfer coefficient larger than the coefficient with a stainless substrate. It is claimed that the difference in heat transfer coefficient is caused by the difference in surface energies. In a different study, to eliminate the surface energy difference factor from the measurements, condensation surface made of different materials is covered by a thin coating of gold.

Measurements in that study showed that different substrates have different heat transfer coefficients although they are covered by a thin gold coating. This difference is attributed to the difference in the thermal conductivities of the substrate material. In general, investigators claim that dropwise condensation heat transfer coefficient increases with an increase in the thermal conductivity of the substrate material. In order to explain the substrate effect various model are developed.

In dropwise condensation, in addition to the thermal resistance of the droplet itself there are two additional thermal resistances: Interfacial thermal resistance at the vapor-liquid interface of the droplet which varies with varying interfacial temperature. The other resistance is called constriction resistance and is caused by the bending of the heat flux lines in the substrate.

In order to study the effect of substrate material in dropwise condensation, Sadhal [19] studied a single droplet on a substrate material. The surface of the substrate which is not covered by the droplet is considered as adiabatic. This model does not represent the events taking place in dropwise condensation exactly. Nevertheless, it is the first mathematical model that gives the non-uniform temperature distribution un-

der the droplet. In his calculations it is shown that if the substrate material has a high thermal conductivity, then the Nusselt number is independent of thermal conductivity of the substrate (no substrate effect). On the other hand, if the thermal conductivity of the substrate is low then the Nusselt number becomes a function of the substrate thermal conductivity. When the thermal conductivity of the substrate decreases, Nusselt number also decreases. This behavior is consistent with the previous observation of dropwise condensation that dropwise condensation heat transfer coefficient increases with an increase in the substrate thermal conductivity.

2.5 The Effect of Sweeping

If the dropwise condensation on a vertical surface is examined, the droplets that grow to large sizes and departs under the effect of gravity forces will be observed. As these large droplets depart from the condensation, surface they slide down and leave a swept surface behind them. New droplets nucleate in the swept region immediately. This process is termed as sweeping process in dropwise condensation. Sweeping rate is affected by three parameters of the dropwise condensation. These are the temperature difference between the vapor and condensation surface, the magnitude of the forces acting on the droplets and the physical dimensions of the condensation surface. As the temperature difference between the surface and the vapor increases the rate of heat transfer, therefore the rate of condensation increases which result in an increase in the sweeping rate. As one goes down the condensation surface the frequency of the sweeping increases which result in higher dropwise condensation heat transfer coefficient there [20]. Analytical and experimental investigations resulted in the following observations:

- a) The faster a location is swept, the higher the heat transfer coefficient there.
- b) The top of the condensation surface is not affected by the sweeping process; since the droplets that reach the departure size do not sweep that location. Therefore, the heat transfer coefficient at that point is low.

CHAPTER III

ANALYTIC MODEL

The analytical formulation of dropwise condensation requires careful understanding of the processes taking place. The most fundamental question that should be asked before proceeding with the analytical description is how the droplets form in the first place. The high speed movie film studies of Mc Cormick-Westwater [11], Peterson-Westwater [21] and experimental studies of Umur and Griffith and Ivanovskii [9-10] removed doubts about the origin of the smallest drop on the surface; it has been concluded that the droplets form by a nucleation process at specific locations called nucleation sites. In the model to be developed, therefore it will be assumed that droplets form at specific sites on the surface and it also will be assumed that the area between the droplets can be considered as thermally insulated. Heat transfer does take place between the vapor and the surface on the bare areas in the form of convection and the transfer of molecular kinetic energy, but these will be neglected when compared to the heat transfer associated with the phase change.

Several mathematical models are introduced in the literature to predict the heat transfer rate and heat transfer coefficient in dropwise condensation. However, none of the proposed theories have explicitly considered the effect of thermal properties of the surface material in spite of the fact that strong experimental evidence have existed showing that this effect is significant. First evidence was given in the work of Tanner et.al., where it was observed that heat transfer coefficient was, in average, about one fifth less in the case of stainless steel than in the case of copper as a material for the condensing surface. They concluded that reduction in heat transfer coefficient was

not associated with any difference in the appearance of the condensing surface and suggested that such a difference could arise from the influence of absorption properties and surface free energy of the interface.

Griffith and Lee [22] conclusively showed that the above explanation for the difference in the heat transfer coefficients for the two metals is invalid. They had their surface prepared identically and gold plated, and the difference in heat transfer coefficients was still present in approximately the same degree. Their conclusion was that non-uniformity in surface temperature under conditions of dropwise condensation causes different heat fluxes for different surface materials and that higher thermal conductivity of the surface would give more uniform surface temperature and therefore higher heat flux (for a fixed temperature difference between condensing vapor and the mean surface temperature).

Since the droplets in dropwise condensation differs in size in a couple of order of magnitude and it is always possible that a large droplet might be surrounded by very small droplets with very small thermal resistances, it is expected that on a surface where dropwise condensation is taking place, there will be large temperature changes in very short distances. This situation will be made even more complicated by the existence of a small resistance at the edge of the droplets.

Consequently in dropwise condensation, thermal resistance on the surface shows sharp changes from location to location which results in drastic changes in temperature distribution. Such variations introduce an additional thermal resistance which is called substrate effect and result in reduction in the heat transfer coefficient of dropwise condensation. In a previous study [23] a numerical solution of heat transfer through a single droplet with its substrate is obtained. Large changes in temperature at the edge of the droplet puts limitation on the interpretation of such solutions. In this study, first, an analytical solution to the temperature distribution in the substrate will be obtained. Taking a statistical average of the droplet size distribution the effect of neighbouring droplets on the heat transfer rate of a droplet of given radius will be studied. Such, an analysis will make it possible to introduce the interference between the droplets as far as the heat transfer rate is concerned.

3.1 Interfacial Heat Transfer Coefficient

In most of the mathematical modelling of dropwise condensation the surface temperature of the droplets is assumed to be equal to the temperature of the surrounding vapor. In the pioneering models this assumption was sufficient to model the dropwise condensation phenomena because in those studies models were simple and do not go into the details of the events taking place. In the mathematical model used in this study, to analyze the substrate effect temperature drop due to the mass diffusion effects will be also considered to make the model more sophisticated. Therefore, the conduction model for individual droplets will also consider the thermal resistance due to the interfacial heat transfer coefficient.

Schrage's equation (3.10) for interphase mass transfer under nonequilibrium conditions is modified by means of the Kelvin-Helmholtz equation and Clausius-Clapeyron relation.

Mass transfer through the interface is given under nonequilibrium conditions by,

$$\omega = \left(\frac{2\gamma}{2-\gamma} \right) \left(\frac{1}{2\pi g} \right)^{1/2} \left[\frac{P_v}{T_v^{1/2}} - \frac{P_i^{**}}{T_i^{1/2}} \right] \quad (3.1)$$

where

- γ : condensation coefficient
- ω : net rate of condensation per unit interfacial area
- P_i^{**} : equilibrium pressure corresponding to the interface temperature T_i .

Using Kelvin-Helmholtz equation,

$$Ln \frac{P_r^{**}}{P_i^*} = \frac{2\sigma v_l}{r \cdot G \cdot T_i} \quad (3.2)$$

where,

- P_r^{**} : equilibrium pressure corresponding to drop radius r
- P_i^* : saturated pressure corresponding to temperature of liquid vapor interface temperature T_i .

By using property of $P_r^{**} = P_i^{**}$ at interface, Equation (3.1) becomes;

$$\omega = \left(\frac{2\gamma}{2-\gamma} \right) \left(\frac{1}{2\pi g} \right)^{1/2} \frac{P_v}{T_v^{1/2}} \left[1 - \frac{P_i^*}{P_v} e^{\frac{2\sigma v_l}{r \cdot G \cdot T_i}} \frac{T_v^{1/2}}{T_i^{1/2}} \right] \quad (3.3)$$

Clasius-Clapeyron equation gives;

$$\ln \frac{P_i^*}{P_v^*} = -\frac{h_{fg}}{G T_e} \left(\frac{T_i}{T_v} \right). \quad (3.4)$$

If vapor is saturated,

$$P_v^* = P_v \quad (3.5)$$

where,

P_v^* : saturation pressure corresponding to vapor temperature

Substituting Equations (3.5) and (3.4) into Equation (3.3)

$$\omega = \left(\frac{2\gamma}{2-\gamma} \right) \left(\frac{1}{2\pi g} \right)^{1/2} \frac{P_v}{T_v^{1/2}} \left[1 - e^{\frac{2\sigma v_i}{r^* G T_i}} e^{-\frac{h_{fg}}{G T_i} \left(1 - \frac{T_i}{T_v} \right)} \frac{T_v^{1/2}}{T_i^{1/2}} \right] \quad (3.6)$$

From Equations (3.2) and (3.4)

$$\ln = \frac{P_i^*}{P_v^*} = -\frac{h_{fg}}{G T_e} \left(1 - \frac{T_i}{T_v} \right) = -\frac{2\sigma v_i}{r^* G T_i} \quad (3.7)$$

and,

$$h_i = \frac{w h_{fg}}{T_v - T_i} \quad (3.8)$$

Therefore, interface heat transfer coefficient becomes,

$$h_i = \frac{h_{fg}}{T_v - T_i} \left(\frac{2\gamma}{2-\gamma} \right) \left(\frac{1}{2\pi g} \right)^{1/2} \frac{P_v}{T_v^{1/2}} \cdot \left[1 - \frac{T_v^{1/2}}{T_i^{1/2}} \exp \left(-\frac{h_{fg}}{G T_i} \left[1 - \frac{T_i}{T_v} \right] \left[1 - \frac{R^*}{R} \right] \right) \right] \quad (3.9)$$

By expanding the exponential function in expression (3.9) and neglecting small terms, the interfacial heat transfer coefficient becomes,

$$h_i = \left(\frac{2\gamma}{2-\gamma} \right) \left(\frac{1}{2\pi} \right)^{1/2} \frac{h_{fg}^2 P_v}{G^{3/2} T_v^{5/2}} \left(1 - \frac{R^*}{R} \right) \quad (3.10)$$

where,

$$R^* = \frac{2T_{sat}\sigma}{h_{fg}\rho_1\Delta T}$$

where,

R^* : critical radius for formation of the droplet

R : the radius of curvature of the interface of the point of interest

ΔT : difference between the vapor and the interface temperatures The term
(= $T_{sat} - T_i$)

ρ_1 : liquid density

R^*/R is quite small for droplets of moderate size (close to departure size) but approaches the value of unity as it comes closer to the critical size. At the critical size it becomes unity, and equivalent heat transfer coefficient on the surface thus becomes zero. At the critical size drop is in unstable equilibrium, neither growing nor collapsing.

Equation (3.10) can be put in a more simplified form such as,

$$h_i = \frac{K_1}{T_i} \left(1 - \frac{K_2}{R\Delta T} \right)$$

where,

$$K_1 = \left(\frac{2\gamma}{2-\gamma} \right) \left(\frac{1}{2\pi} \right)^{1/2} \frac{h_{fg}^2 P_v^*}{G^{3/2} T_v^{3/2}}$$

$$K_2 = \frac{2T_{sat}\sigma}{h_{fg}\rho_1}$$

Assuming circular heat flow lines within the condensate in the neighborhood of the triple interface (Figure 3.1) the thermal resistance associated with the interfacial heat transfer coefficient can be expressed as;

$$R_i = \frac{1}{h_i}$$

Thermal resistance of condensate element becomes,

$$R_c = \frac{X \cdot \theta}{k}$$

where θ and X shown in Figure 3.1.

3.2 Mathematical Model for the Substrate Effect in Dropwise Condensation

The events taking place in dropwise condensation are described before in the previous chapters. The most important phenomena in dropwise condensation is the heat conduction through the droplet and the substrate which results in the transfer of energy and also the formation of the specially shaped isotherms in both substances. Studies of many investigators show that the heat flux lines in the droplet are essentially close to an arc of a circle and using this fact an approximate thermal resistance as a function of the location on the substrate surface can be obtained.

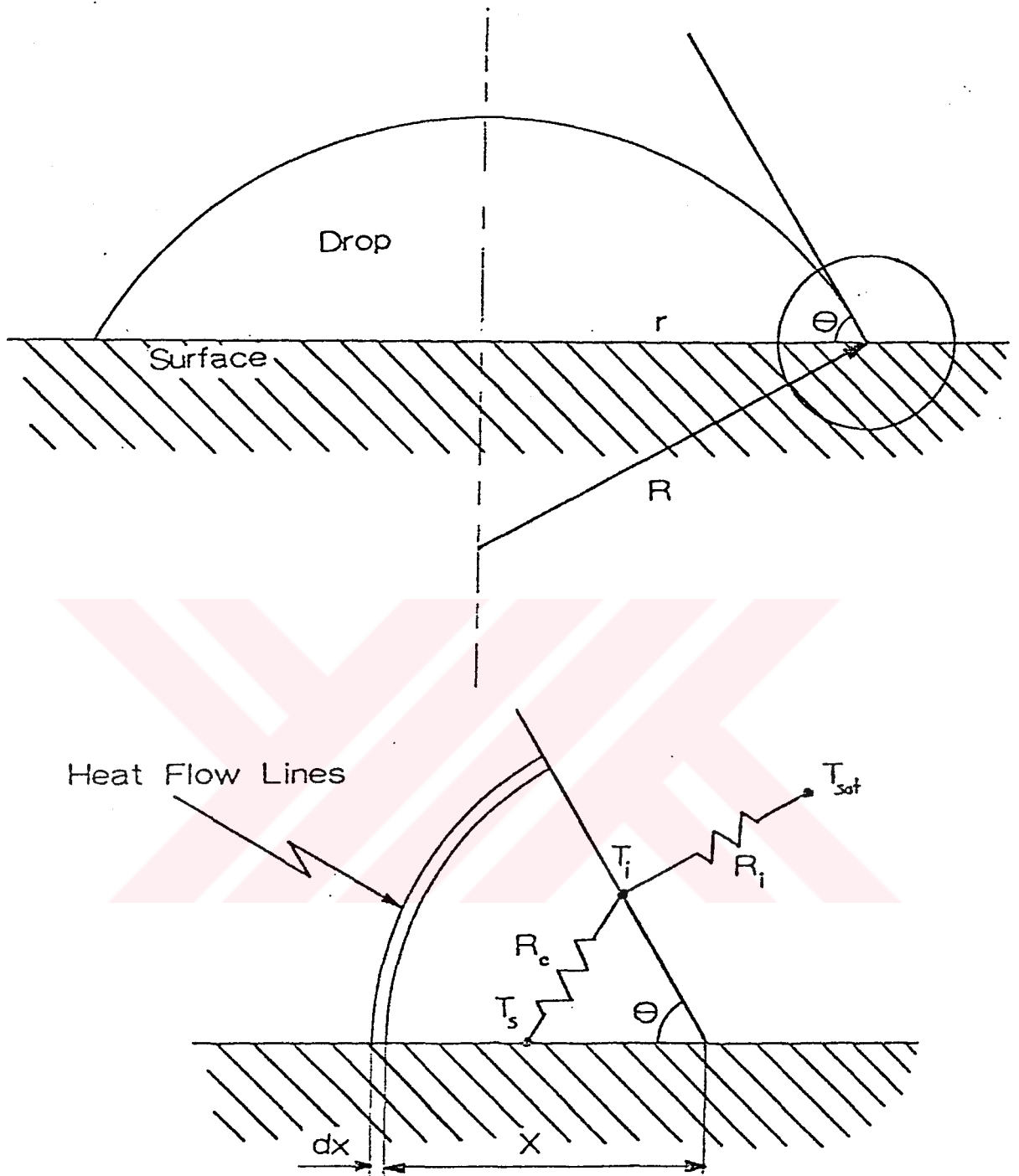


Figure 3.1. Thermal resistance associated to the edge of the droplet.

On the other hand, the shape of the isotherms in the substrate is complicated because of the complicated nature of the heat flux at the interface of the droplet. Smaller resistance due to the shorter heat flux "arcs" near the edge of the droplet cause drastic changes in the temperature in that region, which results in excessive bending in the isotherms in that region. The immediate effect of such drastic changes in the temperature of the substrate material is to raise the temperature at the edge of the droplet in the substrate material which cause a drop in the total heat transfer in the droplet because, such a rise in the temperature reduces the temperature potential between the vapor and the substrate material. The fact that the majority of the heat transfer takes place at the edge of the droplet further strengthens the effect of substrate temperature distribution in reducing the total heat transfer through a droplet.

The reduction of the total heat transfer through a droplet as a result of temperature distribution in the substrate material will be called "primary substrate effect". In a typical dropwise condensation growth and coalescences of the droplets take place continuously and therefore process is highly time dependent. An analysis that take the time dependent behavior of enormously large number of droplets into account is very complex and seems almost an impossible task.

Nevertheless, time constant of the droplets is much smaller than their growth time therefore growth of the droplets may be analyzed by considering a quasi steady approach.

"A secondary substrate effect" comes into picture, in dropwise condensation, due to the fact that individual droplets are not isolated but surrounded by droplets of varying sizes small and large. Droplets that are close to the edge of an individual droplet cause a further rise of the temperature of the substrate in that region and coupled with the fact that majority of the heat transfer takes place there, further reduction in the total heat transfer through a droplet takes place.

In the light of the discussions above, substrate effect in dropwise condensation can be summarized as.

- a) "Primary Substrate Effect" due to the temperature distribution in the substrate material that results from the heat flux of individual droplets.

- b) "Secondary Substrate Effect" due to the temperature distribution in the substrate material resulting from the heat flux of the neighboring droplets.

In the light of the substrate effect classification summarized above the mathematical model to analyze the substrate effect will be established as follows:

Model will be based on the temperature distribution of an isolated individual droplet resting on a semi-infinite substrate with known thermal conductivity. Since it is assumed that the problem is quasi-steady thermal capacity of the substrate is irrelevant to the problem.

3.3 Temperature Distribution in and Heat Flux Through an Isolated Droplet Resting on a Semi-Infinite Substrate with Known Thermal Properties

In order to find the total substrate effect in dropwise condensation, attention will be concentrated on a single droplet. Once the heat flux through a single droplet can be found the total substrate effect can be obtained by integrating the substrate effect on individual droplets over the droplet size distribution.

The coordinate system chosen to solve the temperature distribution in the substrate material under a droplet is shown in Figure 3.2. Following assumptions are made in solving the problem:

1. Temperature distribution is axi-symmetric
2. Steady state temperature distribution determines the effect of the substrate and, time dependent thermal effects are not major concern.
3. Substrate material, although it has a finite thickness in typical applications, will be assumed to be a semi-infinite body since its thickness is considerably large for the majority of the droplets on the surface of condensation.
4. Except the area covered by the droplet, surface of the condensation will be assumed to be insulated since the small amount of heat transfer by convection

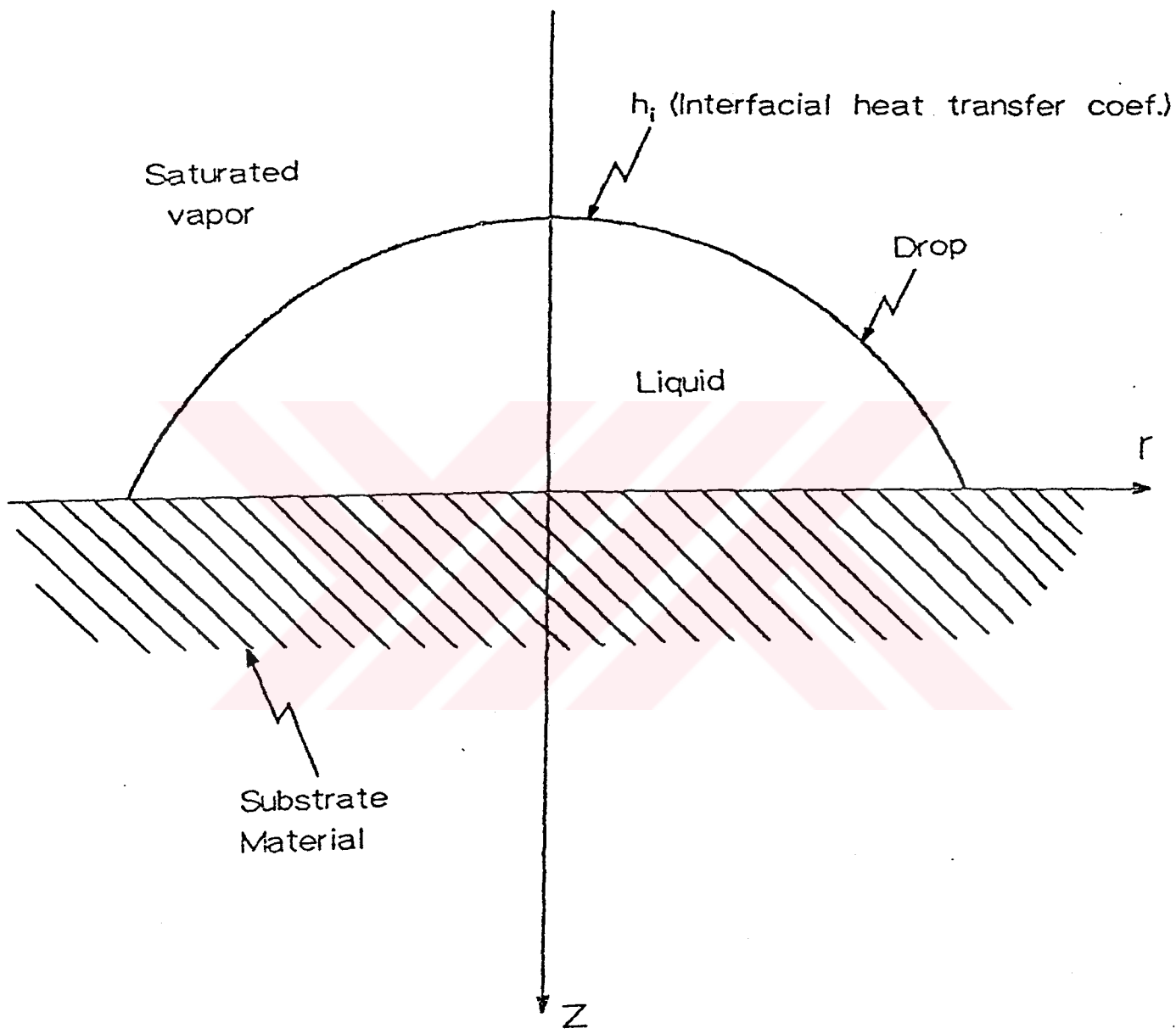


Figure 3.2. Isolated droplet resting on a semi-infinite solid substrate

there is negligible compared to the high rate of heat transfer on the surface of the droplet.

The governing differential equation for heat conduction in the substrate and the droplet can be expressed as:

For the substrate:

$$\frac{\partial^2 T_s}{\partial r^2} + \frac{1}{r} \frac{\partial T_s}{\partial r} + \frac{\partial^2 T_s}{\partial z^2} = 0 \quad (3.11)$$

For the droplet:

$$\frac{\partial^2 T_d}{\partial r^2} + \frac{1}{r} \frac{\partial T_d}{\partial r} + \frac{\partial^2 T_d}{\partial z^2} = 0 \quad (3.12)$$

where, T_s : temperature distribution in the substrate
 T_d : temperature distribution in the drop
 z : axial direction (Figure 3.2)
 r : radial direction (Figure 3.2)

Boundary Conditions.

On the surface of the droplets heat conduction rate can be equated to the heat convected at the interface

$$-k_v \frac{\partial T_d}{\partial n} \Big|_{\text{drop surface}} = h_i (T_{\text{drop surface}} - T_v)$$

where n is the direction, perpendicular to the drop surface

At the interface between the droplet and the substrate conduction rate and the temperatures are equal:

$$+k_s \frac{\partial T_s}{\partial z} \Big|_{z=0} = +k_v \frac{\partial T_s}{\partial z} \Big|_{z=0}$$

$$T_s|_{z=0} = T_d|_{z=0}$$

At large distances in the substrate

$$T_s|_{z \rightarrow \infty} = T_\infty$$

Simultaneous solution of differential Equations (3.11) and (3.12) with the boundary conditions given above yields the temperature distribution in the substrate and

the droplet. By taking the derivative of the temperature at the interface between the droplet and the substrate the heat flux through a droplet can be calculated. Analytical solution of the differential equation system above is quite complicated by the known methods therefore the second differential equation that gives the temperature distribution in the droplet will be eliminated by assuming circular heat flux lines at the edge of the droplet. In view of the fact that majority of the heat transfer in dropwise condensation takes place at the edge of the droplet the heat flux lines are close to circular paths there. A surface heat flux distribution under the droplet will be assumed by taking the interfacial resistance and conduction resistance proportional to the arc length in the droplet into account. With such an assumption one of the differential equations i.e. the differential equation that gives the temperature distribution in the droplet will be eliminated. Accordingly, the formulation of the problem will be reduced into the following form.

$$\frac{\partial^2 T_s}{\partial r^2} + \frac{1}{r} \frac{\partial T_s}{\partial r} + \frac{\partial^2 T_s}{\partial z^2} = 0 \quad (3.13)$$

Boundary conditions:

$$\begin{aligned} -k \frac{\partial T_s}{\partial z} \Big|_{z=0} &= h (T_v - T_s(r, 0)) \quad r \leq R \\ -k \frac{\partial T_s}{\partial z} \Big|_{z=0} &= 0 \quad r > R \\ T_s &= T_\infty \quad \text{as } z \rightarrow \infty \end{aligned} \quad (3.14)$$

$$T_s = T_\infty \quad \text{as } r \rightarrow \infty \quad (3.15)$$

$$\frac{\partial T_s}{\partial r} \Big|_{r=0} = 0$$

Overall heat transfer coefficient h on the surface is defined as,

$$\frac{1}{h} = \frac{1}{h_i} + \frac{\ell}{k_v}$$

where, ℓ is the arc length of the heat flux line in the droplet.

Defining $\theta = T_s - T_\infty$

$$\frac{\partial^2 \theta}{\partial r^2} + \frac{1}{r} \frac{\partial \theta}{\partial r} + \frac{\partial^2 \theta}{\partial z^2} = 0 \quad (3.16)$$

Boundary conditions:

$$-k \frac{\partial \theta}{\partial z} = h(\theta_v - \theta(r, 0)) \quad r < R \quad (3.17)$$

$$-k \frac{\partial \theta}{\partial z} \Big|_{z=0} = 0 \quad r > R$$

$$\theta = 0 \quad \text{as } z \rightarrow \infty \quad (3.18)$$

$$\theta = 0 \quad \text{as } r \rightarrow \infty \quad (3.19)$$

$$\frac{\partial \theta}{\partial r} \Big|_{r=0} = 0 \quad (3.20)$$

In order to nondimensionalize the governing equation and the boundary conditions, to obtain the solutions in the nondimensional terms, the following definitions are introduced:

$$T^* = \frac{T_s - T_\infty}{T_v - T_\infty}, \quad h^* = \frac{h}{h_i}, \quad r^* = \frac{r}{R}$$

$$k^* = \frac{k}{h_i \cdot R}, \quad q^{**} = \frac{q''}{h_i(T_v - T_\infty)}, \quad z^* = \frac{z}{R}$$

where, q'' is the heat flux at the interface between the droplet and substrate. Then, the governing equation and boundary conditions become:

$$\frac{\partial^2 T^*}{\partial r^{*2}} + \frac{1}{r^*} \frac{\partial T^*}{\partial r^*} + \frac{\partial^2 T^*}{\partial z^{*2}} = 0 \quad (3.21)$$

$$-k^* \frac{\partial T^*}{\partial z^*} \Big|_{z^*=0} = h^*(1 - T^*(r^*, 0)) \quad \text{for } r^* < 1 \quad (3.22)$$

$$-k^* \frac{\partial T^*}{\partial z^*} \Big|_{z^*=0} = 0 \quad \text{for } r^* > 1$$

$$T^* = 0 \quad \text{as } z^* \rightarrow \infty \quad (3.23)$$

$$T^* = 0 \quad \text{as } r^* \rightarrow \infty \quad (3.24)$$

$$\frac{\partial T^*}{\partial r^*} \Big|_{r^*=0} = 0 \quad (3.25)$$

Hankel transform will be applied to solve Eqn. (3.21) together with the boundary conditions (3.22) and (3.23).

Hankel transform is defined by,

$$f(\alpha) = \int_0^\infty f(r) r J_0(\alpha r) dr \quad \text{for } \alpha > 0 \quad (3.26)$$

By operational property of Hankel transform,

$$H \left\{ \frac{\partial^2 T^*}{\partial r^{*2}} + \frac{1}{r^*} \frac{\partial T^*}{\partial r^*} \right\} = -\alpha^2 t(\alpha) \quad \text{for } 0 < r < \infty \quad (3.27)$$

where, $t(\alpha)$ is the Hankel transform of T^* . Taking the Hankel transform of Eqn. (3.21),

$$-\alpha^2 t(\alpha, z^*) + \frac{d^2}{dz^{*2}} t(\alpha, z^*) = 0 \quad (3.28)$$

The ordinary differential equations, Eqn. (3.18) can be solved to get,

$$t(\alpha, z^*) = c_1 e^{\alpha z^*} + c_2 e^{-\alpha z^*}$$

where, $c_1 = 0$ to have a finite solution as $z^* \rightarrow \infty$. Then, transformed temperature becomes,

$$t(\alpha, z^*) = c_2 e^{-\alpha z^*} \quad (3.29)$$

In general, c_2 is a function of α ,

$$t(\alpha, z^*) = c_2(\alpha) e^{-\alpha z^*} \quad (3.30)$$

In order to determine $c_2(\alpha)$, the Hankel transform of Eqn. (3.22) will be taken

$$H \left\{ -k^* \frac{\partial T^*}{\partial z^*} \Big|_{z^*=0} \right\} = H \{ h^* (1 - T^*(r^*, 0)) \} = H(q^{*''}(r^*)) = q^{*''}(\alpha) \quad (3.31)$$

$$-k^* \frac{d}{dz^*} t(\alpha, z^*) \Big|_{z^*=0} = q^{*''}(\alpha)$$

Substituting $t(\alpha, z^*)$ from Eqn. (3.30)

$$-k^* \frac{d}{dz^*} [c_2(\alpha) e^{-\alpha z^*}] \Big|_{z^*=0} = q^{*''}(\alpha)$$

$$+k^* \alpha c_2(\alpha) e^{-\alpha z^*} \Big|_{z^*=0} = q^{*''}(\alpha)$$

$$+k^* \alpha c_2(\alpha) = q^{*''}(\alpha)$$

$$c_2(\alpha) = \frac{q^{*''}(\alpha)}{k^* \cdot \alpha}$$

Substituting in Eqn. (3.30):

$$t(\alpha, z^*) = \frac{q^{*''}(\alpha)}{k^* \alpha} e^{-\alpha z^*} \quad (3.32)$$

By taking the inverse Hankel transformation the solution of problem can be found as:

$$T^*(r^*, z^*) = H^{-1} \{ t(\alpha, z^*) \}$$

$$T^*(r^*, z^*) = \int_0^\infty t(\alpha, z^*) \alpha J_0(\alpha r^*) d\alpha \quad (3.33)$$

Substituting Eqn. (3.32) for $t(\alpha, z^*)$ in Eqn. (3.33),

$$T^*(r^*, z^*) = \frac{1}{K^*} \int_0^\infty q^{*''}(\alpha) e^{-\alpha z^*} J_0(\alpha r^*) d\alpha \quad (3.34)$$

where, $q^{*''}(\alpha)$ is given by Eqn. (3.31) as,

$$q^{*''}(\alpha) = H\{h^*(r^*)(1 - T^*(r^*, 0))\} = \int_0^\infty h^*(r^*)(1 - T^*(r^*, 0)) r^* J_0(\alpha r^*) dr^*$$

Since $h^*(r^*) = 0$ for $r^* > 1$,

$$q^{*''}(\alpha) = \int_0^1 h^*(r^*)(1 - T^*(r^*, 0)) r^* J_0(\alpha r^*) dr^* \quad (3.35)$$

This problem can be solved iteratively by the following steps.

1. Assume an initial temperature distribution $T(r^*, 0)$.
2. Evaluate $q^{*''}(\alpha)$ from Eqn. (3.35).
3. Re-evaluate $T^*(r^*, 0)$ from Eqn. (3.34) by,

$$T^*(r^*, 0) = \frac{1}{k^*} \int_0^\infty q^{*''}(\alpha) J_0(\alpha r^*) d\alpha.$$

4. If the distribution of temperature at $z^* = 0$ is not sufficiently close to the distribution used in step 2, repeat the calculation starting from step 2 again.
5. Once $T^*(r^*, 0)$ is obtained. The temperature distribution can be evaluated as follows:

$$T^*(r^*, z^*) = \frac{1}{k^*} \int_0^\infty q^{*''}(\alpha) e^{-\alpha z^*} J_0(\alpha r^*) d\alpha$$

A Special Case: Constant Heat Flux $r \leq 1$:

If there is constant heat flux on the surface, solution obtained directly as shown below.

Eqn. (3.35) becomes,

$$\begin{aligned} q^{*''}(\alpha) &= \int_0^1 q^{*''} r^* J_0(\alpha r^*) dr^* \\ q^{*''}(\alpha) &= q^{*''} \int_0^1 r^* J_0(\alpha r^*) dr^* \\ q^{*''}(\alpha) &= \frac{q^{*''}}{\alpha} \int_0^1 (\alpha r^*) J_0(\alpha r^*) dr^* \\ q^{*''}(\alpha) &= \frac{q^{*''}}{\alpha} [r^* J_1(\alpha r^*)]_0^1 = \frac{q^{*''}}{\alpha} [J_1(\alpha) - 0] \\ q^{*''}(\alpha) &= \frac{q^{*''}}{\alpha} J_1(\alpha) \end{aligned}$$

Substituting in Eqn. (3.34),

$$T^*(r^*, z^*) = \frac{q^{*''}}{k^*} \int_0^\infty \frac{1}{\alpha} J_1(\alpha) e^{-\alpha z^*} J_0(\alpha r^*) d\alpha$$

or $z^* = 0$,

$$T^*(r^*, z^*) = \frac{q^{*''}}{k^*} \int_0^\infty \frac{1}{\alpha} J_1(\alpha) \cdot J_0(\alpha r^*) d\alpha$$

3.4 Temperature Distribution in the Substrate Under Two Neighboring Droplets

In the previous section the temperature distribution under an isolated droplet is formulated. Solution of these equations gives the primary substrate effect when it is integrated over the entire drop population. Nevertheless in dropwise condensation as it is explained before there is a secondary substrate effect as a result of the change of the substrate temperature distribution due to the neighboring droplets on the surface of condensation. In a typical droplet size distribution these droplets range from minimum (critical) size to the maximum (departure) size which complicates the calculation of the substrate effect. Also the distance between the droplets varies from zero clearance to (if droplet sizes are used as reference for comparison) very large distances. So, the problem is reduced to finding the effect of a neighboring droplet of radius, let's say, r_n on the temperature distribution in the substrate material under a given droplet of radius, let's say, r as a function of the distance between the center of the droplets, x .

The geometry of the problem is described in the Fig. 3.3.

There are several approaches to solve such a problem with the geometry described in the Fig. 3.3. to be known by the author, can be described briefly as follows:

1. The temperature distribution obtained by the combination of the two droplets can be obtained by superimposing the individual solutions obtained for each droplet by the equations of the previous section. It is obvious that the resulting solution will not be symmetrical around any axis as the solutions of the individual droplets.
2. Another approach might be solving the general differential equation under the influence of the boundary conditions resulting from heat flux of each droplet on

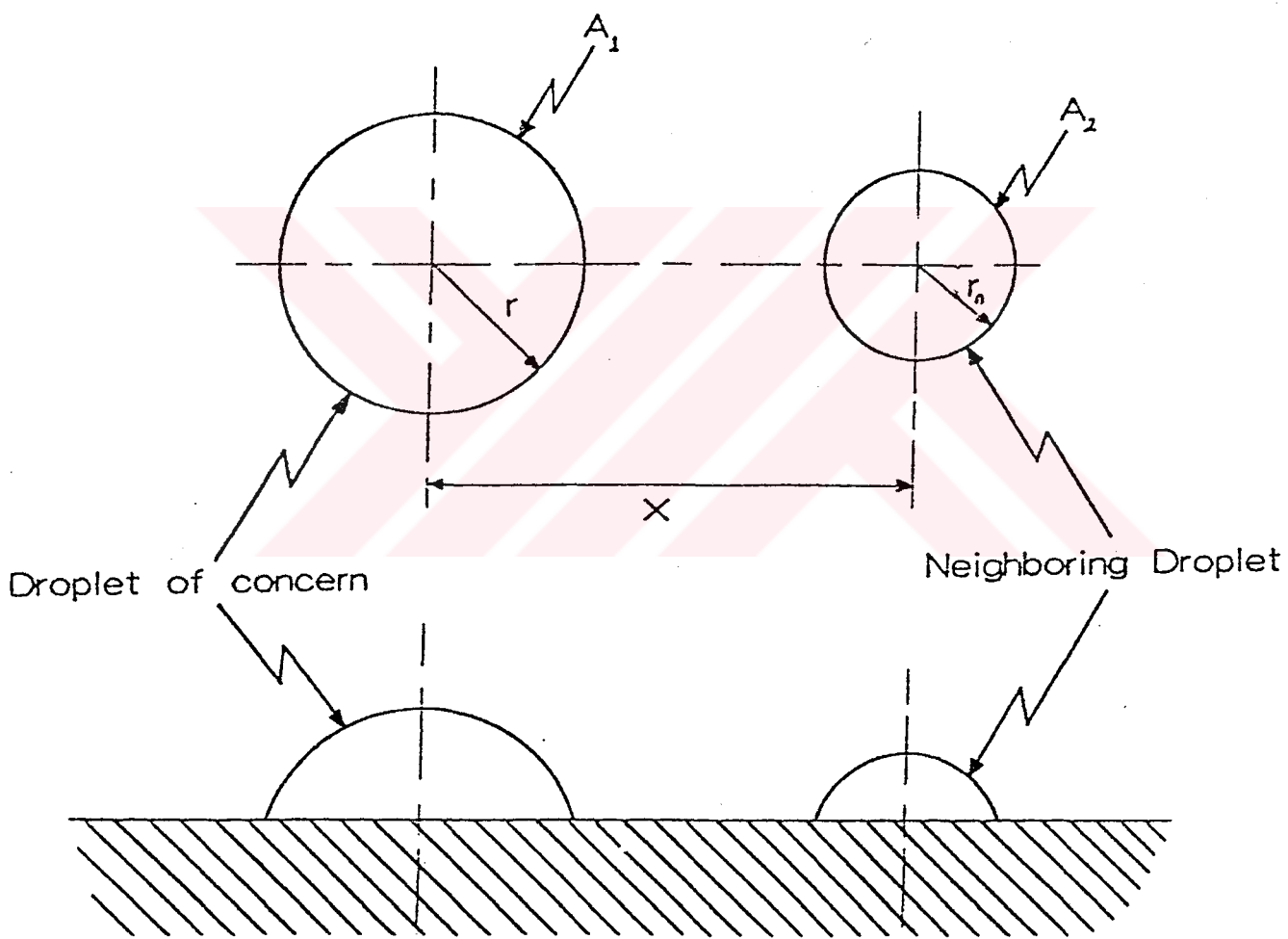


Figure 3.3. Two neighboring droplets resting on a semi-infinite solid surface

the surface of condensation. Such a solution, although not impossible, will be quite complicated since an additional diffusion term in the governing equation (conduction in the substrate) will appear due to the nonsymmetry around any axis.

3. A third approach might be solving the temperature distribution under the droplet of concern not only by the influence of a neighboring droplet at a distance of x , but also under the influence of all the droplets that might possibly occur at a distance x from the center of the droplet of concern with a given diameter of r_n . Then the effect of single droplet may be calculated by the area ratio which will be described later.

Among the three possibilities that are described above, the first method (superposition) will be employed here because of its simplicity. In the light of the Fig. 3.3, the problem can be formulated as follows:

Governing differential equation

$$\frac{\partial^2 T^*}{\partial r^{*2}} + \frac{1}{r^*} \frac{\partial T^*}{\partial r^*} + \frac{\partial^2 T^*}{\partial z^{*2}} + \frac{1}{r^{*2}} \frac{\partial^2 T^*}{\partial \phi^2} = 0 \quad (3.36)$$

Boundary conditions

$$T^*(\phi) = T^*(\phi + 2\pi) \quad (3.37)$$

$$\frac{\partial T^*}{\partial \phi}(\phi) = \frac{\partial T^*}{\partial \phi}(\phi + 2\pi) \quad (3.38)$$

$$T^* \rightarrow 0 \quad \text{as} \quad r^* \rightarrow \infty \quad (3.39)$$

$$\left. \frac{\partial T^*}{\partial r^*} \right|_{r^*=0} = 0 \quad (3.40)$$

$$T^* \rightarrow 0 \quad \text{as} \quad z \rightarrow \infty \quad (3.41)$$

$$-k^* \left(\frac{\partial T^*}{\partial z^*} \right) \Big|_{z^*=0} = 0 \quad (\text{Over the surface area not occupied by the droplets}) \quad (3.42)$$

$$-k^* \left(\frac{\partial T^*}{\partial z^*} \right) \Big|_{z^*=0} = h_1^*(1 - T^*(r^*, 0)) \quad (\text{Over the surface occupied by the droplet of concern}) \quad (3.43)$$

h_1^* is the nondimensional overall heat transfer coefficient for the droplet of concern and depends on the radial distance from the center of the droplet.

$$-k^* \left(\frac{\partial T^*}{\partial z^*} \right) \Big|_{z^*=0} = h_2^*(1 - T^*(r^*, 0)) \quad (3.44)$$

h_2^* is the nondimensional heat transfer coefficient for the neighboring droplet and depends on the radial distance from the center of the droplet.

It should be kept in mind that governing differential equation has an angular coordinate term and problem is not axially symmetrical unlike the problem of an isolated single droplet.

Now to facilitate the solution of the problem formulated above the following conduction problems are devised, the superposition of which gives the conduction problem given above.

Conduction Problem I:

Governing equation

$$\frac{\partial^2 T_1^*}{\partial r^{*2}} + \frac{1}{r^*} \frac{\partial T_1^*}{\partial r^*} + \frac{\partial^2 T_1^*}{\partial z^{*2}} + \frac{1}{r^{*2}} \frac{\partial^2 T_1^*}{\partial \phi^2} = 0 \quad (3.45)$$

Boundary condition

$$T_1^*(\phi) = T_1^*(\phi + 2\pi) \quad (3.46)$$

$$\frac{\partial T_1^*}{\partial \phi}(\phi) = \frac{\partial T_1^*}{\partial \phi}(\phi + 2\pi) \quad (3.47)$$

$$T_1^* \rightarrow 0 \quad \text{as} \quad r^* \rightarrow \infty \quad (3.48)$$

$$\left. \frac{\partial T_1^*}{\partial r^*} \right|_{r^*=0} = 0 \quad (3.49)$$

$$T_1^* \rightarrow 0 \quad \text{as} \quad z^* \rightarrow \infty \quad (3.50)$$

$$-k^* \left(\frac{\partial T_1^*}{\partial z^*} \right) \Big|_{z^*=0} = 0 \quad (\text{Over the surface area not occupied by the droplet}) \quad (3.51)$$

$$-k^* \left(\frac{\partial T_1^*}{\partial z^*} \right) \Big|_{z^*=0} = h_1^*(1 - T_1^*(r^*, 0)) \quad (\text{Over the surface occupied by the droplet of concern}) \quad (3.52)$$

$$-k^* \left(\frac{\partial T_1^*}{\partial z^*} \right) \Big|_{z^*=0} = h_2^*(0 - T_1^*(r^*, 0)) \quad (\text{Over the surface occupied by the neighboring droplet}) \quad (3.53)$$

Conduction Problem II:

Governing equation

$$\frac{\partial^2 T_2^*}{\partial r^{*2}} + \frac{1}{r^*} \frac{\partial T_2^*}{\partial r^*} + \frac{\partial^2 T_2^*}{\partial z^{*2}} + \frac{1}{r^{*2}} \frac{\partial^2 T_2^*}{\partial \phi^2} = 0 \quad (3.54)$$

Boundary condition

$$T_2^*(\phi) = T_2^*(\phi + 2\pi) \quad (3.55)$$

$$\frac{\partial T_2^*}{\partial \phi}(\phi) = \frac{\partial T_2^*}{\partial \phi}(\phi + 2\pi) \quad (3.56)$$

$$T_2^* \rightarrow 0 \quad \text{as} \quad r^* \rightarrow \infty \quad (3.57)$$

$$\left. \frac{\partial T_2^*}{\partial r^*} \right|_{r^*=0} = 0 \quad (3.58)$$

$$T_2^* \rightarrow 0 \quad \text{as} \quad z \rightarrow \infty \quad (3.59)$$

$$-k^* \left(\frac{\partial T_2^*}{\partial z^*} \right) \Big|_{z^*=0} = 0 \quad (\text{Over the surface area not occupied by the droplet}) \quad (3.60)$$

$$-k^* \left(\frac{\partial T_2^*}{\partial z^*} \right) \Big|_{z^*=0} = h_2^*(0 - T_2^*(r^*, 0)) \quad (\text{Over the surface occupied by the droplet of concern}) \quad (3.61)$$

$$-k^* \left(\frac{\partial T_2^*}{\partial z^*} \right) \Big|_{z^*=0} = h_2^*(1 - T_2^*(r^*, 0)) \quad (\text{Over the surface occupied by the neighboring droplet}) \quad (3.62)$$

If the temperature distribution in conduction problem I is T_1^* and the temperature distribution in conduction problem II is T_2^* then the temperature distribution of the original problem (droplet of concern and neighboring droplet resting on a semi-infinite substrate with a distance of x between their center of axis) becomes.

$$T^* = T_1^* + T_2^* \quad (3.63)$$

Summation of the boundary conditions and the governing equation of both conduction problems gives the boundary conditions and the governing equation of the original problem.

The aim of the superposition described above is to express a complicated conduction problem in terms of known simpler problems, solution of which is either known or can be obtained by known methods. Still the examination of the both conduction problems shows that the solutions are not so easy to obtain.

The first conduction problem describes temperature distribution in a semi-infinite solid surface, the contact area of the droplet of concern is convecting heat to the vapor at a nondimensional temperature of unity and the contact area of the neighboring droplet is convecting heat to the vapor at a nondimensional temperature of zero.

On the other hand, the second conduction problem describes conduction in a semi-infinite solid, the contact area of the droplet of concern is convecting heat to the vapor at a nondimensional temperature of zero whereas the contact area of the neighboring droplet is convecting heat to the vapor at a nondimensional temperature of unity.

Consequently, both conduction problem are axially nonsymmetric and is believed to have a complicated solution method. Still, a carefull examination shows a shortcut to the solution of the problems. At infinitely large distances from the surface of the solid, nondimensional temperature is zero. Because of the comperatively large thermal conductivity of the substrate it is expected that a large portion of the surface area has a temperature close to zero (except the regions very close to the droplet convecting heat to the vapor at a temperature of unity. Consequently, it is expected that heat exchange to the vapor at a temperature of zero will be quite small and therefore the surface area might be assumed, essentially, insulated. In the light of this assumption conduction problems I and II are reduced to isolated droplet problem of the previous section. That means the original conduction problem of two neighboring droplets on a semi-infinite surface can be approximately solved by superimposing the solutions of two isolated droplet on a semi-infinite surface.

3.5 Total Substrate Effect in Dropwise Condensation

As it is explained, substrate effect arises from two sources:

1. Effect of the drop itself on the temperature distribution in the solid substrate under the droplet (primary substrate effect).
2. Effect of the neighboring droplets on the temperature distribution in the solid substrate under the droplet (secondary substrate effect).

In the previous sections these effects are solved for isolated droplets. By solving the temperature distribution under an isolated droplet the primary substrate effect, by solving the temperature distribution under two neighboring droplet the secondary substrate effect for a single isolated droplets of concern is found. In dropwise condensation there are large number of droplet of varying sizes that occupies the surface of condensation. Unlike the previous section, in this section the total substrate effect resulting from the entire drop population will be derived.

The derivations will be based on three important drop total heat transfer terms which are defined as follows:

- i) Drop total heat transfer without any substrate effect, $q_0(r)$: It is the value of total heat transfer through a droplet assuming that the substrate temperature is uniform. q_0 is function of the drop radius only.
- ii) Drop total heat transfer under the influence of the primary substrate effect, $q_1(r)$: It is the value of total heat transfer through a droplet assuming that the droplet is isolated i.e. except the area covered by the droplet, condensation surface is completely insulated and heat is conducted to the semi-infinite substrate which has a finite thermal conductivity.
- iii) Drop total heat transfer under the influence of a neighboring droplet, $q_2(r, r_n, x)$: In this case heat transfer through the droplet is affected not only by the heat diffusion to the substrate but also by the additional heat transfer through the neighboring droplets. Total heat transfer, in this case, becomes a function of the distance between the droplets, the radius of the neighboring droplet as well as the radius of the droplet of concern.

Consequently, the primary substrate effect per unit droplet becomes

$$f_{01}(r) \equiv q_0(r) - q_1(r) \quad (3.64)$$

The secondary substrate effect per unit droplet then becomes

$$f_{12}(r, r_n, x) \equiv q_1(r) - q_2(r, r_n, x) \quad (3.65)$$

So, f_{01} and f_{12} gives the reduction of total heat transfer through a drop as a result of the primary and secondary substrate effects, respectively.

$q_0(r)$ can be approximately calculated by taking a uniform substrate temperature and taking circular arc shaped heat flux lines of length $\ell(r)$. If the interfacial heat transfer is h_i then

$$q_0(r) = \left[\int_{(DropBaseArea)} \left(\frac{\ell r}{k_d} + \frac{1}{h_i} \right) dA \right] (T_{vapor} - T_{surface}) \quad (3.66)$$

In the case of q_1 and q_2 , $T_{surface}$ is not constant but should be obtained from the solution of the temperature distribution in the substrate material. Once the substrate temperature distribution is found they can be obtained by an expression similar to Eqn. (4.1)

3.6 Total Primary Substrate Effect

f_{01} represents the decrease in total heat transfer through a droplet of a given size as a result of the primary substrate effect and is, therefore, a function of the size of the droplet.

Drop size distribution in dropwise condensation is given by

$$f_{c0} \left(\frac{r}{r_{max}} \right) = 1 - \left(\frac{r}{r_{max}} \right)^n \quad (3.67)$$

In the equation above f_{c0} represents the fraction of surface area covered by droplets in the size range r to r_{max} i.e.

$$f_{c0} \left(\frac{r}{r_{max}} \right) = \frac{A_{r \rightarrow r_{max}}}{A_{total}} \quad (3.68)$$

Consequently, the fraction of the area covered by the droplets of the size range of r to $r + dr$ becomes

$$df_{c0} = \frac{dA_{r \rightarrow r+dr}}{A_{total}} = \frac{n}{r_{max}} \left(\frac{r}{r_{max}} \right)^{n-1} dr \quad (3.69)$$

The number of droplets in the size range r to $r + dr$, then, becomes (per unit area)

$$\frac{dN}{A_{total}} = \frac{n}{r_{max}} \left(\frac{r}{r_{max}} \right)^{n-1} \frac{dr}{\pi r^2} \quad (3.70)$$

Total primary substrate effect can, now, be expressed as

$$Q_{01} = \int_{r_{\min}}^{r_{\max}} f_{01}(r) \frac{r}{r_{\max}} \left(\frac{r}{r_{\max}} \right)^{n-1} \frac{dr}{\pi r^2} \quad (3.71)$$

3.7 Total Secondary Substrate Effect

Calculation of the total secondary substrate effect is more involved since this effect depends not only on the size of the droplet of concern but also on the distance between the droplets and the size of the neighboring droplets.

In the Fig. 3.4. differential surface area at a distance of x from the droplet of concern is shown. Naturally the dropsize distribution given by Eq. (3.67) also applies here. The function $f_{12}(r, r_n, x)$ gives the reduction in total heat transfer rate through a droplet of size r as a result of a neighboring droplet of r_n at a distance of x . Since there are large number of droplets on the surface, each neighboring droplet will affect the temperature distribution under the droplet of concern and reduce the total heat transfer through it. As a basic assumption here, it will be assumed that the total reduction in heat transfer through the droplet of concern is equal to the summation of the reduction caused by individual neighboring droplets. So, the total reduction of heat transfer through a droplet of radius r as a result of secondary substrate effect can be expressed as

$$q_{II}(r) = \int_{(\text{Entire Drop Population})} f_{12} \times (\text{No of drop size in size range } r_n \text{ to } r_n + dr_n)$$

Coming back to Fig. 3.4, it can easily be seen that in the differential area $2\pi x dx$, the number of droplets in the size range r to $r + dr$ becomes

$$(2\pi \times dx) \left(\frac{n}{r_{\max}} \left(\frac{r_n}{r_{\max}} \right)^{n-1} \frac{dr_n}{\pi r_n^2} \right)$$

Consequently, the reduction in total heat transfer rate through a drop of a given size r as a result of the effect of all the droplets on the surface of condensation becomes

$$q_{II}(r) = \int_{r_n=r_{\max}}^{r_n=r_{\max}} \int_{x=x_{\min}}^{x \rightarrow \infty} f_{12}(r, r_n, x) \left(\frac{n}{r_{\max}} \left(\frac{r_n}{r_{\max}} \right)^{n-1} \frac{2x}{r_n^2} \right) dx dr_n \quad (3.72)$$

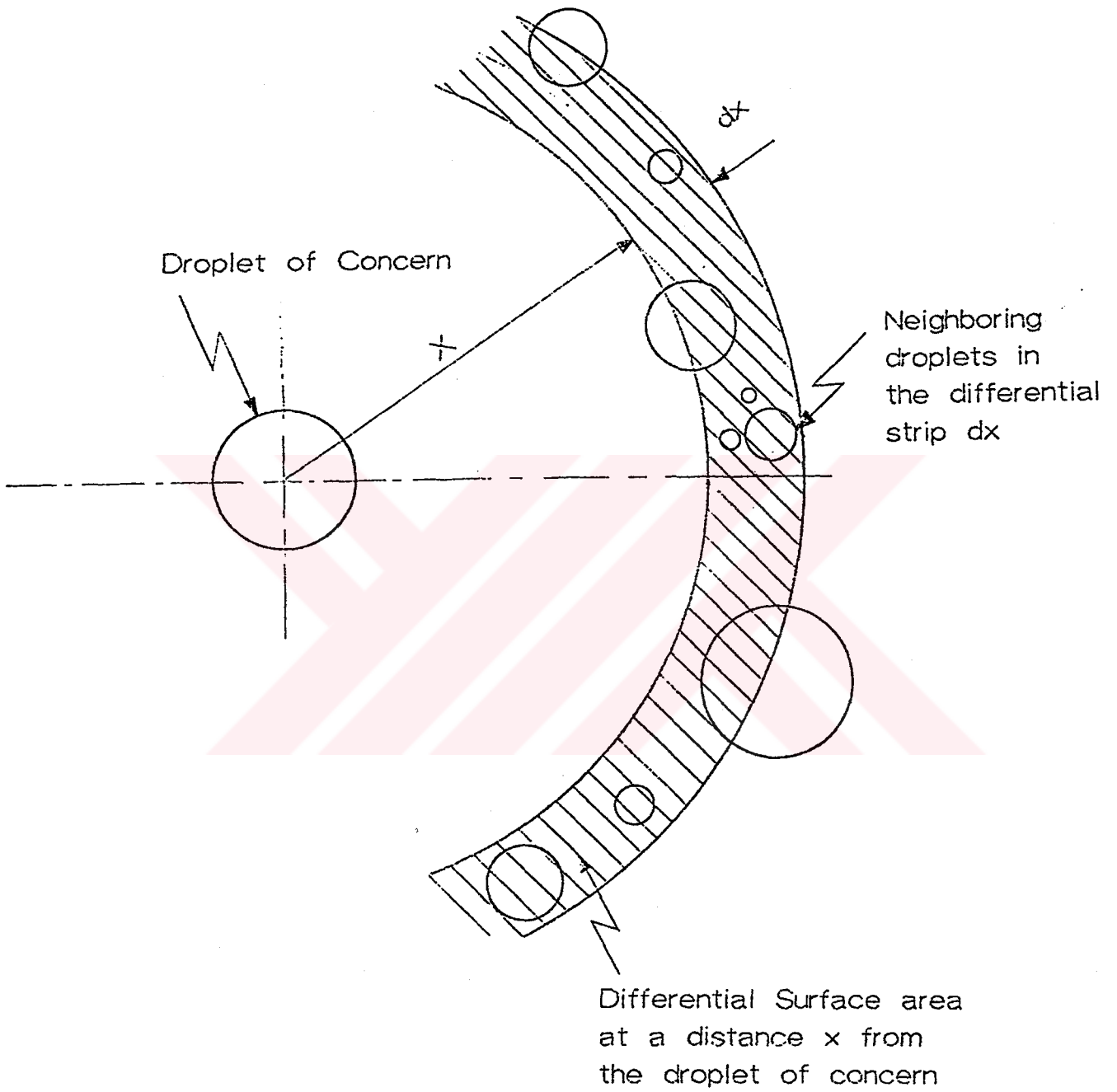


Figure 3.4. Differential area of influence at a distance of x from the droplet of concern

Once the reduction per drop is found (q_{II}) then the total secondary substrate effect can be expressed as:

$$Q_{12} = \int_{r=r_{\min}}^{r_{\max}} q_{II}(r) \left[\frac{n}{r_{\max}} \left(\frac{r}{r_{\max}} \right)^{n-1} \frac{dr}{\pi r^2} \right] \quad (3.73)$$

CHAPTER IV

RESULTS OF COMPUTATION AND DISCUSSION

4.1 Computation Results for the Temperature Distribution Under an Isolated Droplet

To obtain the temperature distribution under the droplet, a computer code is prepared. Computer code follows the following steps:

In the first step, the thermal conductivity of the substrate material and the radius of the droplet is chosen and entered as input data. In the second step, an initial temperature distribution is assumed. An accurate guess of the initial temperature distribution is essential for two reasons: First, a poor choice of the initial temperature distribution may lead to the divergence of the solution in the successive iterations. Secondly, starting value which are close to the true temperature distribution will accelerate the convergence of the iterations.

By using the Eqn. (3.35), the heat flux values are evaluated as a function of the Hankel transformation variable α . In the following step, Eqn. (3.34) is solved to obtain the temperature distribution and, the temperature distribution so obtained is compared to the temperature distribution of the previous iteration. If the difference in the numerical values of successive iteration falls below a specified value (convergence criteria) iteration process is stopped.

Axially symmetric temperature distribution in the substrate for an isolated droplet is shown in Figs. 4.1., 4.2., 4.3., 4.4.

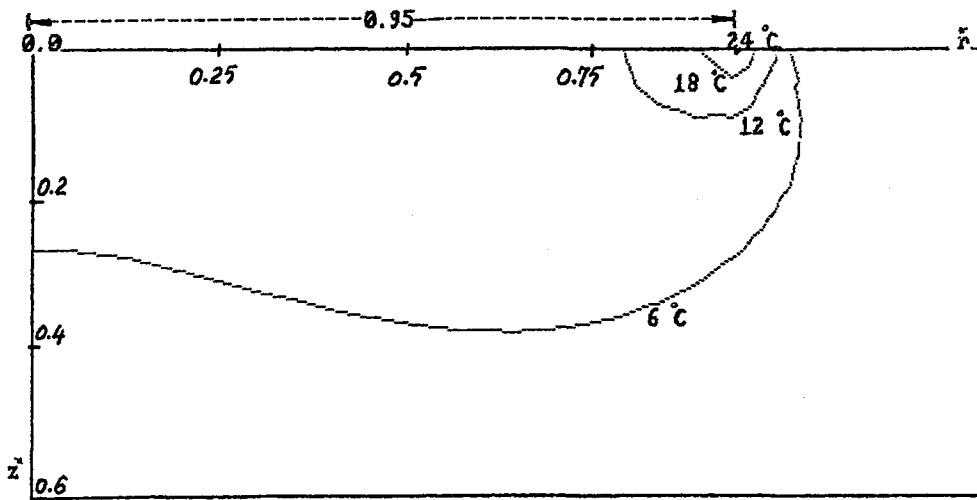


Figure 4.1. Isotherms under an isolated droplet of radius 2 mm.

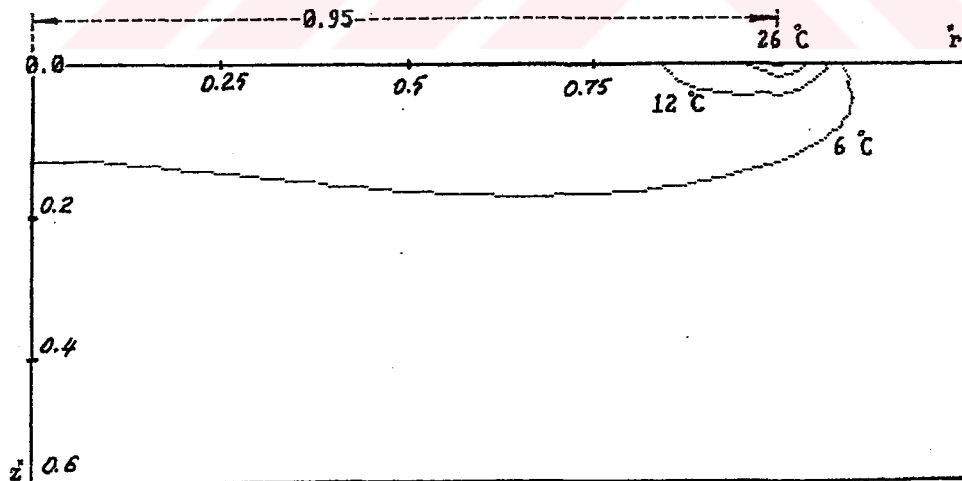


Figure 4.2. Isotherms under an isolated droplet of radius 1 mm.

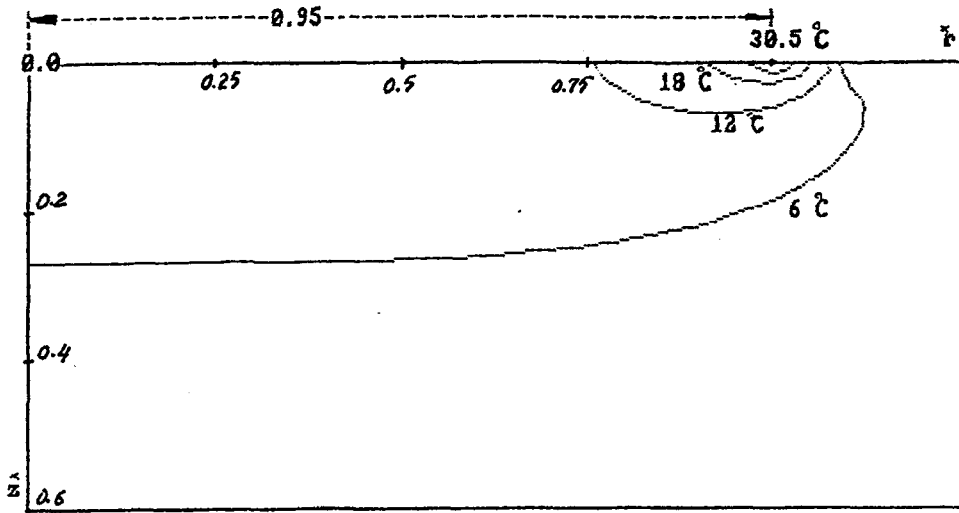


Figure 4.3. Isotherms under an isolated droplet of radius 1 mm.

In these figures isotherms are shown in a rectangular section of the substrate. Vertical axis (z) coincides with the centerline of the droplet and is therefore an axis of symmetry. Horizontal axis represents the radial distance from the center of the droplet. The droplet which rests on the surface is shown with dotted line. Its edge is marked on the surface.

Calculations are carried out for a stainless steel substrate with a thermal conductivity of ($14.038W/mK$). This substance is intentionally chosen since it is the most possible candidate if dropwise condensation is ever used in industrial heat exchanging devices. The result of the computations gives the nondimensional temperature distribution as a function of the nondimensional radial and axial distances. These nondimensional results are converted to dimensional result for a typical application of saturated water condensing on stainless steel substrate. Total temperature difference is taken as the largest difference possible for a typical condensation of water on a metal surface. That is the temperature of the saturated water is taken $100^{\circ}C$ and the temperature of the semi-infinite substrate is taken as $0^{\circ}C$ at infinitely large distances from the surface of condensation.

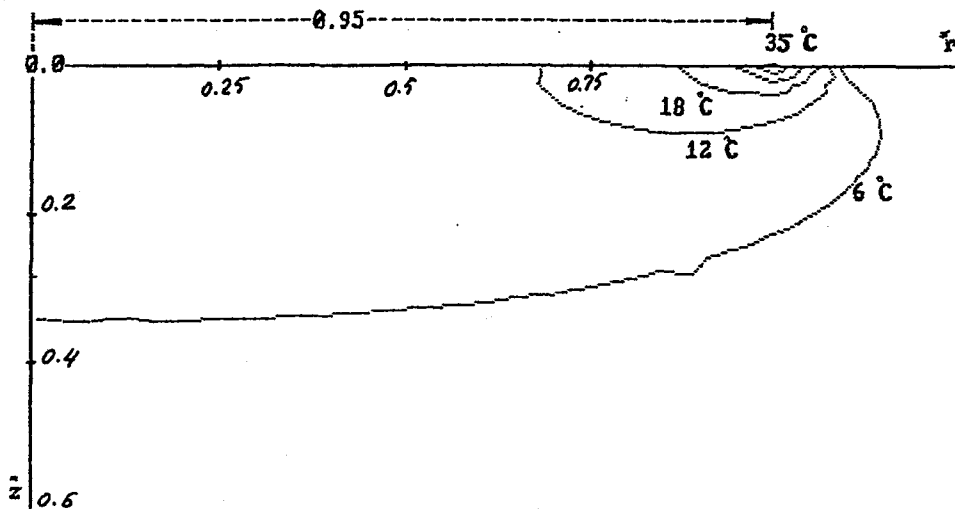


Figure 4.4. Isotherms under an isolated droplet of radius 0.01 mm.

The maximum drop size that should be taken in the calculations should obviously be the departure size of the droplets. Nevertheless, the departure size of the droplets in dropwise condensation depends on various factors like pressure and temperature of the surrounding as well as body forces and surface roughness. Measurements show that on metal surfaces, the departure radius of water droplet is slightly larger than $2mm$. Therefore, in this study the maximum drop radius is taken as $2mm$ for the calculations. The contact angle is taken as $65^{\circ}C$.

In calculations the drop radius is decreased in the order of magnitudewise. That is, the calculations are performed for $2mm$, $1mm$, $0.1mm$ and $0.01mm$ radius droplets. An interfacial heat transfer coefficient is taken on the surface of the droplet to make the model more realistic. Unlike in some of the previous work (2) the interfacial heat transfer is not taken as temperature dependent but rather constant, since an analytical solution is possible only in that special case.

There is an argument on the value of the condensation coefficient. In the past, investigators measured rather small coefficients in the order of 0.01 and also observed large deviations in its value. Recent works showed that the small value and large

deviations are most probably caused by noncondensable gases present in the vapor and, consequently, its value should be close to unity. In the light of these arguments, a condensation coefficient of unity is taken in this study.

The major characteristics of the figures that show the isotherms in the substrate material (Fig's 4.1 through 4.4) is that whatever the size of the droplet is, they are concentrated at the edge of the droplet which is a clear sign of very high heat transfer there. It is also observed that, those ends of the isotherms which are close to the edge of the droplet is perpendicular to the surface of condensation which is an expected result since the surface is insulated there. The other end of the isotherms reach the surface at points far from the edge of the droplet and they are almost (not exactly) perpendicular to the surface of condensation which is a clear indication that the large thermal resistance due to the large thickness of the droplet in regions close to the droplet center acts almost like an insulator and therefore central regions are essentially ineffective as far as the heat transfer is concern. Substrate temperature distribution and the isotherms also clearly show the direction of the heat flow lines. Another important observation in (Fig's 4.1 through 4.4) is that even for droplets of small sizes (0.01mm for instance) temperature on the surface of the droplet is quite small and essentially close to the temperature of the substrate at large distances from the surface. Except at very small volume around the edge of the droplet, substrate temperature can essentially be taken in the order of the temperature of the cooling medium. This result supports the assumption made in the previous chapter that if any part of the substrate surface is convecting heat to a medium at a zero nondimensional temperature, this heat transfer is quite small and surface can be assumed insulated, for all practical purposes.

Comparison of (Fig's 4.1 through 4.4) show that isotherms of larger drops are curved more and larger percentage of larger drops are inactive as far as heat transfer is concerned. This supports the general notion among the researchers of dropwise condensation that large droplets act as insulators as far as heat transfer in dropwise condensation is concerned.

One difficulty in the calculation of the isotherms in the substrate material under an isolated droplet is encountered during the evaluation of the integral terms in Eqn. (3.35). Because of the fast changes that occurs around the edge of the droplet smaller

increments should be taken as one gets closer to the edge of the droplet. Another calculational complication, right at the edge of the droplet arises because of the fact that there is a sharp change on the boundary condition there. Boundary condition changes from convection with interfacial heat transfer coefficient to insulated surface at that point. So, there is a mathematically singular point there. The effect of the above argued calculational difficulties are seen in Fig's 4.5., 4.6., 4.7., 4.8.



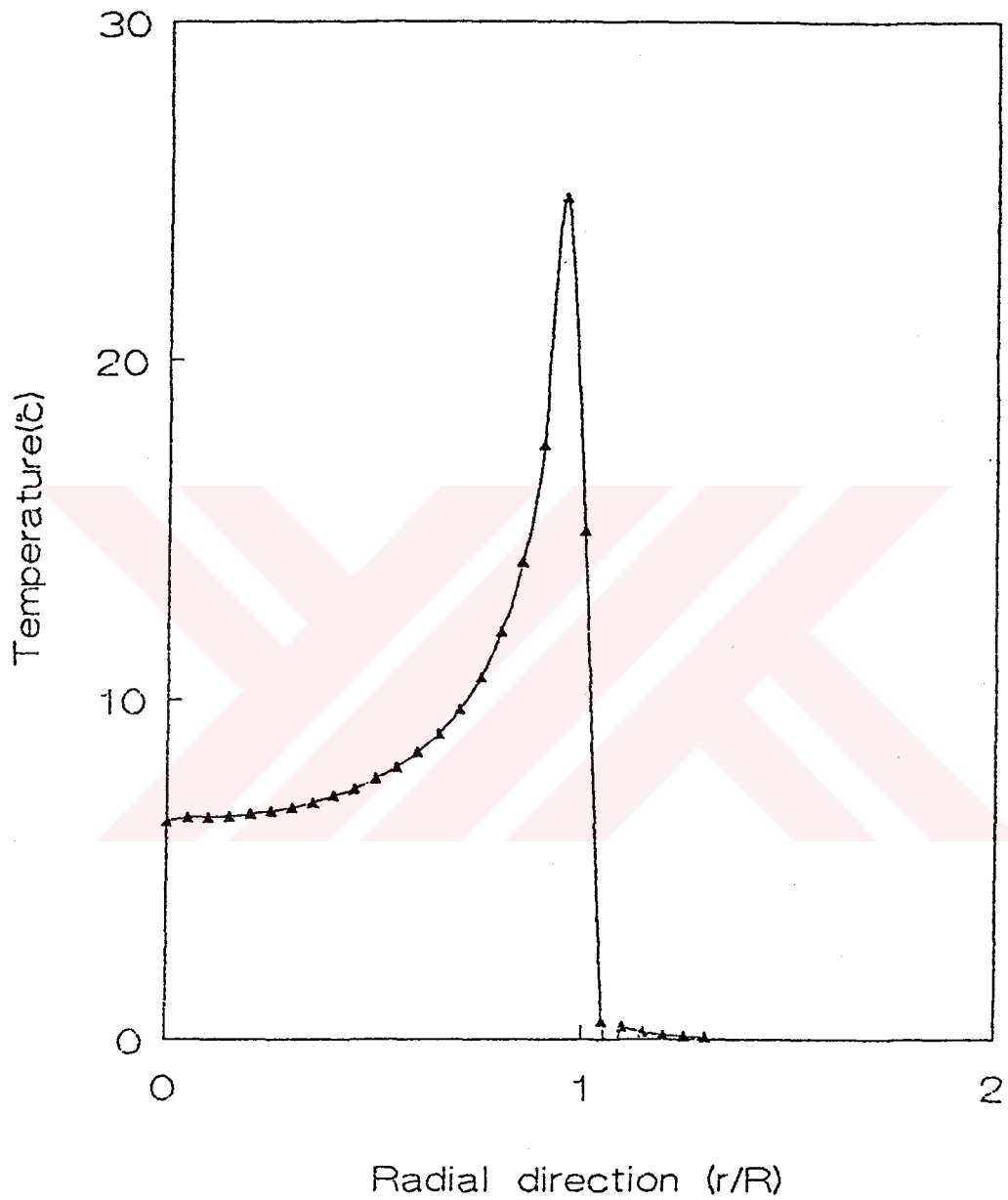


Figure 4.5. Variation of the stainless steel substrate surface temperature under an isolated droplet as a function of radial distance ($r = 2mm$).

As it can be seen in these figures the maximum temperature does not occur right at the edge ($r/R = 1$) of the droplet but rather at a point slightly toward the center of the droplet. By taking smaller divisions in numerical calculations the region in error can be made even narrower but it is not possible to eliminate it completely because of the points argued above. Fig's 4.5., through 4.8. show the variation of the surface temperature of the substrate as a function of the radial distance for droplets of various sizes. These figures also clearly show the sharp changes that occurs under any droplet. The sharp change on surface temperature indicates that there might be considerable thermal stresses on the surface of the substrate which might be the reason for the short operation life of gold plating in dropwise condensation.

An important observation in Fig's 4.5. through 4.8. is that right beyond the edge of the droplets substrate temperature drops almost to zero and is affected very little by the large temperature at the edge of the droplet.

Fig's 4.9., and 4.10. show the computational results of substrate temperature under an isolated droplet for nickel and copper substrates respectively.

The thermal conductivities of nickel and copper are taken ($60W/mK$) and ($401W/mK$) respectively. Fig. 4.5. also shows the variation of surface temperature for steel substrate. Consequently, Fig's 4.5., 4.9., 4.10. are drawn to see the effect of varying substrate thermal conductivities in surface temperature distribution. In all these figures total temperature difference is taken as $100^{\circ}C$. Even for such a large temperature difference the maximum surface temperature for copper substrate is smaller than $2^{\circ}C$.

Fig's 4.11., 4.12., 4.13., 4.14. show the variation of the local heat flux on the surface of the droplet as a function of the nondimensional radial distance (r/R) for drops of various sizes.

Substrate material is again stainless steel with thermal conductivity of ($14.038W/mK$). One can easily see in these figures how the heat flux drops rapidly in the central regions as the radius of the droplet increases. For droplets which has a radius of $0.01mm$ and smaller heat flux is not negligible in the central regions and should be considered in the calculations. For larger droplets heat flux in central regions

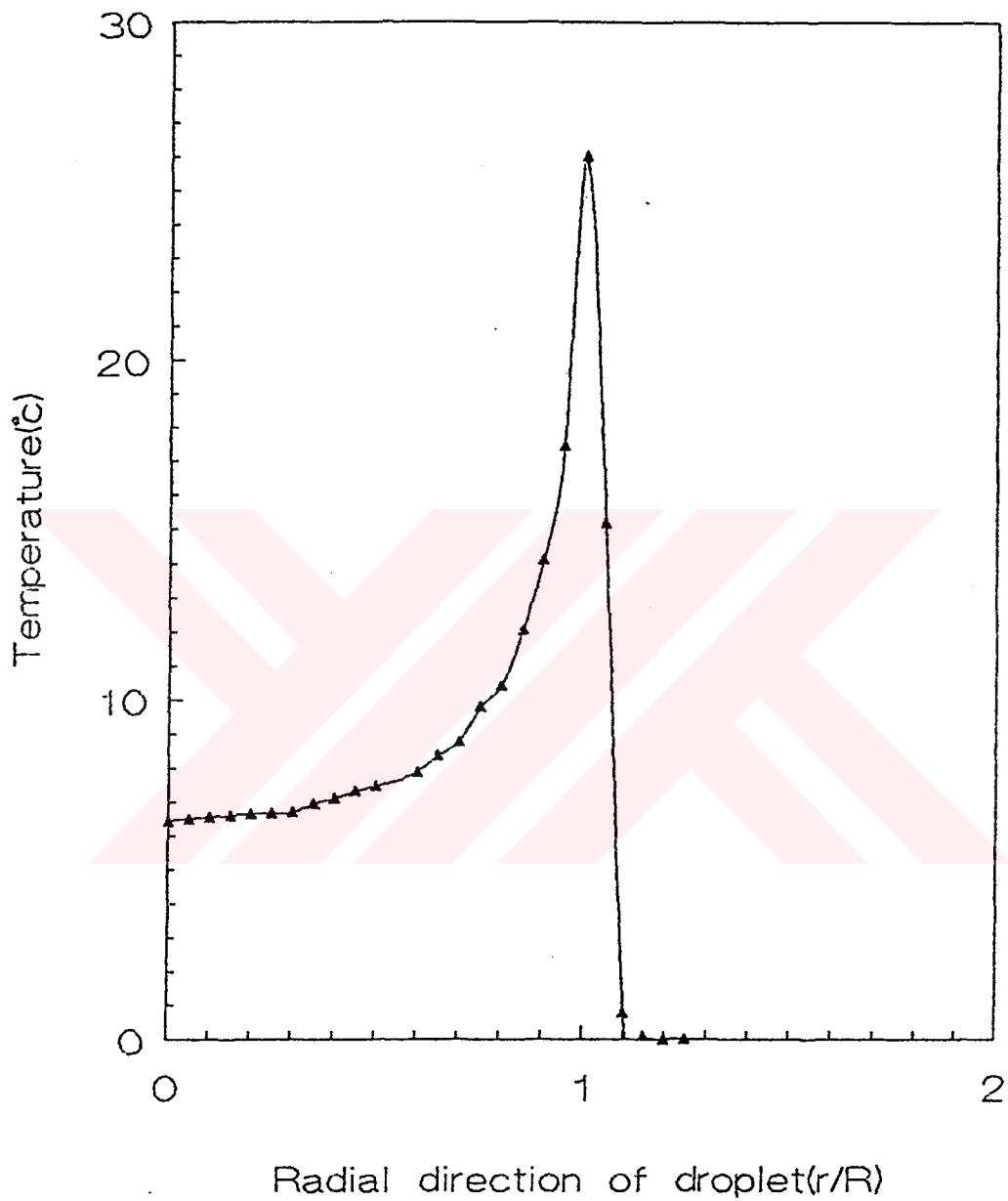


Figure 4.6. Variation of the stainless steel substrate surface temperature under an isolated droplet as a function of radial distance ($r = 1mm$).

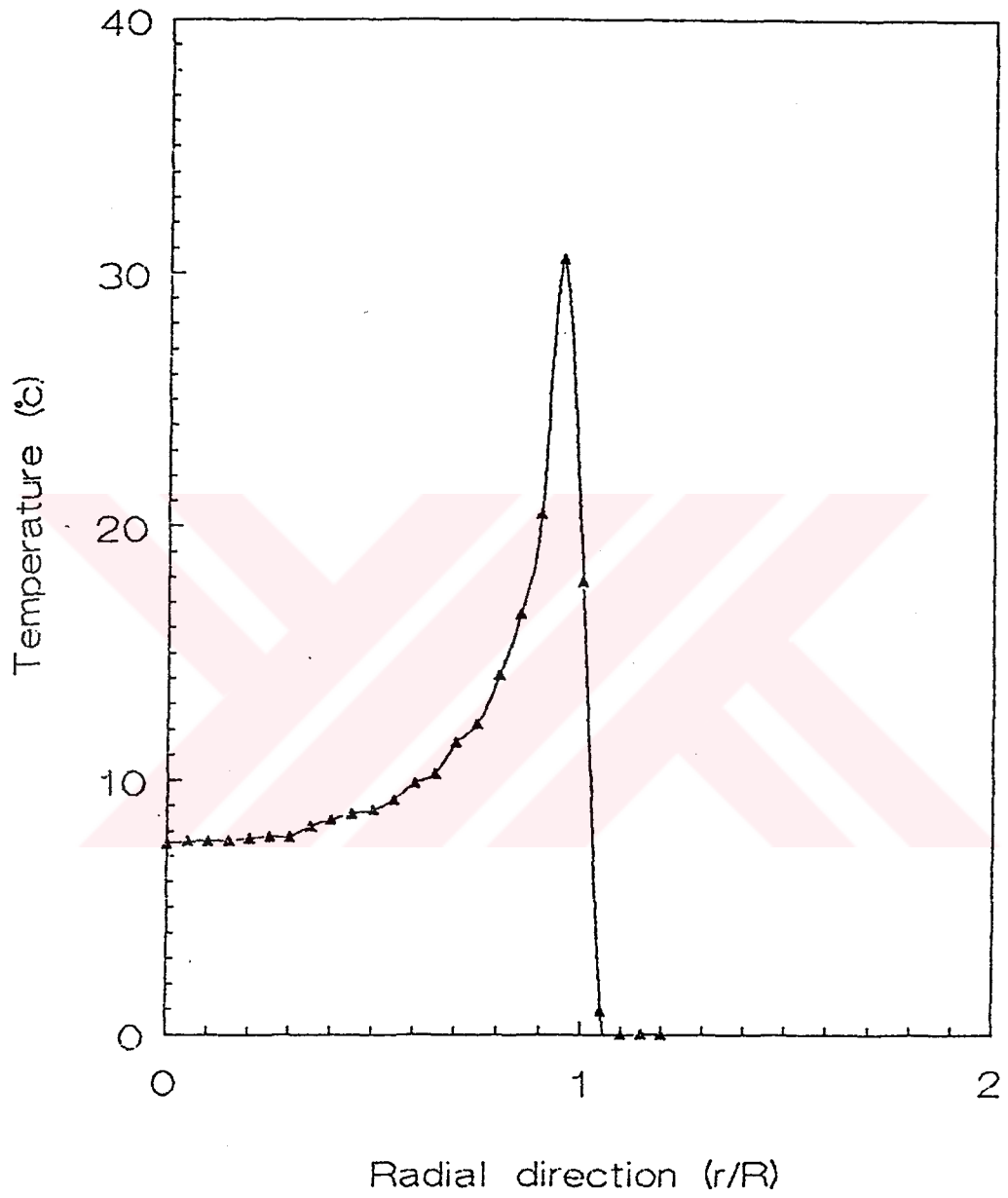


Figure 4.7. Variation of the stainless steel substrate surface temperature under an isolated droplet as a function of radial distance ($r = 0.1mm$).

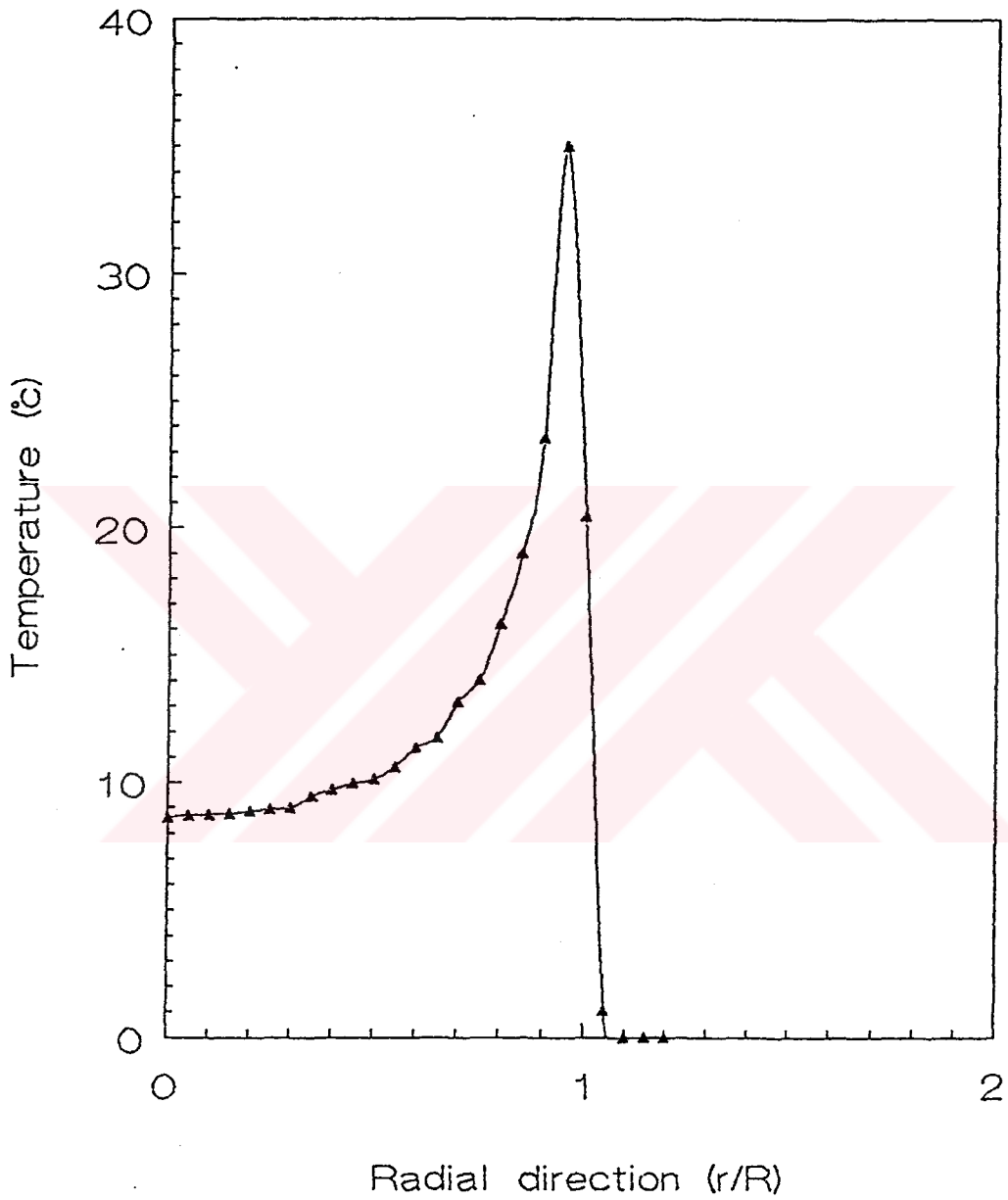


Figure 4.8. Variation of the stainless steel substrate surface temperature under an isolated droplet as a function of radial distance ($r = 0.01mm$).

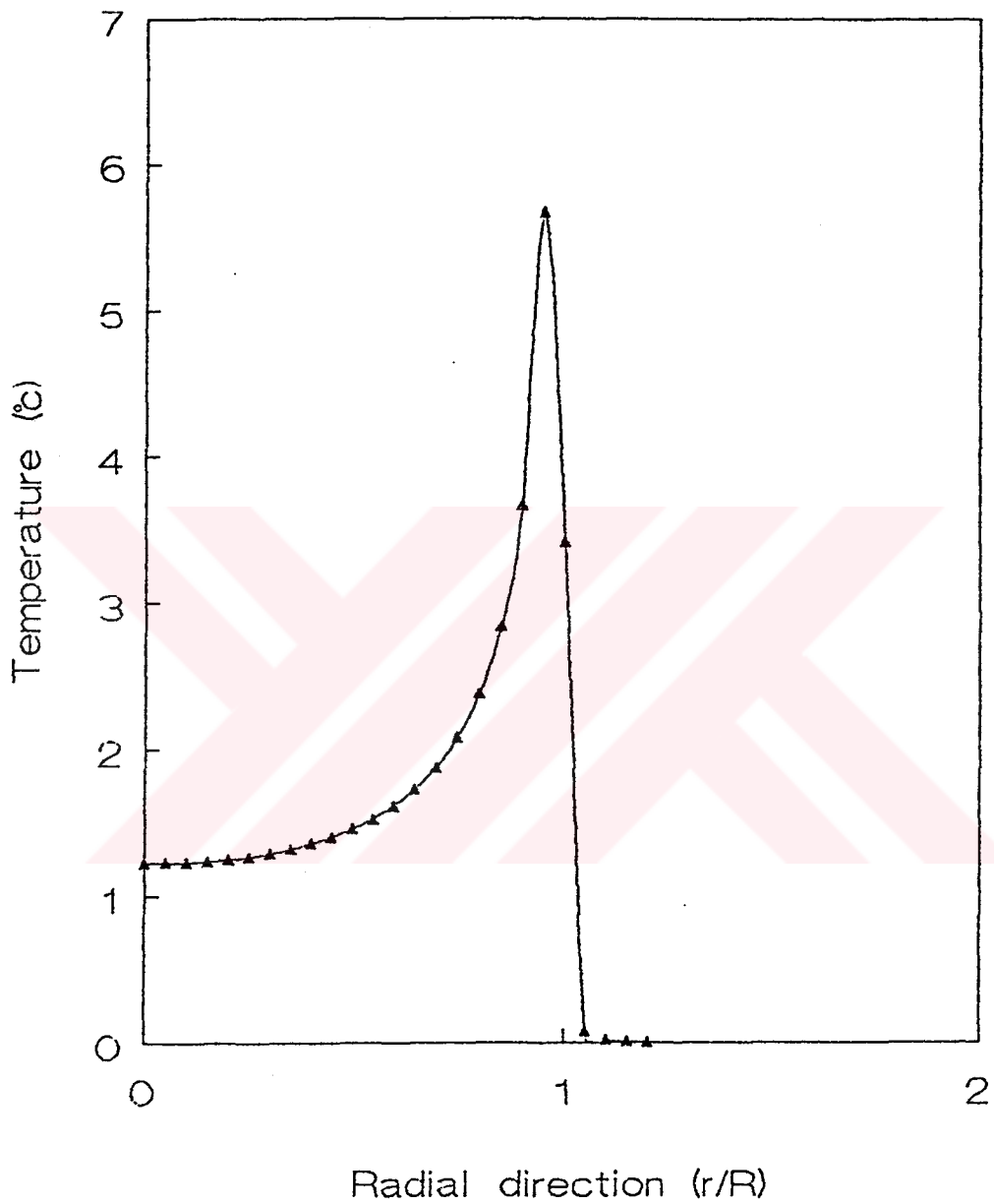


Figure 4.9. Variation of the nickel substrate surface temperature under an isolated droplet as a function of radial distance ($r = 2\text{mm}$).

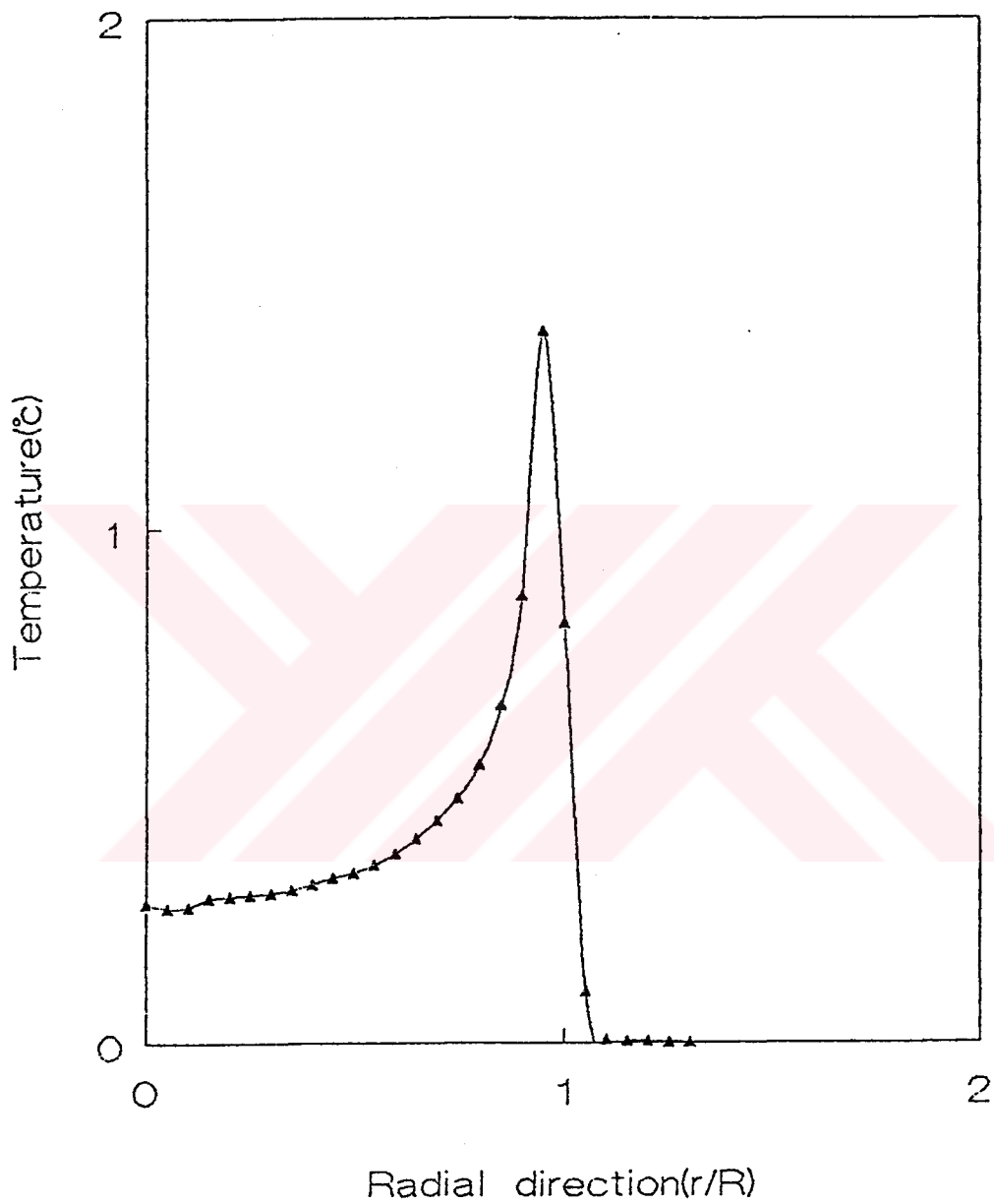


Figure 4.10. Variation of the copper substrate surface temperature under an isolated droplet as a function of radial distance ($r = 2mm$).

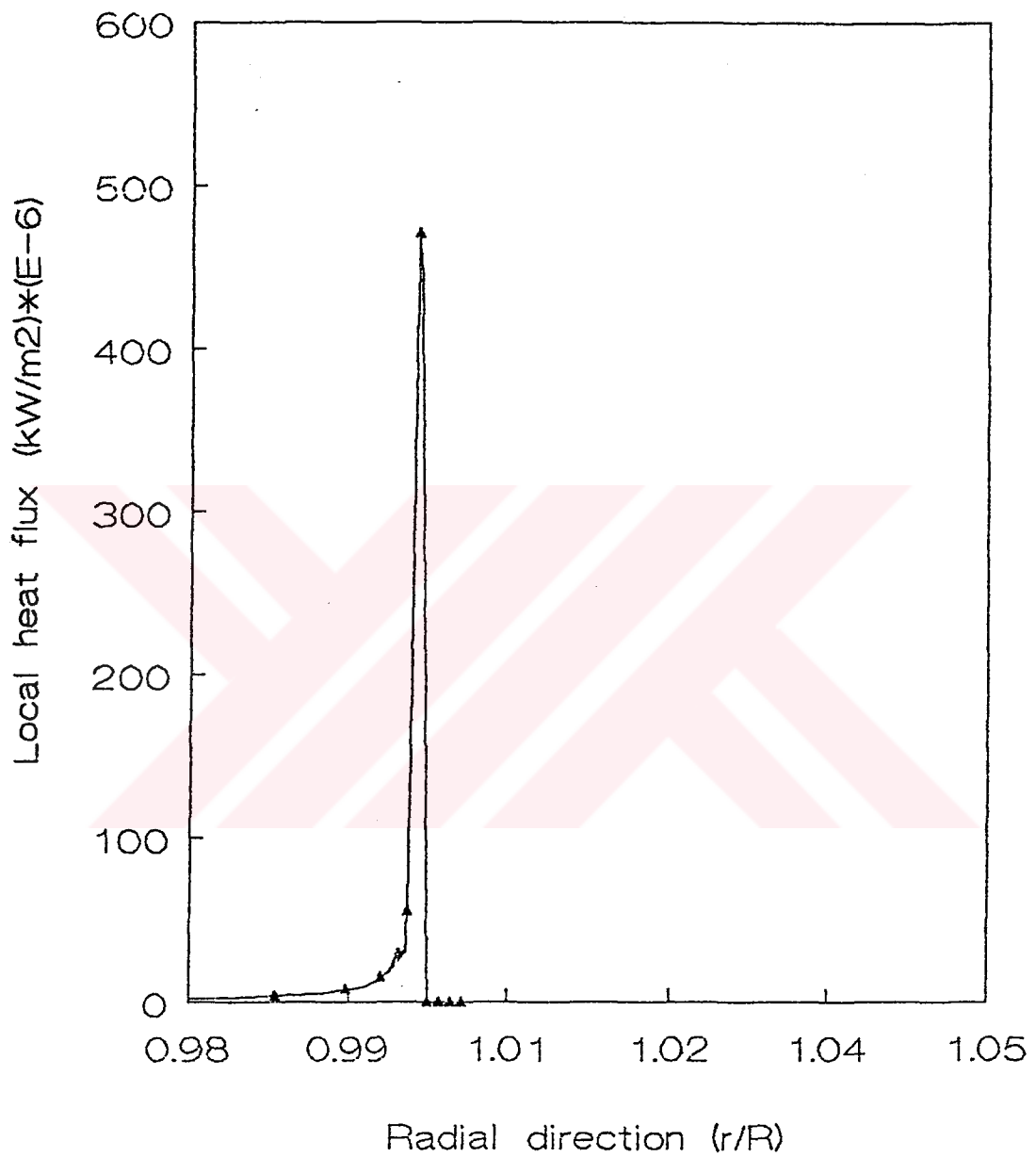


Figure 4.11. Surface local heat flux under an isolated droplet versus nondimensional radial distance ($r = 2mm$).

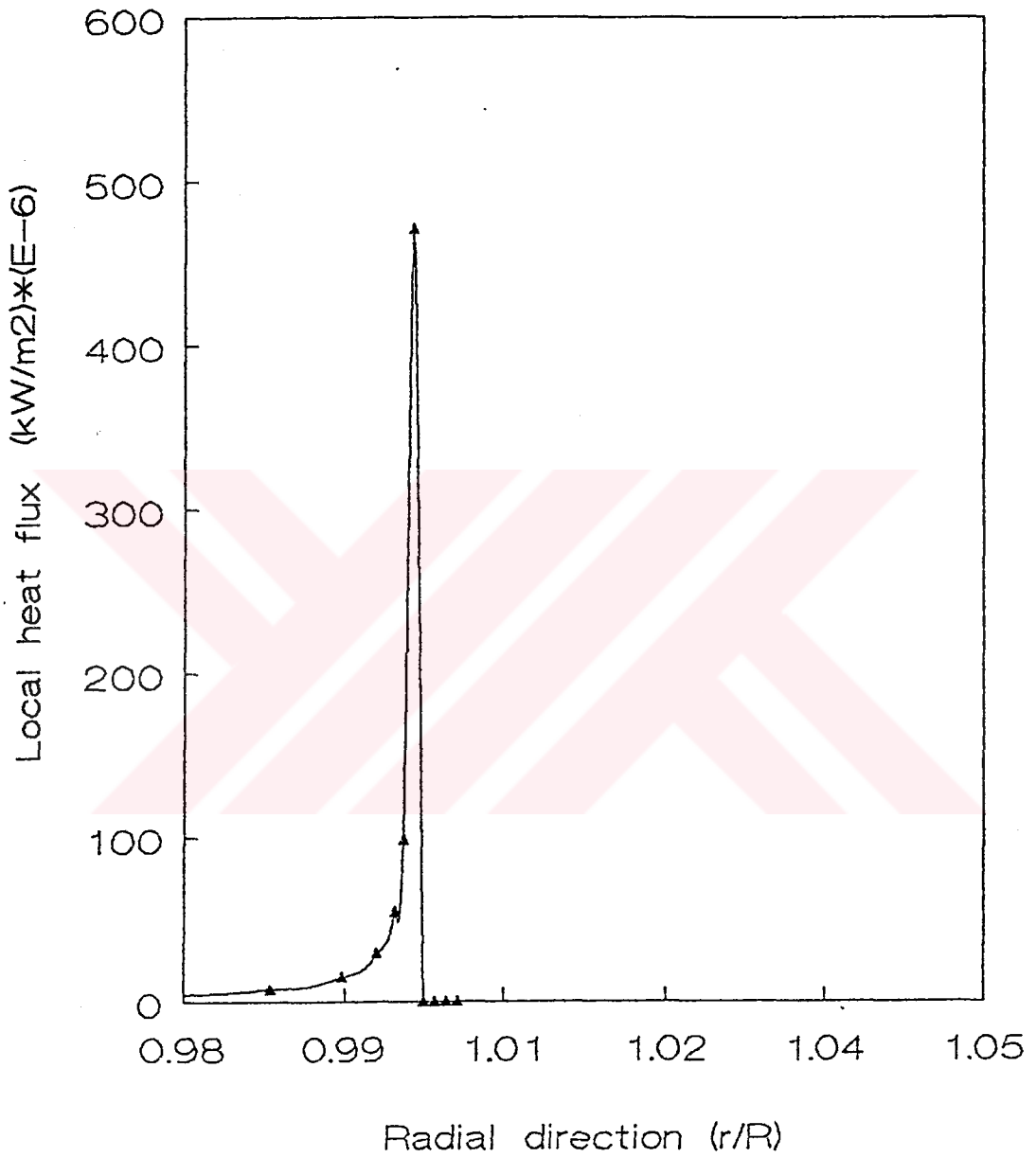


Figure 4.12. Surface local heat flux under an isolated droplet versus nondimensional radial distance ($r = 1\text{mm}$).

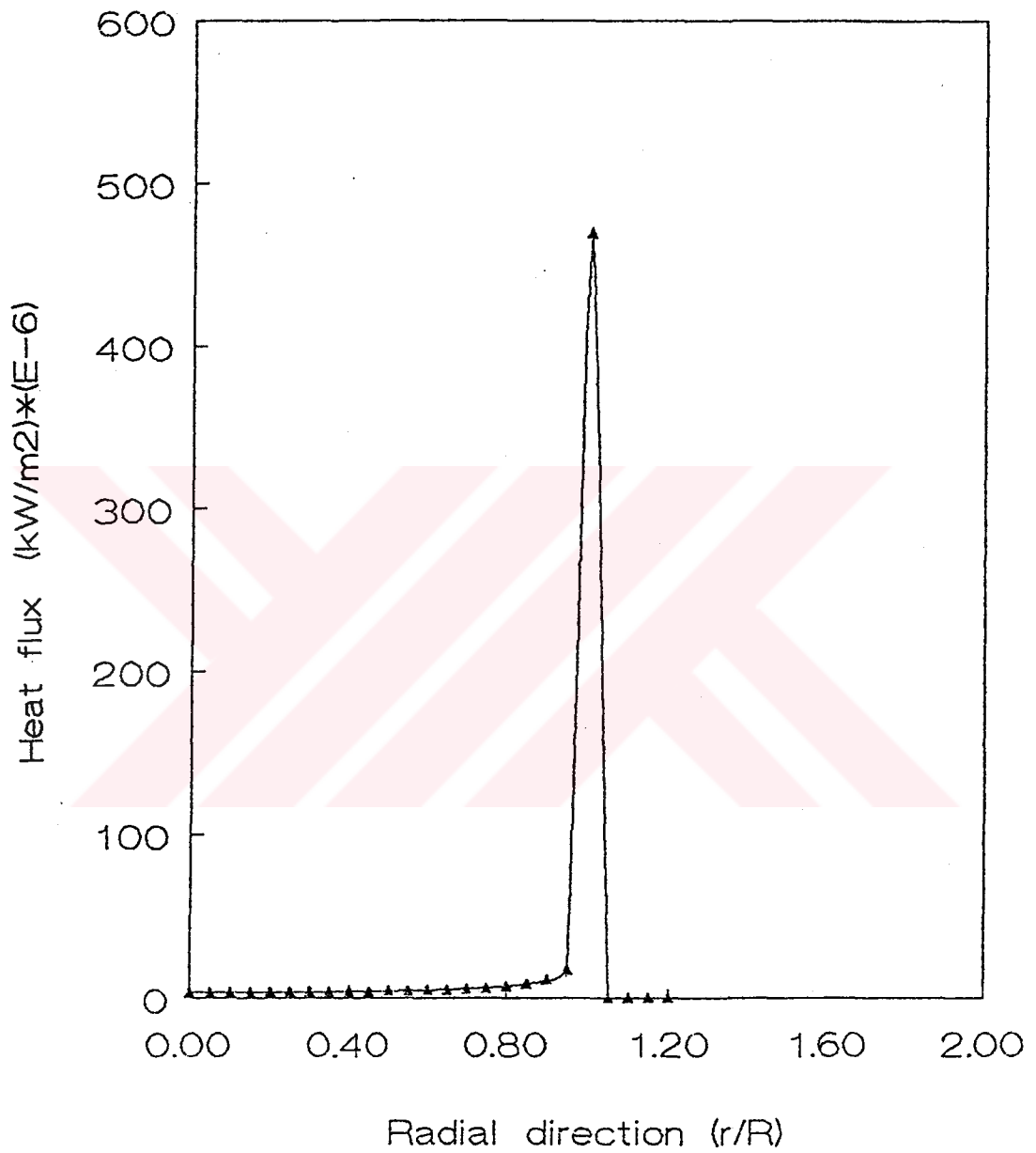


Figure 4.13. Surface local heat flux under an isolated droplet versus nondimensional radial distance ($r = 0.1mm$).

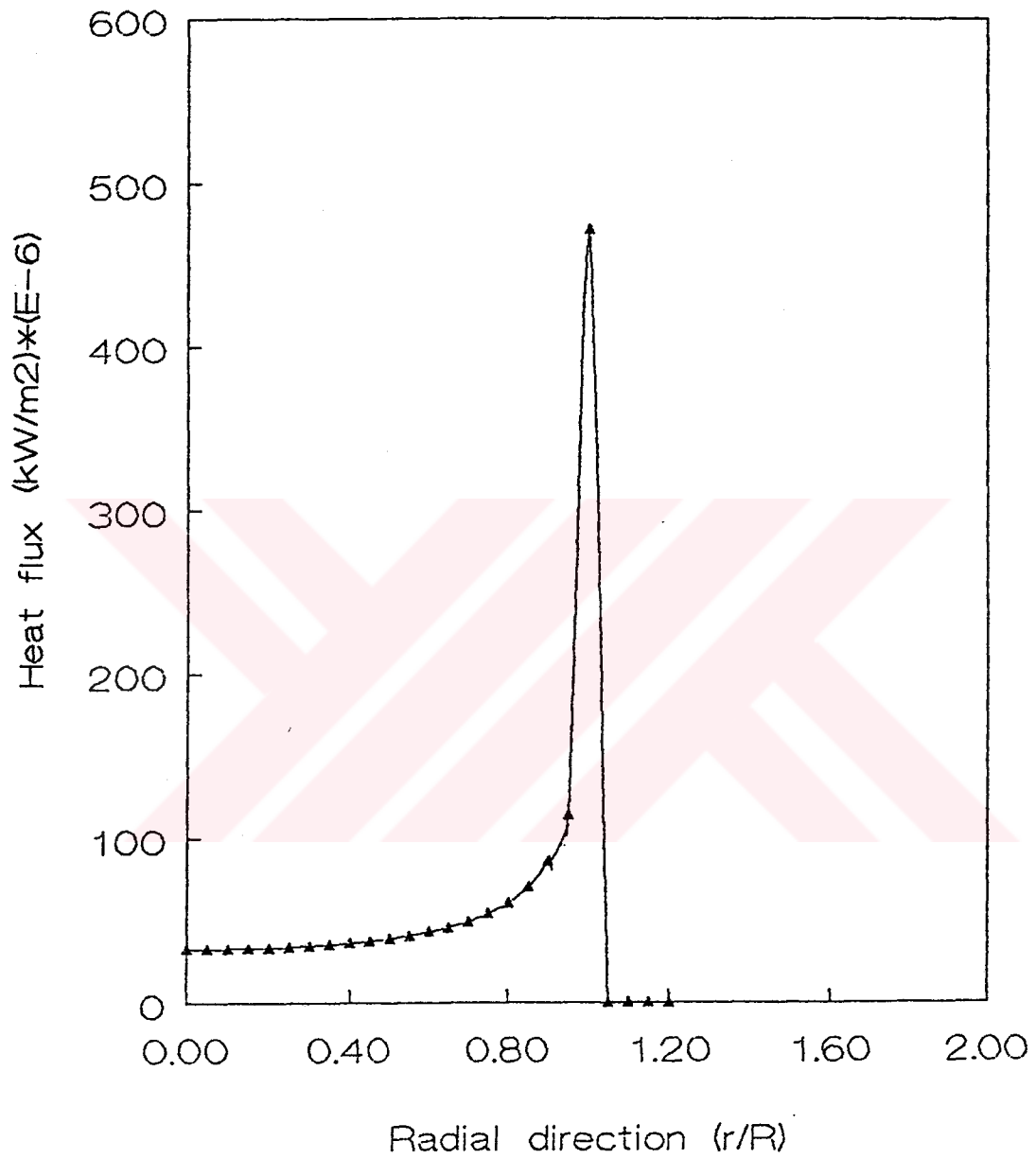


Figure 4.14. Surface local heat flux under an isolated droplet versus nondimensional radial distance ($r = 0.01mm$).

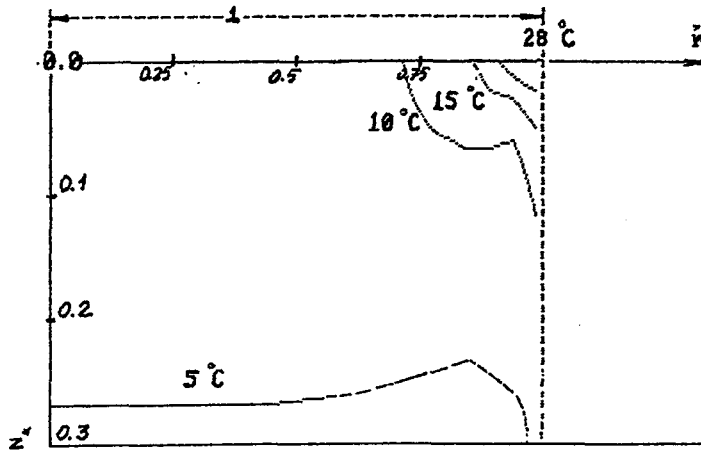


Figure 4.15. Isotherms under two neighboring droplets of radius 2 mm and axial distance 4.0 mm.

are negligible for all practical purposes. Local heat flux at the edge of the droplets is almost independent of the size of the droplet.

4.2 Computation Results for the Temperature Distribution Under Two Neighboring Droplets

Fig's 4.15., 4.16., 4.17., 4.18., 4.19., 4.20 show the temperature distribution under two neighboring droplets.

The substrate material is stainless steel. The location of the droplet and the distance between them are shown on the figures. When there are two neighboring droplets on the surface axial symmetry around the center of the droplet no longer exists, therefore Fig's 4.15 through 4.20 represents the temperature distribution on the plane that passes through the axis of both droplets. Sharp peaks seen on some of the isotherms are due to the lack of sufficiently close computational points and therefore slightly deviates from the actual situation.

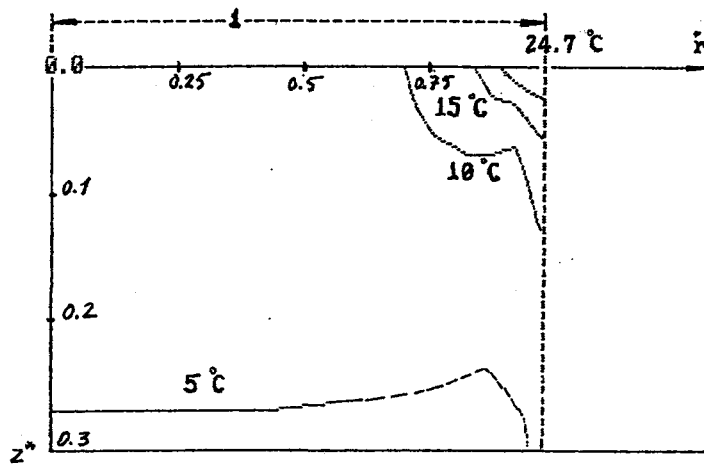


Figure 4.16. Isotherms under two neighboring droplets of radius 2 mm and radial distance 4.02 mm.

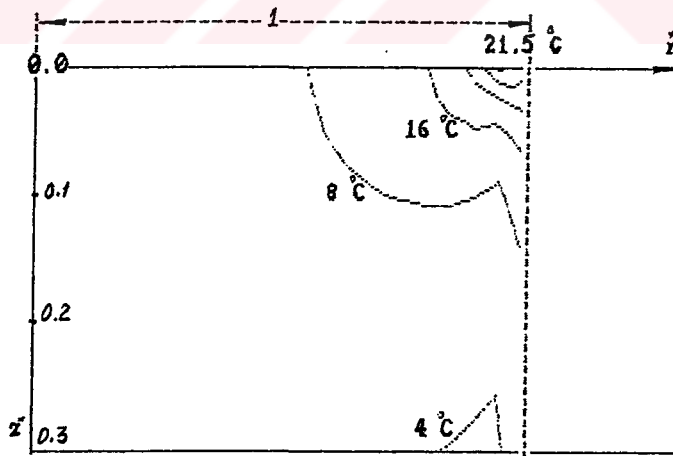


Figure 4.17. Isotherms under two neighboring droplets of radius 2 mm and radial distance 4.04 mm.

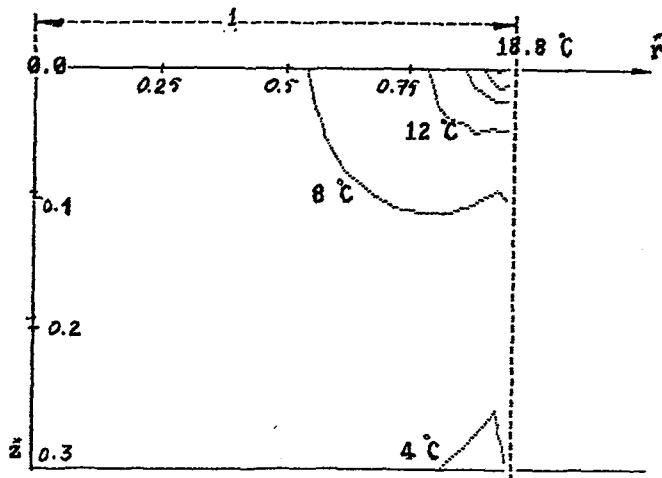


Figure 4.18. Isotherms under two neighboring droplets of radius 2 mm and radial distance 4.06 mm.

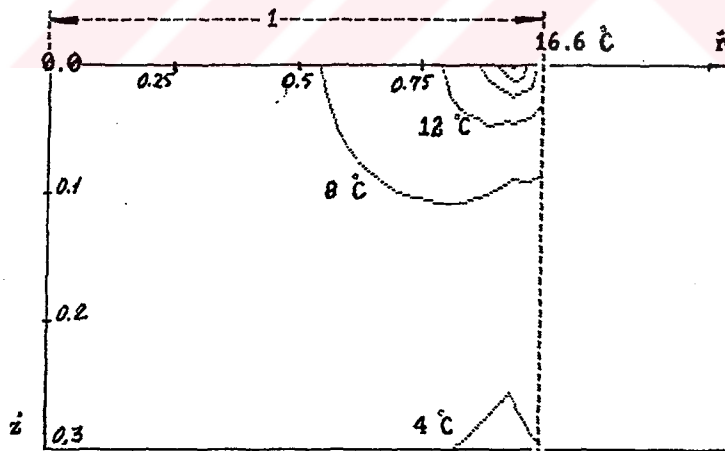


Figure 4.19. Isotherms under two neighboring droplets of radius 2 mm and radial distance 4.08 mm.

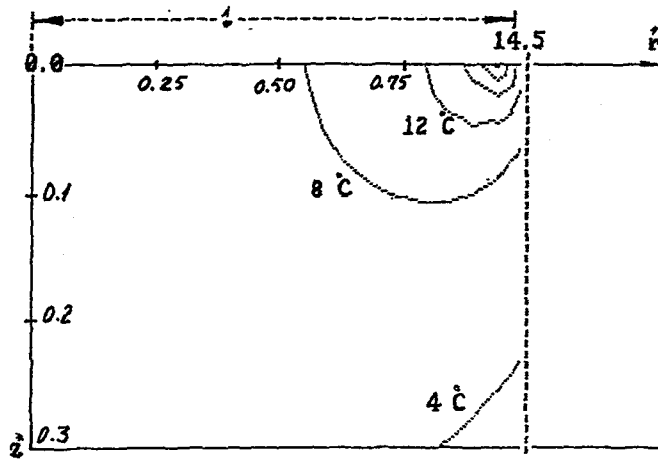


Figure 4.20. Isotherms under two neighboring droplets of radius 2 mm and radial distance 4.10 mm.

Fig's 4.21., 4.22., 4.23., 4.24 represents the temperature distribution on the surface of the substrate along the line connecting the center of the droplets.

Radial direction is taken from the center of one of the droplets towards the center of the other droplet. Fig. 4.21 shows the above described temperature distribution for droplets of 2mm diameter with zero clearance between them. The maximum temperature which occurs at the edge of the droplet is obviously larger than the temperature at the edge of an isolated single droplet which is expected to reduce the local heat flux there, because of the decreasing temperature potential.

As the clearance between the droplets increases not only the maximum temperature decreases but also a low temperature region enters between the droplets. Temperature distribution under the droplet of concern is obviously influenced by the presence of the neighboring droplets and as it is understood from the Fig's 4.21 through 4.24, this effect is such that it increases the temperature under the droplet of concern. As the distance between the droplets increases the resulting effect should be such that total heat flux through the droplet of concern increases. The relation between the distance

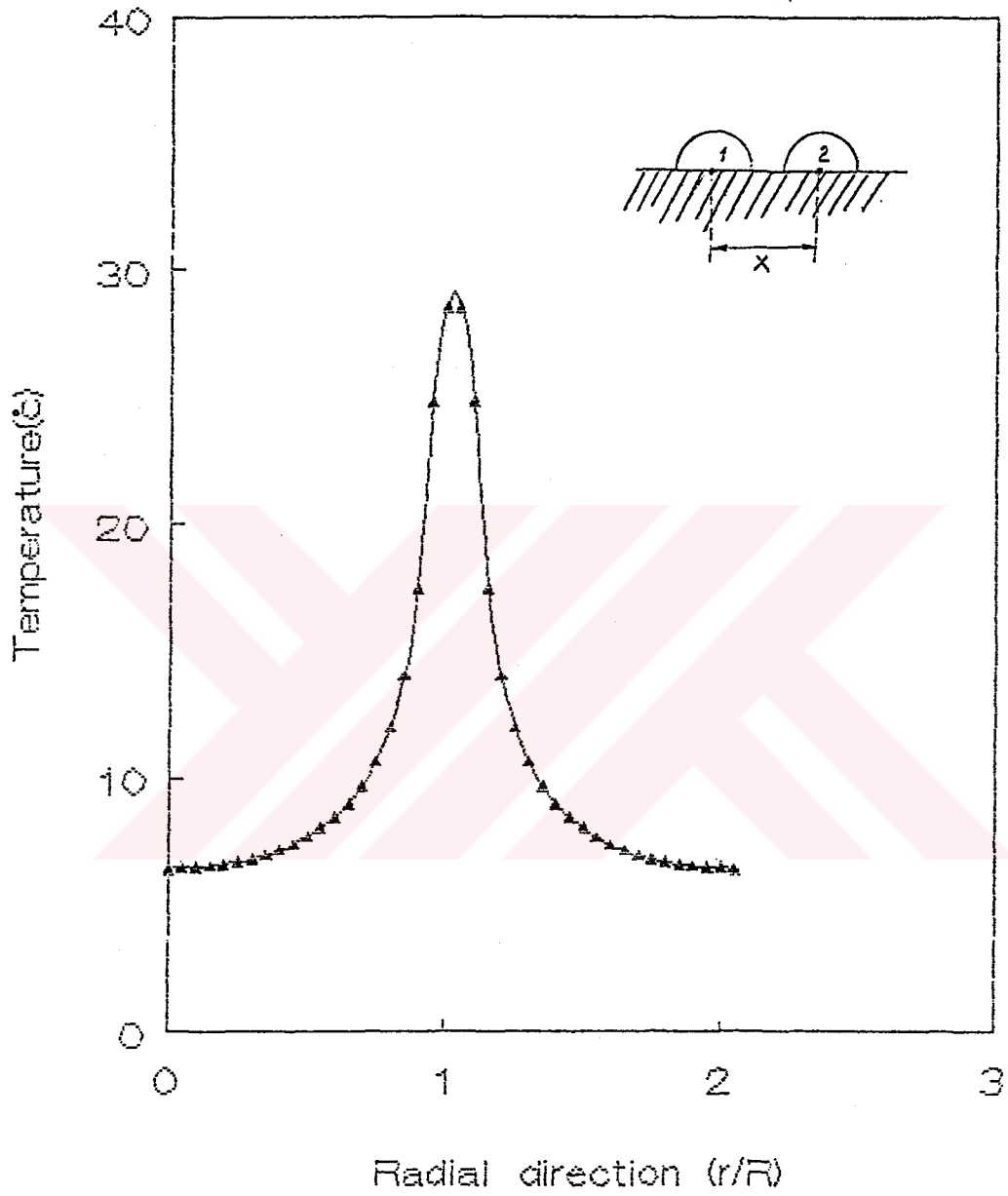


Figure 4.21. Temperature of the substrate surface along the line joining the center of the droplets ($x = 4.0mm$, $d_1 = 2mm$, $d_2 = 2mm$).

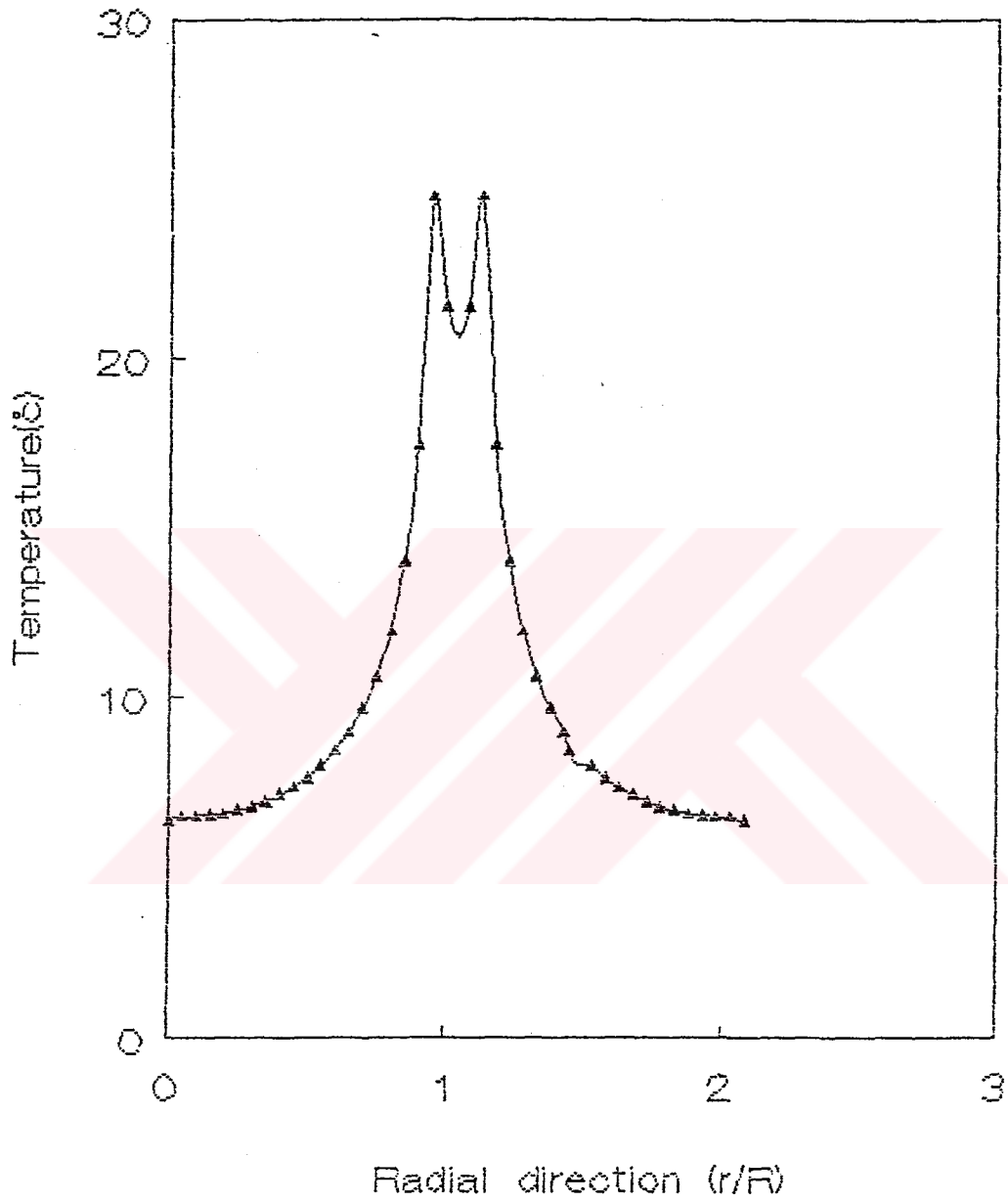


Figure 4.22. Temperature of the substrate surface along the line joining the center of the droplets ($x = 4.06\text{mm}$, $d_1 = 2\text{mm}$, $d_2 = 2\text{mm}$).

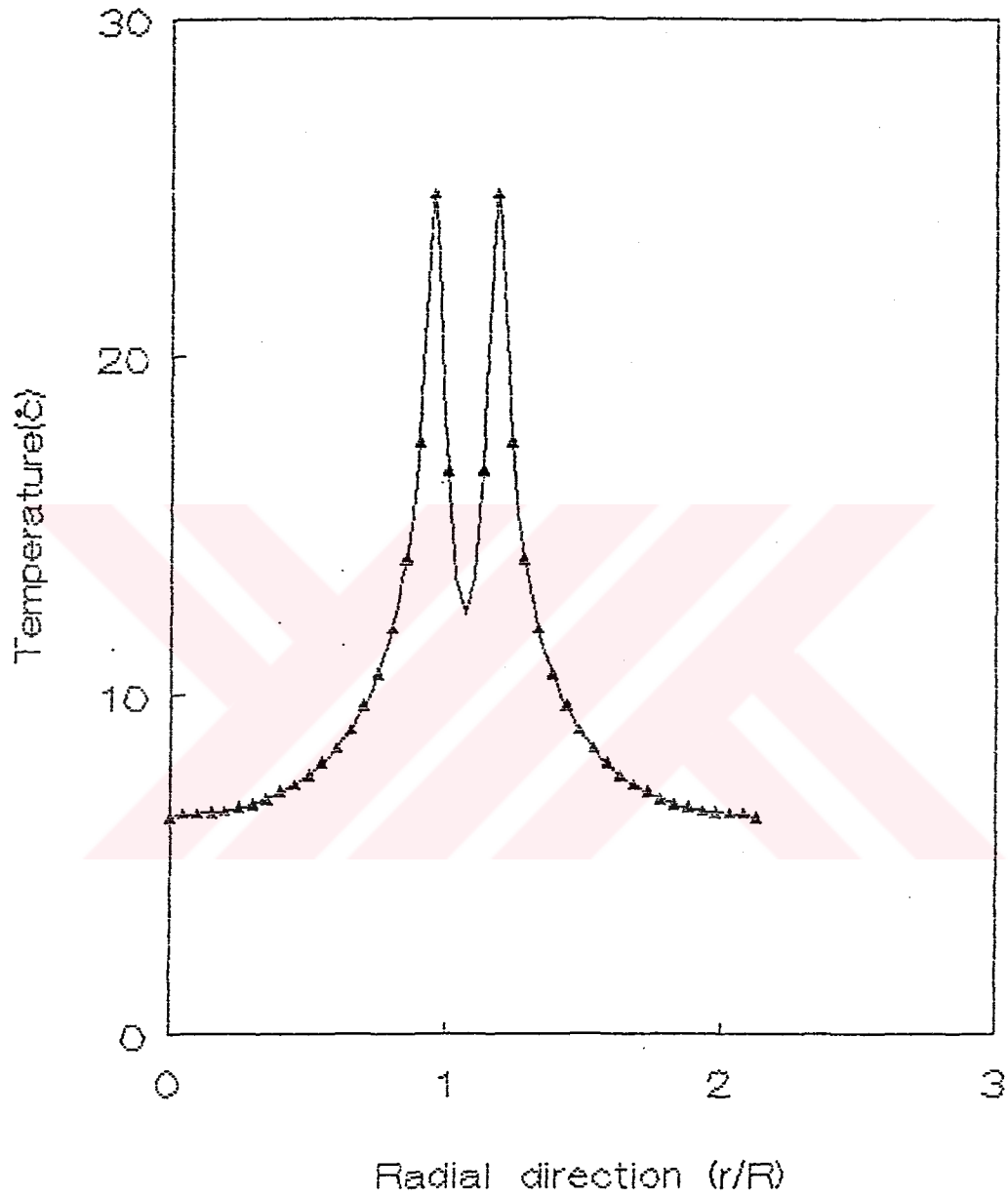


Figure 4.23. Temperature of the substrate surface along the line joining the center of the droplets ($x = 4.08\text{mm}$, $d_1 = 2\text{mm}$, $d_2 = 2\text{mm}$).

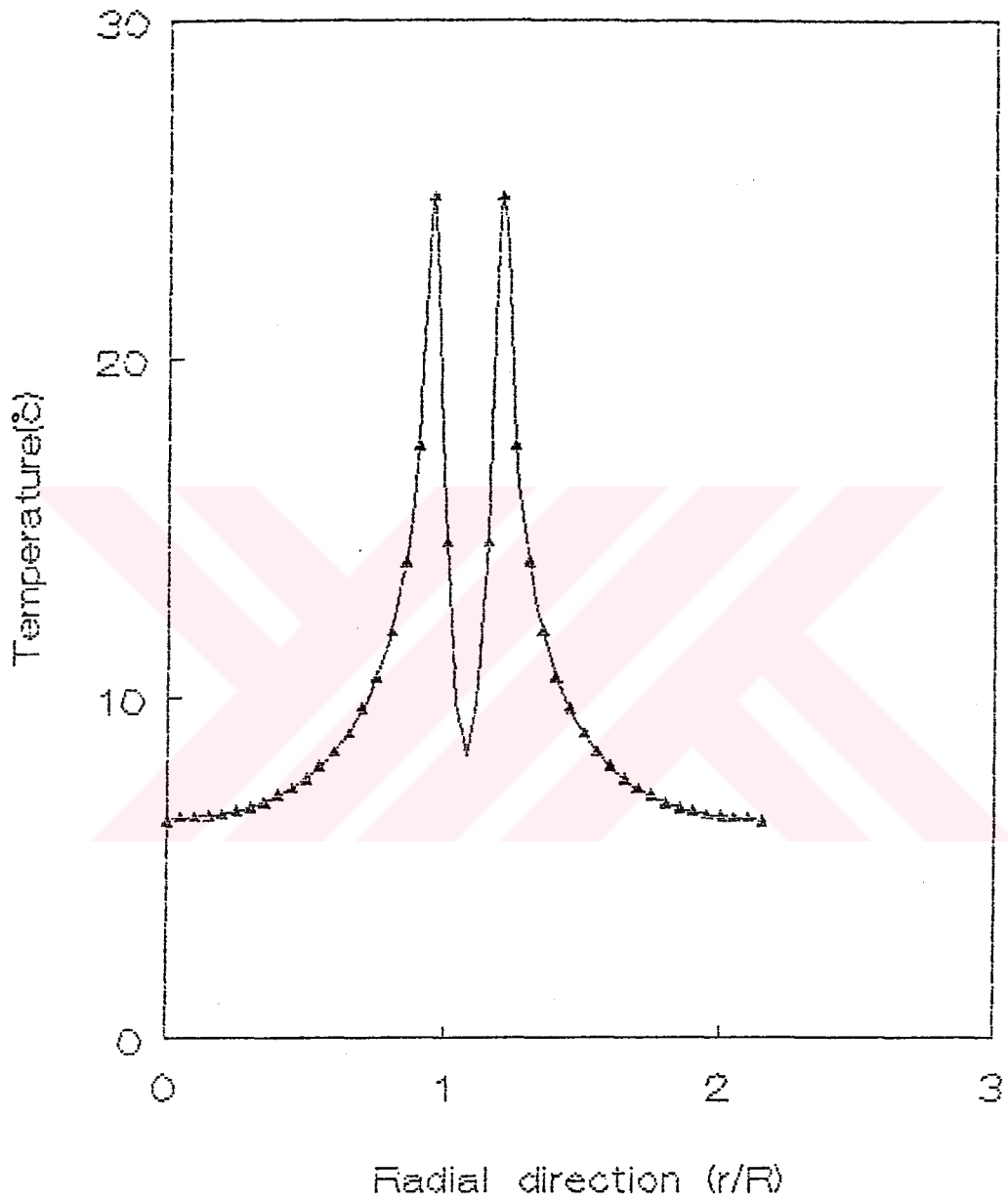


Figure 4.24: Temperature of the substrate surface along the line joining the center of the droplets ($x = 4.10\text{mm}$, $d_1 = 2\text{mm}$, $d_2 = 2\text{mm}$).

between the droplets and the total heat transfer through the droplet of concern is important. This relation is shown for neighboring droplets of various sizes in Fig's 4.25., 4.26., 4.27.

In these figures size of the neighboring droplet is the same in all figures but the size of the droplet of concern is changed. There are various observations that can be deduced from these figures. First of all, total heat flux through the droplet of concern increases as the neighboring droplets moves away from the droplet of concern. This decrease is comperatively larger if the neighboring droplet is comperatively larger than the droplet of concern. That means if a small droplet is placed next to the droplet of concern, the effect in reducing the total heat transfer through it is smaller than the situation in which a large droplet is placed next to the droplet of concern.

Another observation is that the effect of the neighboring droplet drops very fast as the distance between the droplets changes and the total heat transfer through the droplet of concern reaches to an asymptotic value for a clearence equal to a small fraction of the drop radius. One more important observation that can be obtained from Fig's 4.25 through 4.27 is that for large droplets the total heat transfer is not proportional to drop contact surface area but instead is proportional to the periphery. That is expected since the central regions are almost insulated for all practical purposes for such droplets and majority of the heat transfer takes place in a narrow region close to the periphery.

4.3 Computation Results of the Total Substrate Effect

4.3.1 Total Primary Substrate Effect

Total primary substrate effect will be calculated by means of Eqn. (3.71) which requires the value of $f_{01}(r)$, the difference between the total heat transfer through a droplet of radius r with a substrate of infinitely large thermal conductivity (i.e. uniform temperature distribution) and the total heat transfer through the droplet with a substrate of finite thermal conductivity under the effect of no neighboring droplet. This second total drop heat transfer corresponds to the maximum values in Fig. 4.25

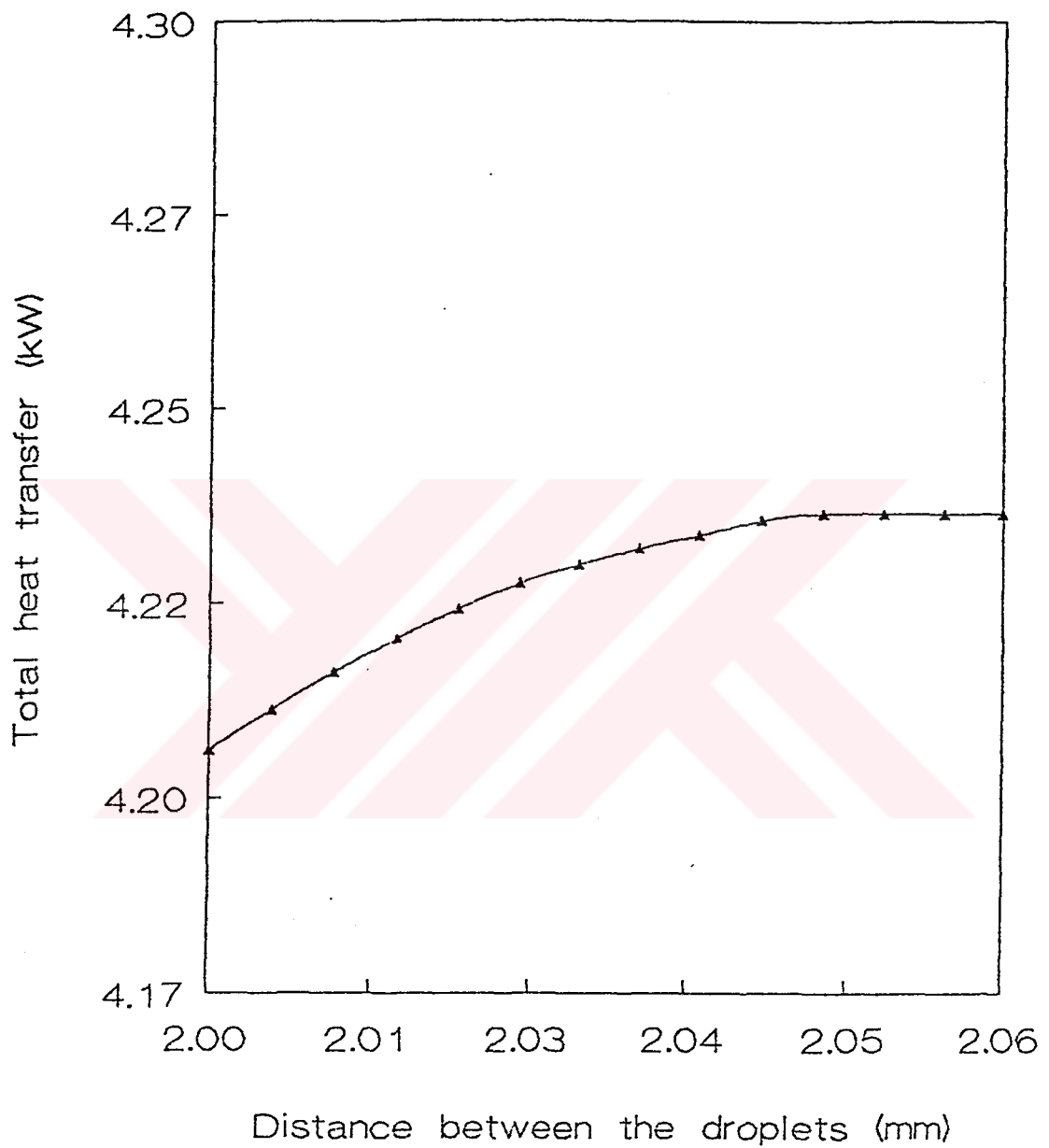


Figure 4.25. Total heat flux through the droplet of concern ($d = 1mm$) under the influence of the neighboring droplet ($d = 1mm$) versus center to center distance between the droplets.

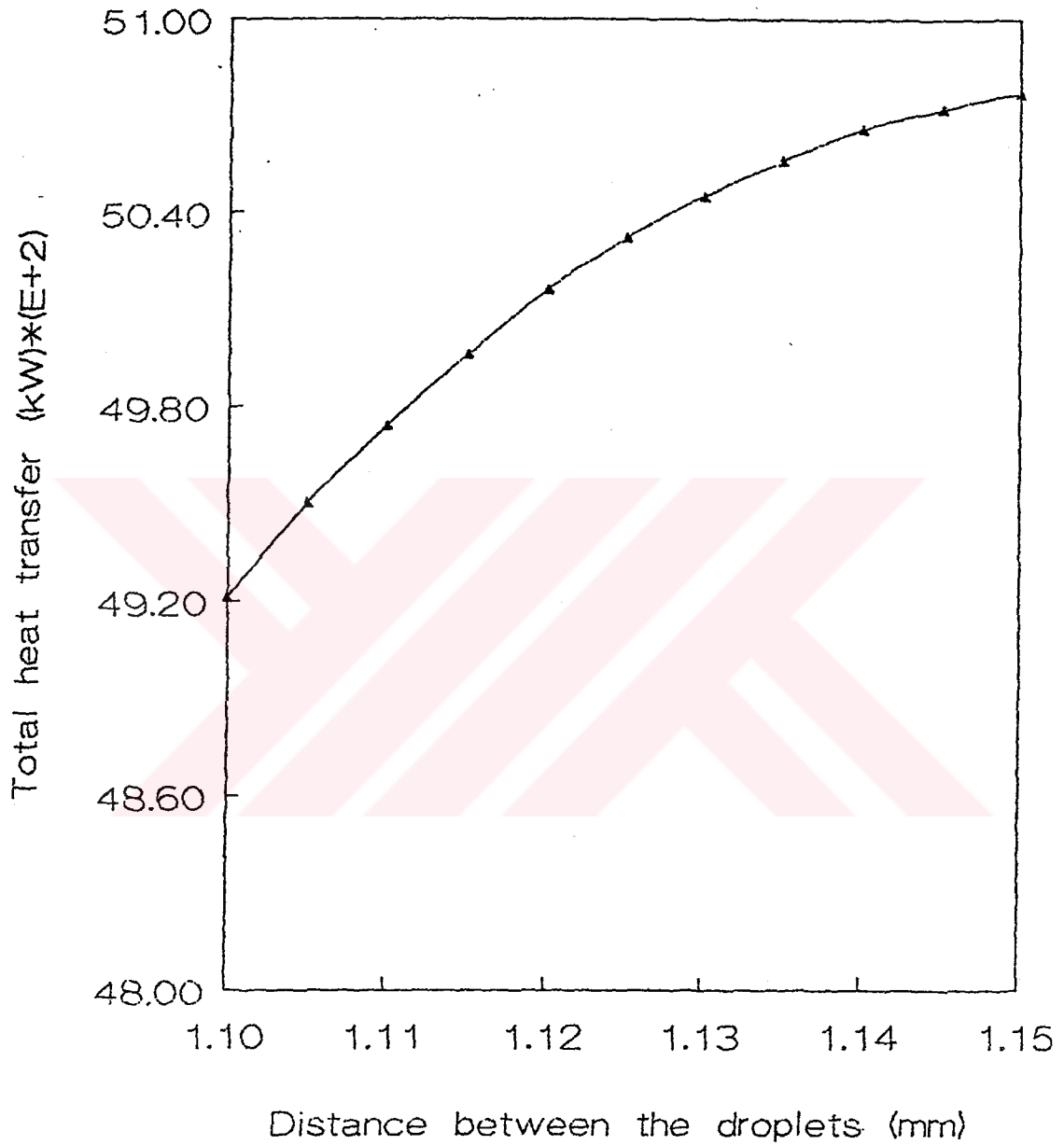


Figure 4.26. Total heat flux through the droplet of concern ($d = 0.1mm$) under the influence of the neighboring droplet ($d = 1mm$) versus center to center distance between the droplets.

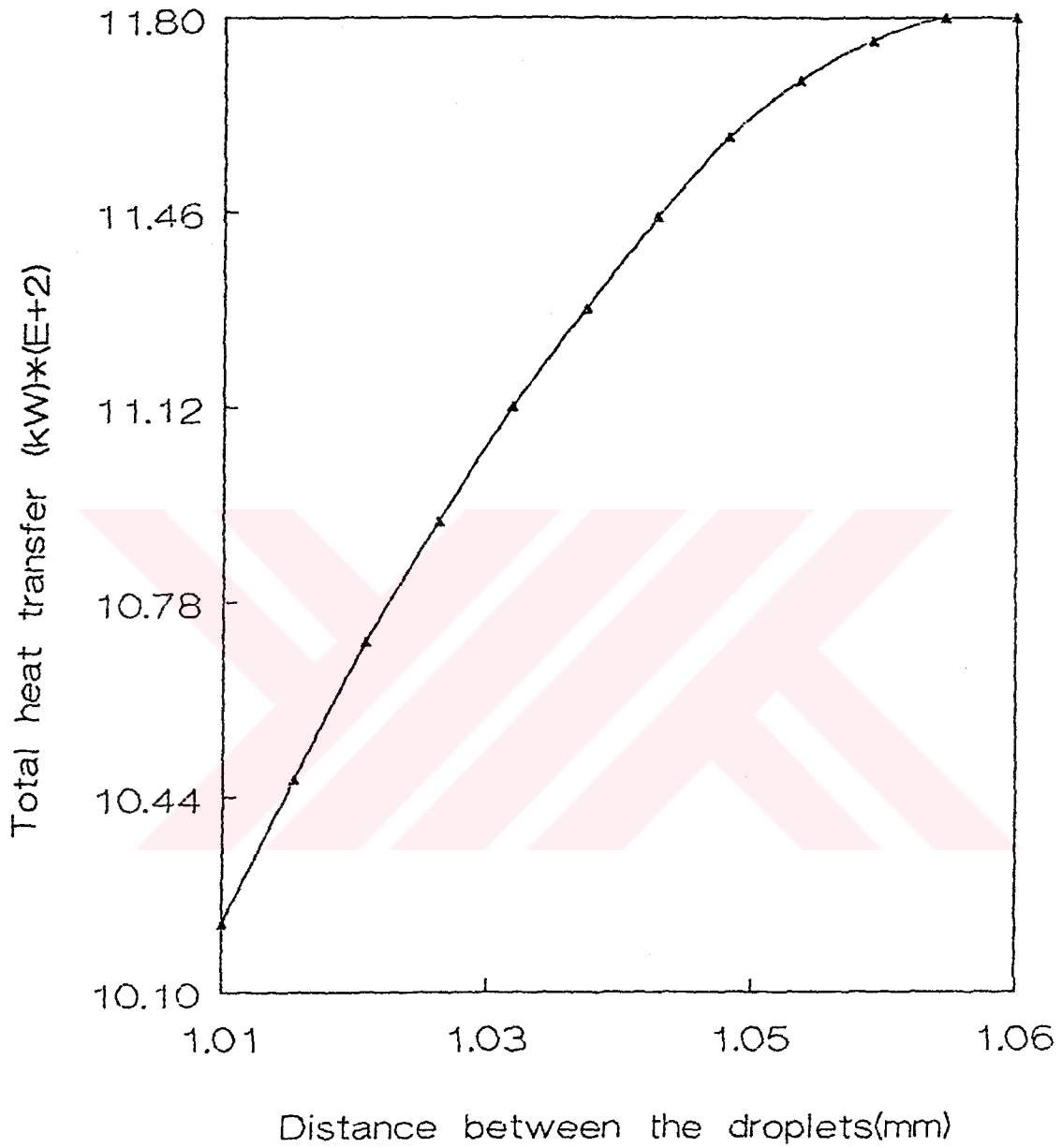


Figure 4.27. Total heat flux through the droplet of concern ($d = .01mm$) under the influence of the neighboring droplet ($d = 1mm$) versus center to center distance between the droplets.

through 4.27. (Neighboring droplet is far enough so that it has no effect on the heat transfer through the droplet of concern.) Numerical computation of integral in Eqn. (3.71) requires the value of $f_{01}(r)$ at each incremental change in the value of r which is not practical for computational purposes. So, instead of doing that, the value of $f_{01}(r)$ is calculated at certain values of r ($2mm, 1mm, 0.1mm$ and $0.01mm$) and using a logarithmic scale and least square curve fitting technique an expression that gives f_{01} as a function of r is obtained as below:

$$f_{01}(r) = 0.728 + 0.754(\ln r) + 0.281(\ln r)^2 + 3.36 \times 10^{-2}(\ln r)^3 \quad (4.1)$$

where r is in mm and f_{01} is in kJ .

To take the fast changes of the integral in Eqn. (3.71) a variable transformation is applied by

$$s = \ln r \quad (4.2)$$

which transforms the integral of Eqn. (3.71) to the following form:

$$Q_{01} = \int_{\ln r_{\min}}^{\ln r_{\max}} f_{01}(s) \frac{n}{r_{\max}} \left(\frac{\exp(s)}{r_{\max}} \right)^{n-1} \frac{ds}{\pi \exp(s)} \quad (4.3)$$

Evaluation of this integral for $n = 1/3$ gives the value of the total primary substrate effect (i.e. the reduction in total dropwise condensation heat transfer as a result of the temperature distribution in the substrate material as $3.0569 \times 10^6 W/m^2$ for the numerical values chosen for various parameters in this study.

4.3.2 Total Secondary Substrate Effect

Total secondary substrate effect is calculated by using first Eqn. (3.72) and then Eqn. (3.73). Evaluation of the integral in Eqn. (3.72) requires the computation of f_{12} , the reduction of the total heat transfer through a droplet due to the effect of a neighboring droplet. It is obvious that f_{12} is function of not only the radius of the droplet itself but also function of the radius of its neighboring droplet as well as the distance between them. To evaluate the integral in Eqn. (3.72) f_{12} is expressed as a function of the distance between the droplets, x using the least square curve fitting method. Since the range of the clearance distance between the droplets are quite different for droplets of different sizes, using a normalization procedure, this clearance

is expressed in such a manner that it changes from 0 to 1. The normalization parameter then becomes a function of the radius of the neighboring droplets. Then, a second curve fitting is applied to the coefficient of the expression found between f_{12} and x to obtain an expression that gives f_{12} as a function of x and the radius of the neighboring droplet. The same procedure is applied for droplets of various sizes to obtain q_{II} as a function of r . The result of the computation to obtain the value of the total secondary substrate effect shows that for the parameters chosen in this study its value is around $0.0286 \times 10^6 W/m^2$.

4.4 Total Dropwise Condensator Heat Transfer Including the Substrate Effect

Total dropwise heat transfer under the influence of primary and secondary substrate effects can be obtained by the expression.

$$Q_{dc} = \int_{r=r_{\min}}^{r=r_{\max}} \int_{r_n=r_{\min}}^{r_n=r_{\max}} \int_{x=x_{\min}}^{x \rightarrow \infty} q_2(r, r_n, x) \left(\frac{n}{r_{\max}} \right)^{n-1} \frac{2x}{r_n^2} \frac{n}{r_{\max}} \left(\frac{r}{r_{\max}} \right)^{n-1} \frac{dx dr_n dr}{\pi r^2} \quad (4.4)$$

The expression above is obtained using the procedure described for the total secondary substrate effect in the previous section. For the numerical values used for various parameters in this study the value of total dropwise condensation heat transfer rate is found to be $10.5666 \times 10^6 W/m^2$.

4.5 Comparison with Experimental Results

Several experimental work exist in the literature to study the effect of substrate material on the heat transfer in dropwise condensation.

Tanner et.al. (18) observed that the dropwise condensation heat transfer coefficient with copper as a substrate material is about one fifth as large when compared with stainless steel. They suggest that such a difference could arise from the influence of adsorption properties and surface free energy of the interface. In another work Grif-

fith and Lee (22) coated two surfaces of different materials with a thin layer of gold so as to present the same surface energy characteristics. The differences between the heat transfer coefficients were quite large, and attributed to the differences in the thermal conductivities. As a matter of fact, measurements showed that the ratio of heat transfer coefficient for a zinc substrate to that of the copper substrate is 0.45 whereas the ratio of heat transfer coefficient for a stainless steel substrate to that of the copper substrate is 0.2 in this work.

Computational results of this study shows that when the substrate effect is taken into account the resulting heat transfer rate is only 71 % of the heat transfer rate without any substrate effect. The experimental results of Tanner et.al. is a little bit smaller than the computational results of this study. However, it should be kept in mind that in actual dropwise condensation, movement and coalescences of the droplets occur which might help to eliminate some of the substrate effect. Very high substrate effect measured by Griffith and Lee in their work is somehow unexpected and it is believed that uncontrolled factors during the experiments might be the cause.

CHAPTER V

CONCLUSIONS AND RECOMMENDATION

A novel method to calculate the substrate effect in dropwise condensation is proposed in this study. The characteristics of the method is to separate the total substrate effect into two parts namely, primary and secondary substrate effects resulting from the temperature distribution under the droplet and the effect of the neighboring droplets respectively.

Computations showed that total primary substrate effect is around 30 percent of the total heat transfer rate in dropwise condensation. This effect may be smaller if time dependency due to the movement of the droplets is introduced into model.

It is found that total secondary substrate effect, that is the effect of neighboring droplets on each other is small. However, it should be noted that this effect depends on the temperature distribution under the neighboring droplets and approximate in nature. In addition, computational time limitations of the mainframe computer system established in Middle East Technical University Computer Center made it possible to perform calculation down to $0.01mm$ radius droplets only. For a temperature difference of $100^{\circ}C$ it is expected that the surface is covered by droplets of sizes smaller than $0.01mm$. Secondary substrate effect is more important at that small sizes. So, computations performed at smaller size droplets might reveal the importance of the total secondary substrate effect.

Sweeping effect is not considered in the model. Sweeping effects the drops size distribution. Introducing the sweeping into the model might improve the accuracy of the model.

High heat flux at the edge of the droplet makes it necessary to take smaller increments there for the numerical calculations.



REFERENCES

- [1] O'Neill, G.A. and Westwater, J.W., "Dropwise Condensation of Steam on Electroplated Silver Surface", Int. S. Heat Mass Transfer, Vol.27, pp.1539-1549, 1984.
- [2] Yamah, C., Dropwise Condensation Under High Gravity and at Large Subcooling, Ph.D. Thes., Michigan, 1983.
- [3] Stylianou, S.A. and Rose, J.W., "Drop-to-Filmwise Condensation Transition: Heat Transfer Measurements for Ethanediol", Int. J. Heat Transfer, Vol.26, pp.742-760, 1983.
- [4] Woodruff, D.W. and Westwater, J.W., "Steam Condensation", Ind. Engn. Chem. 57, 49-52, 1965.
- [5] Mc Cormick, J.L. and Baer, E., "On the mechanism of Heat Transfer in Dropwise Condensation of Steam", J. Colloid Sci. 18, 208-232, 1963.
- [6] Erb, R.A. and Thelen, E., "Dropwise Condensation", First International Symposium on Water Desalination, Washington, D.C. Oct. 3-9, 1965.
- [7] Welch, J.F. and Westwater, J.W., "Microscopic Study of Dropwise Condensation", International Heat Transfer Conference, p.302, 1961.
- [8] Mc Cormick, J.L. and Baer, E., "Dropwise Condensation in Horizontal Surfaces", Developments in Mechanics, Pergamon Press, N.Y., pp.7299-75, 1965.
- [9] Umur, A. and Griffith, P., "Mechanism of Dropwise Condensation", Trans. ASME, Journal of Heat Transfer, 87C, pp.275-282, 1965.
- [10] Ivanovskii, M.N., Subbotin, and Milovanov, Yu, V., "Heat Transfer with Dropwise Condensation of Mercury Vapor", Teplotenergetika, 14, pp.15-22, 1967.
- [11] Mc Cormick, J.L. and Wastwater, J.W., "Drop Dynamics and Heat Transfer During Dropwise Condensation of Water Vapor on a Horizontal Surface", Chemical Engineering Progress Symposium Series, Vol.62, No.64, pp.120-134, 1966.

- [12] Fatica, N. and Katz, D.L., "Dropwise Condensation", Chem. Eng. Progress, 45, pp.661-74, 1949.
- [13] Hurst, C.J. and Olson, D.R., "Conduction Through Drops During Dropwise Condensation", J. Heat Transfer, 95, pp.12-20, 1973.
- [14] Graham, C. and Griffith, P., "Dropwise Distributions and Heat Transfer in Dropwise Condensation", Int. J. Heat Mass Transfer, 16, p.337, 1973.
- [15] Le Feure, E.J. and Rose, J.W., "A Theory of Heat Transfer by Dropwise Condensation", Proc. of 3rd Intern. Heat Transfer Conf., 2, pp.362-375, 1966.
- [16] Tanaka, H., "Measurements of Dropwise Distributions During Transient Dropwise Condensation", Trans. ASME, Journal of Heat Transfer, 97, pp.341-346, 1975.
- [17] Hasson, D., Luss, D. and Navon, V., "An Experimental Study of Steam Condensation of a Laminar Water Sheet", Int. J. Heat Mass Transfer, 7, pp.983-1001, 1964.
- [18] Tanner, D.W., Pope, D., Potter, C.J. and West, D., "Heat Transfer in Dropwise Condensation of Low Steam Pressures in the Absence and Presence of Non-Condensable Gas", Int. J. Heat Mass Transfer, 11, pp.181-190, 1968.
- [19] Sadhal, S.S. and Plesset, M.S., "Effect of Solid Properties and Contact Angle in Dropwise Condensation Theory", Transactions of the ASME, Journal of Heat Transfer, 101, p.603, 1979.
- [20] Chiba; Yoichi, Suzuki, Mutsumi, and Ohtani, Shigemori, "Heat Transfer in Dropwise Condensation of Steam-Effect of Falling Drops", Kageku Kogaku Ronbunshu, 11, 520-527, 1985.
- [21] Peterson, A.C. and Westwater, J.W., "Dropwise Condensation of Ethylene Glycol", Presented at the 8. National Heat Transfer Conference A.I.Ch.Eb ASME, Los Angeles, California, 1965.
- [22] Griffith, P. and Lee, M.S., "The Effect of Surface Thermal Properties and Finish on Dropwise Condensation", Int. J. Heat Mass Transfer, 10, pp.697-707, 1967.

[23] Eser, A., An Analytical Model for Dropwise Condensation Including the Effect of the Substrate Material, Master Thesis, December 1989.

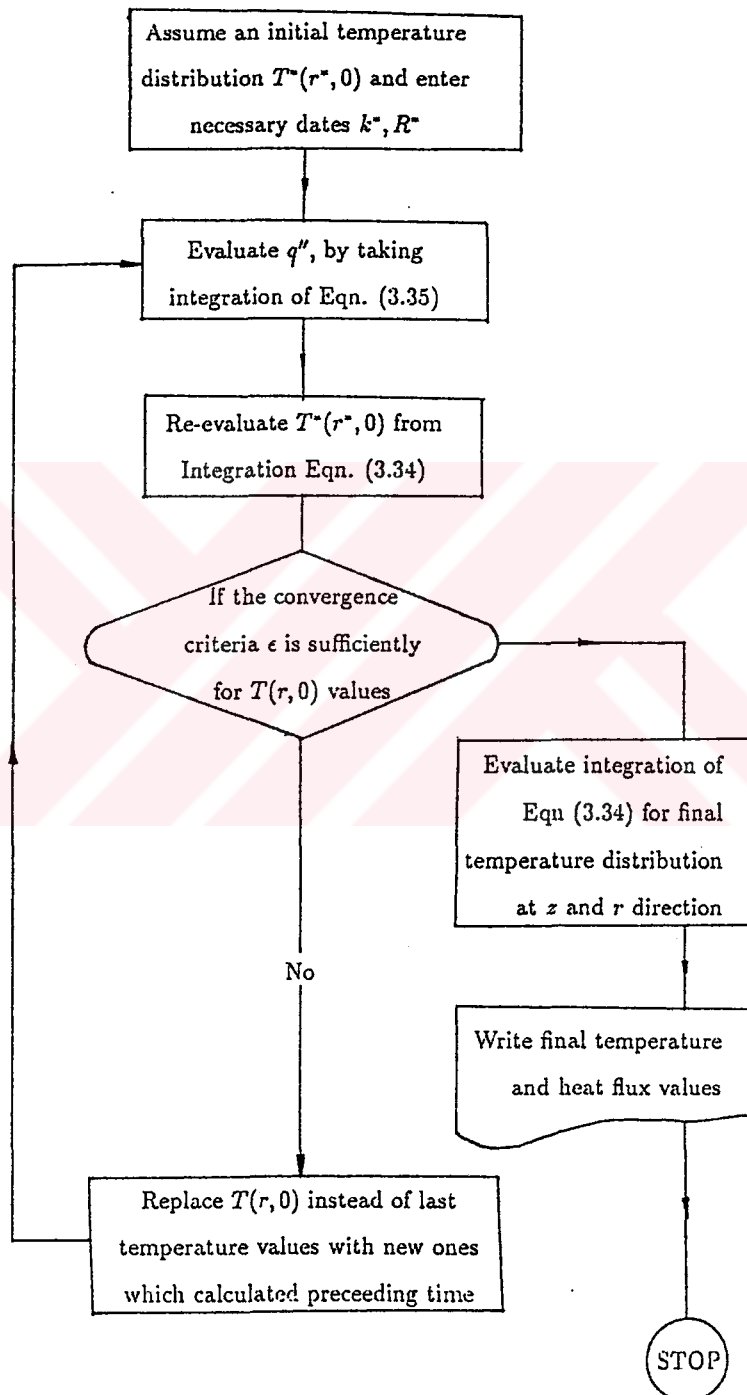


APPENDICES



APPENDIX A

FLOW CHART OF THE SOLUTION PROCEDURE



APPENDIX B
LIST OF THE MAIN PROGRAM

```
IMPLICIT REAL*8(A-H,O-Z)  
DIMENSION HR(1000),QR(1000),T(1000),QA(51000),SN(1000)  
*,TN(51000),F(1000)
```

```
C*****
```

```
C  
C THIS PROGRAM CALCULATES THE TEMPERATURE DISTRIBUTION  
C  
C (FOR THE DROPLET R=2MM)IN THE PLATE FOR COPPER SUBSTRATE.  
C  
C HEAT CONDUCTION COEFF. FOR COPPER=345.00 KCAL/M.K.H)
```

```
C
```

```
C*****
```

```
OPEN(8,FILE='/GAUSS4 OUT A')  
PRINT*,'  
KMJ=1500  
KLL=1  
PRINT*, 'TEMPERATURE CALCULATION FOR STAINLESS STEEL PLATE'  
TKT=3.8164
```

```
C*****
```

```
C  
C INITIAL TEMPERATURE VALUES
```

```
C
```

```
C*****
```

```
DO 55 LI=1,21  
T(LI)=0.5  
55 CONTINUE
```

```
C*****
```

```
C MAIN PROGRAM CALLES SUBROUTINE ANA  
C AND TEMP
```

```
C*****
```

```
NN=1
```

```
Z=0.0
DO 53 LL=1,50
CALL ANA(KLL,T,QA,KMJ)
DO 97 LH=1,21
RR=(LH-1.0)*0.05
CALL TEMP(LH,RR,QA,TN,KMJ,Z)
SN(LH)=3.816*TN(LH)
```

```
97 CONTINUE
```

```
C
```

```
Z=0.0
```

```
WRITE(8,232) Z,LL
```

```
232 FORMAT(1X,'Z=',F3.1,2X,'ITERASYON SAYISI=',I3)
```

```
DO 344 LT=1,21
```

```
WRITE(8,433) SN(LT)
```

```
433 FORMAT(1X,F11.9)
```

```
344 CONTINUE
```

```
C
```

```
DO 89 JJ=1,21
```

```
F(JJ)=ABS(SN(JJ)-T(JJ))
```

```
T(JJ)=SN(JJ)
```

```
89 CONTINUE
```

```
EPS=0.000001
```

```
DO 587 IKJ=1,21
```

```
ENB=F(IKJ)
```

```
IF(ENB.GT.EPS) GO TO 53
```

```
587 CONTINUE
```

```
GO TO 17
```

```
53 CONTINUE
```

```
C
```

```
17 DO 330 LI=1,51
```

```
Z=(LI-1)*0.1
```

```
WRITE(8,202) Z
```

```
202 FORMAT(1X,'Z=',F10.5)
```

```
DO 546 KK=1,501
```

```
RA=(KK-1)*0.01
```

```

CALL TEMP(KK,RA,QA,SN,KMJ,Z)
SN(KK)=3.816*SN(KK)
C
WRITE(8,177) SN(KK)
177 FORMAT(1X,F11.9)
C
546 CONTINUE
330 CONTINUE
STOP
END
C*****
C
C THIS SUBROUTINE CALCULATES THE FINAL TEMPERATURE
C DISTRIBUTION WITH RESPECT TO AL
C AND SENDS THE VALUES TO MAIN PROGRAM
C
C*****
SUBROUTINE TEMP(LH,ST,QA,TN,KMJ,Z)
IMPLICIT REAL*8(A-H,O-Z)
DIMENSION QA(51000),TN(51000),AL(43),WE(43),CIL(51000)
*,R(51000),COEFF(51000)
C*****
C
C INTEGRATION PROGRAM USED
C GAUSS QUADRATURE METHOD
C
C*****
AL(1)=0.0005190346563414
AL(2)=0.0031239146898052
AL(3)=0.0084075682191570
AL(4)=0.0163865807168469
AL(5)=0.0269263916107437
AL(6)=0.0399503329247996
AL(7)=0.0554358423344078
AL(8)=0.0733183177083414

```

AL(9)=0.0934737095762340
AL(10)=0.115780018262161
AL(11)=0.1401382737139876
AL(12)=0.1664305979012938
AL(13)=0.1945014381051170
AL(14)=0.2241905820563901
AL(15)=0.2553520455521657
AL(16)=0.2878289398962806
AL(17)=0.3214373731700395
AL(18)=0.3559893415987994
AL(19)=0.3913099530641356
AL(20)=0.4272190729195524
AL(21)=0.4635163762021047
AL(22)=0.5000000000000000

C

WE(1)=0.0013977406162058
WE(2)=0.0039091686510621
WE(3)=0.0066523213035442
WE(4)=0.0092800277044381
WE(5)=0.0117870995415145
WE(6)=0.0142592132851025
WE(7)=0.0167012731604038
WE(8)=0.0190415767267325
WE(9)=0.0212484664405592
WE(10)=0.0233486623657572
WE(11)=0.0253485988982588
WE(12)=0.0272093375891918
WE(13)=0.0289052287488048
WE(14)=0.0304493401023310
WE(15)=0.0318478076245504
WE(16)=0.0330747889079756
WE(17)=0.0341103531305126
WE(18)=0.0349648825041994
WE(19)=0.0356466731818923
WE(20)=0.0361377411110170

```
WE(21)=0.0364228264152542
WE(22)=0.0365137439813845
```

C

```
DO 911 I1=23,43
AL(I1)=1-AL(44-I1)
WE(I1)=WE(44-I1)
```

911 CONTINUE

C

```
BB=0.0
CIL(1)=0.0
DO 545 LLJ=1,KMJ
CIL(LLJ+1)=CIL(LLJ)+0.05
```

545 CONTINUE

```
KKK=KMJ-1
```

C

```
DO 105 I3=1,KKK
COEFF(I3)=CIL(I3+1)-CIL(I3)
DO 106 I=1,43
R(I)=CIL(I3)+COEFF(I3)*AL(I)
DX=ST*R(I)
CALL AJZERO(DX,GKK)
BB1=EXP(-R(I)*Z)
BB=BB+(R(I)*GKK*BB1*COEFF(I3)*WE(I)*QA(I3))
```

106 CONTINUE

105 CONTINUE

C

```
TN(LH)=BB
RETURN
END
```

C*****

C

C THIS SUBROUTINE CALCULATES THE RESISTANCE
C OF DROPLET AND HEAD FLUX INTEGRATION

C

C*****

```

SUBROUTINE ANA(KLL,T,QA,KMJ)
IMPLICIT REAL*8(A-H,O-Z)
DIMENSION HR(1000),QR(1000),T(1000),QA(51000)

```

```

C*****

```

```

C

```

```

C RESISTANCE OF DROPLET AND HEAT FLUX VALUES

```

```

C

```

```

C*****

```

```

      DO 79 KI=1,21
      YC=KI-1.0
      YRC=(YC/20.)
      IF(YRC.GT.1.0) GO TO 802
      IF(YRC.EQ.1.0) GO TO 902
      RR=1.0+2247.292*(SQRT(1.21749-(YRC**2)))-0.466358231)
      HR(KI)=1.0/RR
      QR(KI)=HR(KI)*(1.0-T(KI))
      GO TO 79
802 QR(KI)=0.0
      GO TO 79
902 HR(KI)=1.0
      QR(KI)=HR(KI)*(1.0-T(KI))
79 CONTINUE

```

```

C

```

```

      DO 188 IJ=1,KMJ
      TT1=IJ-1.0
      AD=(TT1/20.0)
      CALL INTEG2(KLL,AD,QR,RES,KMJ)
      QA(IJ)=RES
188 CONTINUE
      RETURN
      END

```

```

C*****

```

```

C

```

```

C THIS SUBROUTINE CALCULATES HEAT FLUX VALUES

```

```

C AND IS CALLED BY ANA PROGRAM

```


C

C*****

```
SUBROUTINE INTEG2(KLL,DL,QR,S,KMJ)
  IMPLICIT REAL*8(A-H,O-Z)
  DIMENSION AL(43),WE(43),CIL(51000),COEFF(51000),
  *R(51000),HR(1000),QR(1000)
```

C

```
AL(1)=0.0005190346563414
AL(2)=0.0031239146898052
AL(3)=0.0084075682191570
AL(4)=0.0163865807168469
AL(5)=0.0269263916107437
AL(6)=0.0399503329247996
AL(7)=0.0554358423344078
AL(8)=0.0733183177083414
AL(9)=0.0934737095762340
AL(10)=0.1157800182621610
AL(11)=0.1401382737139876
AL(12)=0.1664305979012938
AL(13)=0.1945014381051170
AL(14)=0.2241905820563901
AL(15)=0.2553520455521657
AL(16)=0.2878289398962806
AL(17)=0.3214373731700395
AL(18)=0.3559893415987994
AL(19)=0.3913099530641356
AL(20)=0.4272190729195524
AL(21)=0.4635163762021047
AL(22)=0.5000000000000000
```

C

```
WE(1)=0.0013977406162058
WE(2)=0.0039091686510621
WE(3)=0.0066523213035442
WE(4)=0.0092800277044381
WE(5)=0.0117870995415145
```

```

WE(6)=0.0142592132851025
WE(7)=0.0167012731604038
WE(8)=0.0190415767267325
WE(9)=0.0212484664405592
WE(10)=0.0233486623657572
WE(11)=0.0253485988982588
WE(12)=0.0272093375891918
WE(13)=0.0289052287488048
WE(14)=0.0304493401023310
WE(15)=0.0318478076245504
WE(16)=0.0330747889079756
WE(17)=0.0341103531305126
WE(18)=0.0349648825041994
WE(19)=0.0356466731818923
WE(20)=0.0361377411110170
WE(21)=0.0364228264152542
WE(22)=0.0365137439813845

```

C ***** COMPUTATION OF THE REST OF THE NODES *****

```

DO 11 I1=23,43
AL(I1)=1-AL(44-I1)
WE(I1)=WE(44-I1)

```

11 CONTINUE

C ***** END OF NODE VALUES *****

```

S=0.0
CIL(1)=0.0
DO 166 KK=1,19
CIL(KK+1)=CIL(KK)+0.05

```

166 CONTINUE

```

CIL(21)=1.00
NNN=20

```

C

```

DO 1 I3=1,NNN
COEFF(I3)=CIL(I3+1)-CIL(I3)
DO 2 I=1,43
R(I)=CIL(I3)+COEFF(I3)*AL(I)

```

```

DO 2 I=1,43
R(I)=CIL(I3)+COEFF(I3)*AL(I)
XXX=R(I)*DL
CALL AJZERO(XXX,BB)
S=S+((R(I)*BB*COEFF(I3)*WE(I))*QR(I3))
2 CONTINUE
1 CONTINUE
RETURN
END

```

```

C*****

```

```

C   SUBROUTINE CALCULATES THE BESSEL
C   FUNCTION

```

```

C*****

```

```

SUBROUTINE AJZERO(X,ZF)
IMPLICIT REAL*8(A-H,O-Z)
IF(ABS(X)-3.E0)10,10,30
10 Y=(X*X)/9.E0
ZF((((((0.00021E0*Y-.0039444E0)*Y+.0444479E0)*Y-.3163866E0)*Y+1
*.2656208E0)*Y-2.2499997E0)*Y+1.E0
RETURN
30 Y=3.E0/ABS(X)
F0((((((0.00014476E0*Y-.00072805E0)*Y+.00137237E0)*Y-.00009512E0)
**Y-.0055274E0)*Y-.00000077E0)*Y+.79788456E0
THETAO((((0.00013558E0*Y-.00029333E0)*Y-.00054125E0)*Y
*+.0026257E0)*Y-.00003954E0)*Y-.04166397E0)*Y-.78539816E0+ABS(X)
ZF=(1.E0/(SQRT(ABS(X))))*F0*COS(THETAO)
RETURN
END

```

APPENDIX C

LIST OF THE PROGRAM TO CALCULATE THE NEIGHBOR EFFECT

IMPLICIT REAL*8(A-H,O-Z)

DIMENSION TTOP(37,21),T(21),QF(37,21),QN(37,21),Q(37,21),Q1(37,21

DIMENSION QFT(36,20),QFA(37,21),QFTT(37,21),AL(20),QG(36,20)

*,QFT1(36,20),QFF(36,20),QFFF(37,21),QWS(37,21),QWS1(37,21),QWSS(3

*,20),QWSS1(36,20),QTD(37,21),QTDD(36,20),QTDD1(36,20)

C*****

C THIS PROGRAM CALCULATES SUBSTRATE EFFECT OF THE NEIGHBOR DROPLET *

C AND SUBSTRATE EFFECT DUE TO TEMPERATURE DISTRIBUTION *

C UNDER THE DROPLET *

C X :DISTENCE OF CENTRE BETWEEN THE DROPLET *

C R1 : RADIUS OF THE DROPLET WHICH HAS SUBSTRATE EFFECT *

C R2 :RADIUS OF DROPLET WHICH IS EFFECTED BY THE NEIGHBOURING *

C DROPLET (MAIN DROPLET) *

C T1 :TEMPERATURE OF THE MAIN DROPLET *

C TS1 :TEMPERATURE INCREASING BECAUSE OF SUBSTRATE EFFECT *

C TTOP:FINAL TEMPERATURE OF THE MAIN DROPLET AFTER SUPERIMPOSING *

C CS :NON-DIMENSIONAL HEAT TEANSFER COEFF.OF SUBSTRATE *

C*****

OPEN(9,FILE='SSI.DAT')

R2=2.00

R1=1.0

HI=1318037

CS=14.038/(HI*R2*0.001)

CV1=0.5865

CV2=CV1/(HI*R2*0.001)

CV=1.0/CV2

PRINT*, 'CV=', CV

DO 121 LL=1,22

TOP=0.0

X=(R1+R2)+((LL-1)/200.)

DO 32 I=1,37

TE=((I-1)*5./180.)*3.14159

```

BE=(I-1)*5.0
DO 57 J=1,21
R=((J-1)/20.)*R2
T1=7.6476-28.042*R-2507.128*(R**2)+448963.515*(R**3)-17506113.463
&(R**4)+313230056.346*(R**5)-2983225133.989*(R**6)+5580965634.*(R*
&7)+170049111965.921*(R**8)+1972377830242.006*(R**9)-3965589358720
&5.78*(R**10)-49871176007212.2*(R**11)-2622783110277558.*(R**12)+
&2.707647467929581D+16*(R**13)+2.365620027477119D+17*(R**14)+3.
&516316520771877D+18*(R**15)-4.545747642557848D+19*(R**16)
T(J)=T1
X1=SQRT((R**2)+(X**2)-2*R*X*COS(TE))
SS=1.05*R1
IF(X1.GE.SS) GO TO 10
TS1=3147.6791-5850.3671*X1+2717.2888*(X1**2)
IF(TS1.LT.0.0) GO TO 10
GO TO 65
10 TS1=0.0
65 TTOP(I,J)=TS1+T(J)
57 CONTINUE
32 CONTINUE
DO 77 I=1,37
TETA=(I-1)*5.0
DO 39 J=1,21
YC=J-1.0
YRC=(YC/20.0)
RR=1.0+CV*(SQRT(1.21749-(YRC**2))-0.466358231)
QWS(I,J)=HI*100*CS*(1.0/RR)/100000
Q(I,J)=CS*(1.0-(T(J)/100.0))/RR
Q1(I,J)=4.18*HI*100*Q(I,J)/1000000
IF(I.GT.1) GO TO 107
write(9,777) q1(i,j)
QN(I,J)=CS*(1.0-(TTOP(I,J)/100.0))/RR
QF(I,J)=HI*100*QN(I,J)/100000
QFA(I,J)=Q1(I,J)-QF(I,J)
QWS1(I,J)=QWS(I,J)-QF(I,J)

```

```

      QTD(I,J)=QWS(I,J)-Q1(I,J)
39  CONTINUE
77  CONTINUE
777  FORMAT(2X,'HFX=',F16.8,/)
      DO 97 I=1,36
      DO 88 J=1,20
      IF(J.GT.1) GO TO 100
      QTDD(I,J)=(QTD(I,J)+QTD(I,J+1)+QTD(I+1,J+1))/3.0
      QWSS(I,J)=(QWS1(I,J)+QWS1(I,J+1)+QWS1(I+1,J+1))/3.0
      QFF(I,J)=(QF(I,J)+QF(I,J+1)+QF(I+1,J+1))/3.0
      QFT(I,J)=(QFA(I,J)+QFA(I,J+1)+QFA(I+1,J+1))/3.0
      QFT1(I,J)=(Q1(I,J)+Q1(I,J+1)+Q1(I+1,J+1))/3.0
      GO TO 88
100  QFT(I,J)=(QFA(I,J)+QFA(I,J+1)+QFA(I+1,J+1)+QFA(I+1,J))/4.0
      QFT1(I,J)=(Q1(I,J)+Q1(I,J+1)+Q1(I+1,J+1)+Q1(I+1,J))/4.0
      QFF(I,J)=(QF(I,J)+QF(I,J+1)+QF(I+1,J+1)+QF(I+1,J))/4.0
      QWSS(I,J)=(QWS1(I,J)+QWS1(I,J+1)+QWS1(I+1,J+1)+QWS1(I+1,J))/4.0
      QTDD(I,J)=(QTD(I,J)+QTD(I,J+1)+QTD(I+1,J+1)+QTD(I+1,J))/4.0
88  CONTINUE
97  CONTINUE
      DO 398 KJ=1,20
      AL(KJ)=0.0
398  CONTINUE
      QFFF(37,21)=0.0
      DO 71 II=1,36
      DO 24 JJ=1,20
      RF=(JJ/20.)*R2
      IF(JJ.EQ.1) GO TO 43
      AL(JJ)=((5.0*3.14159*(RF**2))/360.0)-AL(JJ-1)
      GO TO 98
43  AL(JJ)=(5.0*3.14159*(RF**2))/360
98  QFTT(II,JJ)=(AL(JJ)*QFT(II,JJ))/10.0
      QTDD1(II,JJ)=(AL(JJ)*QTDD(II,JJ))/10.0
      QWSS1(II,JJ)=(AL(JJ)*QWSS(II,JJ))/10.0
      QFFF(II,JJ)=(AL(JJ)*QFF(II,JJ))/10.0

```

```

      QG(II, JJ)=(AL(JJ)*QFT1(II, JJ))/10.0
24  CONTINUE
71  CONTINUE
      DO 189 KK=1,36
      DO 200 KL=1,20
      SOP=SOP+QFTT(KK, KL)
      SOP1=SOP1+QG(KK, KL)
      TSWS=TSWS+QWSS1(KK, KL)
      TTDD=TTDD+QTDD1(KK, KL)
      TSHF=TSHF+QFFF(KK, KL)
200  CONTINUE
189  CONTINUE
      TTDD1=TTDD1+2.0*(4.18)*TTDD
      TSHF1=2.0*(4.18)*TSHF
      TSWS1=2.0*(4.18)*TSWS
      WRITE(8,197) TTDD1
197  FORMAT(2X, 'TTDD1=', F20.9, /)
      IF(SOP.EQ.0.0) GO TO 107
121  CONTINUE
107  STOP
      END

```

APPENDIX D

LIST OF THE PROGRAM TO CALCULATE DOUBLE INTEGRATION OF THE
HEAT FLUX

```

C*****
C THIS PROGRAM CALCULATES DOUBLE INTEGRATION      *
C OF THE HEAT FLUX WHICH FUNCTION OF THE X AND R *
C X= DISTANCE BETWEEN THE DROPLETS              *
C R= RADIUS OF THE DROPLET                       *
C*****
      DOUBLE PRECISION ZF,X,BJK,BALY,Y
      OPEN(8,FILE='/DOUB.OUT A')
      AD=1.00
      CALL INTEG2(AD,RES)
      PRINT*,'INT=',RES
      WRITE(8,666) RES
666 FORMAT(1X,1(F10.6))
      STOP
      END
C *****
C*          SUBROUTINE CALCULATES DOUBLE INTEGRATION      *
C*          BY USING SIMPSON 3/8 RULE                      *
C*****
      SUBROUTINE INTEG2(AD,SON)
      R1=1.0
      KKK=2
      SON=0.0
      KK=4
      LI=4
      NNN=201
      PNT=0.0
      TOP=0.0
      GN=0.3333
      DM=2.00
      PI=3.141

```



```

SM=GN-1
DO 901 II=1,NNN
TOP=0.0
SOP=0.0
KK=4
H=(4.60517+0.69314718)/(NNN-1)
IF(II.EQ.1) GO TO 61
SH=((II-1)*H)-4.60517
GO TO 48
61 SH=-4.60517
48 R=SH
F=0.015579+0.010031*R+0.002578*(R**2)+0.00023644*(R**3)
AA=0.05+0.05583*R+0.02173*(R**2)+0.002593*(R**3)
A1=1.00
BB=-1.986176+0.053078*R+0.09087877*(R**2)+0.012464*(R**3)
CC=1.1609986-0.076754*R+0.128499*(R**2)-0.0232163*(R**3)
DD=-0.1712+0.027128*R+0.0383241*(R**2)+0.010619*(R**3)
DO 310 I=1,KKK
HH=(1./(KKK-1))
IF(I.EQ.1) GO TO 93
SSH=(I-1)*HH
GO TO 26
93 SSH=0.0
26 R=SH
X=SSH
QQ=0.09615+F*(A1+SSH*BB+(SSH**2)*CC+(SSH**3)*DD)
A=2*(GN/DM)*QQ*(EXP(R)/DM)**SM*(1.0/EXP(R))*AA*(AA*SSH+EXP(R))+0.1
IF(I.EQ.1) GO TO 800
IF(I.EQ.KKK) GO TO 800
IF(KK.EQ.I) GO TO 200
SOP=SOP+3*A
GO TO 310
200 SOP=SOP+2*A
KK=I+3
GO TO 310

```

```
800 SOP=SOP+A
310 CONTINUE
    TOP=SOP*(3.0/8.0)*HH
    IF(II.EQ.1) GO TO 90
    IF(II.EQ.NNN) GO TO 90
    IF(LI.EQ.II) GO TO 80
    PNT=PNT+3*TOP
    GO TO 901
80 PNT=PNT+2*TOP
    LI=II+3
    GO TO 901
90 PNT=PNT+TOP
901 CONTINUE
    SON=H*(3.0/8.0)*PNT
76 RETURN
    END
```

APPENDIX E

LIST OF THE PROGRAM TO CALCULATE THE MESH POINTS OF THE TEMPERATURE DISTRIBUTION PROBLEM

```

C*****
c   This program calculates the mesh points           *
c   of the temperature distribution problem           *
C*****
      dimension x(5001),y(5001),iel(10000,3),t(5001)
C*****
c   nx=number of nodes in radial direction           *
c   ny=number of nodes in z direction                *
c   dx=increment in the radial direction             *
c   dy=increment in z direction                      *
c   iel(i,1)=first node of element i                 *
c   iel(i,2)=second node of element i                *
c   iel(i,3)=third node of element i                 *
C*****
      print*, 'nx,ny,dx,dy'
      read(*,*)nx,ny,dx,dy
      PRINT*, '
      PRINT*, ' Program is writing the elemental nodes of the'
      print*, ' problem to "MESH.DAT" file'
      y(1)=0.
      x(1)=0.
      n1=nx*ny-nx+1
      do 8 i=nx+1,n1,nx
8     x(i)=x(i-nx)
      do 9 i=1,nx
9     y(i)=0.
      do 1 i=nx+1,n1,nx
      do 1 j=i,i+nx-1
1     y(j)=y(j-nx)+dy
      do 2 i=1,n1,nx
      do 2 j=i+1,i+nx-1

```

```

2  x(j)=x(j-1)+dx
   l=1
   do 3 i=1,ny-1
     jj=i*(nx-1)*2
     j=1
5  m=l+1
   iel(1,1)=j+(i-1)*nx
   iel(1,2)=j+i*nx
   iel(1,3)=iel(1,2)+1
   iel(m,1)=iel(1,1)
   iel(m,2)=iel(1,3)
   iel(m,3)=iel(1,1)+1
   if(m.eq.jj) l=m+1
   if(m.eq.jj) go to 3
   l=m+1
   j=j+1
   go to 5
3  continue
   nnode=nx*ny
   nel=2*(nx-1)*(ny-1)
   open(unit=6,file='MESH.DAT')
   WRITE(6,12)nel,nnode,nx,ny
12  format(2i10)
   do 6 i=1,nx*ny
     6  write(6,10)i,x(i),y(i)
10  format(i5,2f10.4)
   do 7 i=1,2*(ny-1)*(NX-1)
     7  write(6,11)i,iel(i,1),iel(i,2),iel(i,3)
11  format(4i5)
   close (unit=6)
   stop
   end

```

APPENDIX F

THE LIST OF THE PROGRAM TO DRAW THE ISOTHERM LINES

```

10 CLS
20 SCREEN 2
30 OPEN "i", #1, "c:\WATFOR\MESH.DAT"
40 INPUT #1, NEL, NNODE
50 DIM XN(NNODE), YN(NNODE), T(NNODE), IEL(NEL, 3), X(2)
60 KEY OFF
70 GOSUB 550
80 LOCATE 9,8: INPUT "temperature increment?", DT
90 CLS
100 LOCATE 8,8 : INPUT "SCALE FACTOR FOR X=", SX
110 LOCATE 9,8: INPUT "SCALE FACTOR FOR Y=", SY
111 LOCATE 10,8: INPUT "SIFT FACTOR FOR X=", XS
112 LOCATE 11,8: INPUT "SIFT FACTOR FOR Y=", YS
120 CLS
130 FOR I=1 TO NEL
140 I1=IEL(I,1)
150 I2=IEL(I,2)
160 I3=IEL(I,3)
170 FOR J=TMIN TO TMAX STEP DT
180 GOSUB 270
190 NEXT J
200 NEXT I
210 REM LOCATE 4,20: INPUT "DO YOU WANT TO RUN AGAIN (Y/N) ?", C$
220 REM IF C$="Y" OR C$="y" THEN CLS
230 REM IF C$="Y" OR C$="y" THEN 80
240 REM IF C$="N" OR C$="n" THEN END
250 REM IF C$<>"Y" OR C$<>"N" OR C$<>"n" OR C$<>"y" THEN 190
260 END
270 K=0
280 IF T(I2)=T(I1) OR T(I1)=T(I3) OR T(I2)=T(I3) THEN RETURN
290 XX=(J-T(I1))/(T(I2)-T(I1))
300 IF XX>=0 AND XX<=1 GOTO 320
310 GOTO 350
320 K=K+1
330 X(K)=(XN(I2)-XN(I1))*XX+XN(I1)
340 Y(K)=(YN(I2)-YN(I1))*XX+YN(I1)
350 XX=(J-T(I2))/(T(I3)-T(I2))
360 IF XX>=0 AND XX<=1 GOTO 380
370 GOTO 420
380 K=K+1
390 X(K)=(XN(I3)-XN(I2))*XX+XN(I2)
400 Y(K)=(YN(I3)-YN(I2))*XX+YN(I2)
410 IF K=2 GOTO 520
420 XX=(J-T(I3))/(T(I1)-T(I3))
430 IF XX>=0 AND XX<=1 GOTO 450
440 GOTO 520
450 K=K+1

```

```

460 X(K)=(XN(I1)-XN(I3))*XX+XN(I3)
470 Y(K)=(YN(I1)-YN(I3))*XX+YN(I3)
480 LINE(XS+XN(1)*SX,YS+YN(1)*SY)-(XS+XN(NX)*SX,YS+YN(NX)*SY)
490 LINE(XS+XN(NX)*SX,YS+YN(NX)*SY)-(XS+XN(NX*NY)*SX,YS+YN(NX*NY)*
500 LINE(XS+XN(NX*NY)*SX,YS+YN(NX*NY)*SY)-(XS+XN(NX*(NY-1)+1)*SX
+1)*SY)
510 LINE(XS+XN(1)*SX,YS+YN(1)*SY)-(XS+XN(NX*(NY-1)+1)*SX,YS+YN
520 LINE(XS+X(1)*SX,YS+Y(1)*SY)-(XS+X(2)*SX,YS+Y(2)*SY)
530 RETURN
540 END
550 REM OPEN"i",#1,"c:\WATFOR\MESH.DAT"
560 INPUT #1,NX,NY
570 FOR I=1 TO NNODE
580 INPUT #1,II,XN(I),YN(I)
590 NEXT I
600 FOR I=1 TO NEL
610 INPUT #1,IJ1,IJ2,IJ3,IJ4
620 IEL(I,1)=IJ2:IEL(I,2)=IJ3:IEL(I,3)=IJ4
630 REM IEL(47,1)=27:IEL(47,2)=26:IEL(47,3)=35
640 NEXT I
650 CLOSE #1
660 OPEN"i",#2,"c:\gw\temp.dat"
670 FOR I=1 TO NNODE
680 INPUT #2,T(I)
690 NEXT I
700 CLOSE #2
710 TMAX=T(1)
720 TMIN=T(1)
730 FOR I=1 TO NNODE
740 IF T(I)>TMAX THEN TMAX=T(I)
750 IF T(I)<TMIN THEN TMIN=T(I)
760 NEXT I
770 RETURN

```